Phosphorylation and protein turnover regulate epithelial cell migration and membrane ruffling

Elizabeth Steenkiste

A dissertation

submitted in partial fulfillment of the

requirements for the degree of

Doctor of Philosophy

University of Washington

2020

Reading Committee:

Jonathan A. Cooper, Chair

Jihong Bai

Barry M. Gumbiner

Program Authorized to Offer Degree:

Molecular and Cellular Biology

University of Washington

Abstract

Phosphorylation and protein turnover regulate epithelial cell migration and membrane ruffling

Elizabeth Steenkiste

Chair of the Supervisory Committee:
Jonathan A. Cooper, Ph.D.
Biochemistry

Cell migration is crucial for the development and maintenance of multi-cellular animal life. This complex, dynamic process must be coordinated properly, as disruption of mechanisms and signaling pathways that regulate migration contribute to diseases such as cancer. Cullin5-RING E3 ubiquitin ligase (CRL5) and substrate adaptors from the suppressors of cytokine signaling (SOCS) protein family serve to negatively regulate tyrosine phosphorylated proteins through ubiquitination and degradation. We have shown that Cul5, in combination with SOCS2, SOCS4, SOCS5, and SOCS6, inhibits epithelial cell transformation, including inhibition of migration and membrane ruffling. The turnover of focal adhesion (FA) adaptor protein, p130Cas (Cas), is regulated by CRL5-SOCS6 at the leading edge of migrating cells to inhibit FA turnover and membrane ruffling. However, overexpression of Cas alone does not stimulate migration, suggesting that turnover of other CRL5-SOCS substrates contribute to this mechanism. In an

effort to characterize novel substrates of CRL5-SOCS, we identified breast cancer antiestrogen resistance 3 (BCAR3) as a candidate, as two BCAR3 phosphopeptides are increased in cells lacking functional CRL5. BCAR3 is a Cas binding partner in FAs and has been shown to regulate migration and invasion in breast cancer cell lines. However, little is known about the regulation of BCAR3. I found that the turnover of BCAR3 is regulated by CRL5-SOCS6, dependent on the proteasome. Additionally, CRL5-SOCS6-mediated regulation of BCAR3 is independent of Cas, as BCAR3-SOCS6 association occurs in the absence of Cas and under conditions where BCAR3 cannot bind Cas. Binding studies using BCAR3 and SOCS6 mutants show that BCAR3-SOCS6 association require a functional SOCS6 SH2 domain and BCAR3 Y117, suggesting that pY117-BCAR3 is bound by SOCS6 through the SOCS6 SH2 domain. Consistent with these data, BCAR3 Y117F protein levels are not regulated by CRL5. Next, I determined whether BCAR3 regulates migration in normal epithelial cells. While BCAR3 is important for individual cell migration and invasion towards epidermal growth factor (EGF) independent of CRL5, BCAR3 is required for the increased collective migration and membrane ruffling of Cul5-deficient cells in the absence of EGF. While I hypothesized that BCAR3 Y117F would be a gain-of-function mutant because it is not degraded through CRL5, BCAR3 Y117F is not functional. Expressing BCAR3 Y117F does not induce membrane ruffling, as wildtype BCAR3 does and expressing BCAR3 Y117F at normal levels in the absence of endogenous BCAR3 does not support the increased migration and membrane ruffling observed in Cul5-deficient cells. Collectively, these data suggest that BCAR3 Y117 is required for both degradation and function. In addition to Y117, I also found that the BCAR3 SH2 domain and Cas-binding sites are required for BCAR3 function in regulating migration and membrane ruffling. Interestingly, these three sites are all required to promote tyrosine phosphorylation of

Cas at the leading edge of migrating cells, which is known to stimulate membrane ruffling. Taken together, these data identify and characterize novel mechanisms through which BCAR3 is regulated and through which BCAR3 regulates pY-Cas and collective migration. In addition to investigating BCAR3, I also studied FA protein exchange and FA structure and stability. FA proteins are dynamic and constantly associate with and disassociate from the adhesion. This protein exchange is rapid, with 40-80% of FA protein exchanging over a couple minutes and the remaining protein being considered immobile. Such rapid dynamics raise questions about how the adhesion maintains its structure and propagates downstream signals over long periods of time. I found that the population of FA protein previously considered immobile exchanges slowly with cytoplasmic protein over longer periods of time and hypothesize that this slow-exchanging population is actively regulated and participates in signaling. Collectively, my results establish novel regulatory mechanisms of FA proteins BCAR3 and Cas, FA structure and the leading edge of migrating cells.

TABLE OF CONTENTS

LIST OF FIGURES

LIST OF TABLES

ACKNOWLEDGEMENTS

Thank you to Jon Cooper for his mentorship. Jon, thank you for the time you have spent teaching me how to think critically and how to design the best experiment to answer the question being asked. Over the last six years, our conversations have evolved from primarily discussing methods into discussions about possible models and general thoughts about molecular biology. This growth is in large part due to the scientific example you set and I truly value the knowledge and experience you have shared with me. Your true passion for biology is unique and inspiring. Thank you for the patience and encouragement you showed me when experiments were not working and everything seemed challenging. You always had a thoughtful suggestion which helped keep me motivated. I also appreciate your encouragement as I worked to gain valuable teaching experience that will help me in my future career. My experiences working with SEP and teaching at UW were important to me and I thank you for allowing me to devote time to those experiences.

I would also like to thank all the members of my thesis committee for their advice and encouragement through this process, which included both scientific and career-focused advice. Thank you to Jihong Bai, Barry Gumbiner and Jon Cooper for taking the time to read and make thoughtful comments on this dissertation.

Many thanks to the wonderful people who I've gotten to work with in the Cooper lab over the past 6 years. In particular, I would like to thank Anjali Teckchandani and Jason Berndt for their valuable mentorship and experimental help during different stages of this process.

I am grateful to the staff of the Fred Hutch Scientific Imaging Core for their assistance with microscopy in several projects. In particular, I would like to thank Lena Schroeder for her time and expertise.

Finally, I would like to thank all of the people in my life whose support was invaluable over the last 6 years. I would specifically like to thank my parents, Ann and Peter Steenkiste, for their support and encouragement, particularly when I was doubting myself. I am also grateful for my wonderful network of friends, whose support I could always count on.

Chapter 1. GENERAL INTRODUCTION

1.1 CELL MIGRATION AND FOCAL ADHESIONS

Cell migration is crucial for many biological processes, including embryonic development, tissue repair, immune response and cancer metastasis. Developmental processes, such as gastrulation, are essential for the formation of multi-cellular organisms and require extensive cell movement, as cells must migrate long distances in the forming embryo [1]. Following injury to a tissue, epithelial cells must proliferate and migrate collectively into the wound area to repair the epithelium and maintain tissue homeostasis [2, 3]. While cell migration is critical for the development and maintenance of multi-cellular animal life, many diseases, such as cancer, rely on cell motility to propagate. A key component of cancer metastasis is cell migration, as clusters of cells must move through vasculature and invade through tissue to colonize at a secondary site [2-4].

In vivo, cell must migrate through tissue and within the extracellular matrix (ECM). Mesenchymal cell migration is a mode of 3D cell migration that is defined by an elongated, polarized cell body and adhesion to ECM. Actin polymerization drives the formation of leading edge protrusions called lamellipodia. Strong sites of adhesion to other cells or to ECM provide traction and contractile stress fibers help pull the cell forward through the dense matrix. Matrix-adhesion sites must be disassembled under the cell body [5-7] (Figure 1.1). While specific sites of adhesion have been characterized as essential components of cell migration, studies have shown that adhesions are not always required for 3D migration, where dense ECM helps maintain cell-matrix contact [8].

Several molecular processes are coordinated at the leading edge of migrating cells. Components of the cytoskeleton are crucial. Microtubules provide pathways for intracellular transport required for vesicle traffic and delivery of molecules to the leading edge and also contribute to the structure of the protrusions [9]. Broad, flat protrusions called lamellipodia are formed due to the force generated by actin polymerization that pushes the plasma membrane forward. These dense networks of branched actin are formed when the small GTPase, Rac, is active. Rac

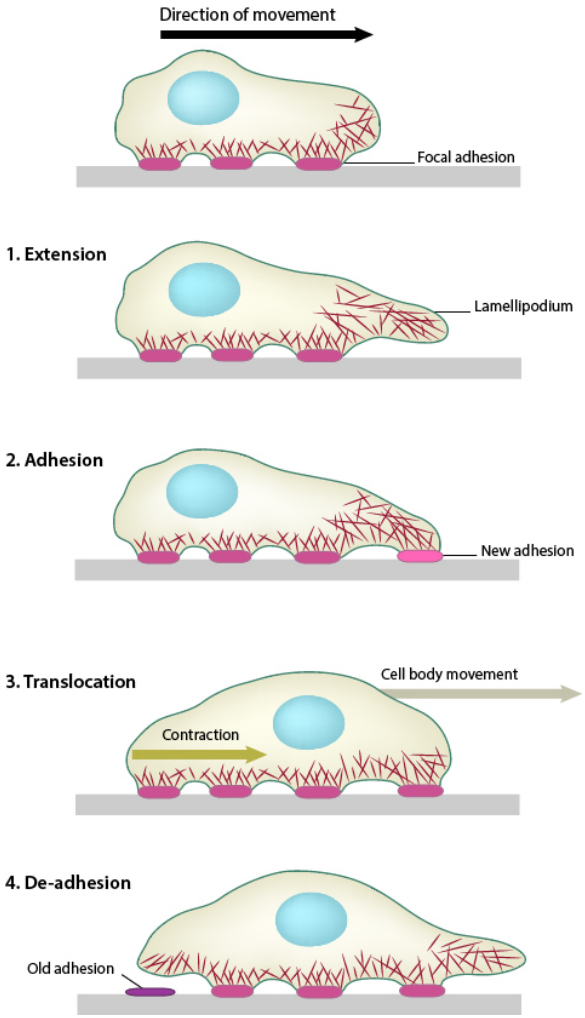

Figure 1.1 Mechanism of cell migration. Polymerization of actin filaments drives the extension of the cell membrane to form a protrusion in the direction of motion. Sites of adhesion are assembled at the leading edge to attach the protrusion to the surrounding matrix. Actomyosin contraction and rearward actin flow generate the force required for translocation of the cell body. Adhesion disassembly under the cell body is required for retraction at the back of the cell. Image used with permission from MBInfo: www.mechanobio.info.

activates a nucleation-promoting factor, WAVE, which in turn activates an actin nucleator, actin-related protein 2/3 (Arp2/3) complex. Arp2/3 generates new actin filaments that branch off of existing filaments [10-12]. Other types of protrusions, such as filopodia, are regulated differently. Filopodia are finger-like protrusions that are stimulated by a different small GTPase, Cdc42, and WASP. As actin polymerization pushes the cell membrane forward, a rearward actin flow is generated that aids in forward movement. Integrin transmembrane receptors are activated and form clusters when they engage with the ECM. These integrin-containing sites of adhesion act as a

mechanical clutch by facilitating transient interactions between the ECM and the moving actin. Traction force is placed on the ECM as the force generated by the actin polymerization is transmitted through the integrin adhesion sites [13, 14].

Integrin-containing adhesion sites recruit proteins to interact with the integrin tails and form complexes called focal adhesions (FAs), which are protein complexes that form a bridge between the ECM and the actin cytoskeleton. Transmembrane integrin receptor proteins engage extracellularly with the ECM and intracellularly with a network of proteins that serve structural, signaling and adaptor roles. FAs are molecularly complex, as they are made up of hundreds of molecules, each of which can be post-translationally modified and potentially interact with more than one binding partner. How such a dynamic and complex structure is differentially regulated in different parts of the cell and at different times is not well understood.

The molecular organization of FAs is composed of multiple layers with different functions [15-18]. Closest to the membrane is an integrin signaling layer that includes paxillin and FAK in addition to the activated cytoplasmic tails. Next is a layer composed of proteins responsible for transducing the force generated that stabilizes the adhesion, such as vinculin and talin. Furthest from the membrane and integrin tails is a layer of proteins like zyxin and α-actinin that bind and regulate actin [15]. All the signaling pathways required for integrin signaling, force transduction and the regulation of actin need to cooperate in order for FA assembly, stabilization and disassembly to occur properly. This coordination is achieved by biophysical, force-induced changes in mechanosensing proteins and biochemical processes, including activation and inactivation of GTPases, lipid modifications and, of particular interest here, protein phosphorylation.

1.2 PHOSPHOTYROSINE SIGNALING IN FOCAL ADHESIONS

1.2.1 *Kinases regulate FA assembly and disassembly*

The activities of tyrosine kinases focal adhesion kinase (FAK) and Srk family kinases (SFKs, primarily Src and Fyn) are crucial for transducing signals of activated integrins. SFKs were first identified as the transforming protein of Rous sarcoma virus, v-Src, which is a mutant variant of a highly conserved cellular protein [19-21]. FAK was identified as a substrate of v-Src that localizes

to adhesion sites and is highly phosphorylated [22, 23]. These kinases phosphorylate several key FA proteins responsible for regulating assembly and disassembly of FAs, which makes them essential for proper adhesion turnover and migration.

Early work showed that FAK is rapidly tyrosine phosphorylated and activated in response to cell adhesion to the ECM [23, 24]. Tyrosine phosphorylation of FAK mediates interactions with other proteins that link key pathways of cell migration. Interactions with phosphatidylinositol lipids, vinculin and paxillin facilitate localization to sites of adhesion. Once at these nascent adhesions, clustering and interactions with membrane can activate FAK autophosphorylation at Y397, which recruits and activates Src. Src then phosphorylates Y576 and other sites in FAK, as well as other proteins in the FA. Many functions of FAK can be explained by FAK serving as a scaffold to activate Src and other proteins for phosphorylation by Src. Ultimately, the FAK-Src signaling complex leads to regulation of small GTPase proteins, Rho, Rac, Cdc42, and Ras by binding or phosphorylating activators or inhibitors of GTPases. By regulating local small GTPase activity, FAK-Src direct the formation of lamellipodia, filopodia and stress fibers required for cell migration.

As opposed to being activated primarily by adhesion to matrix, SFKs can be activated by many different receptors, including growth factor receptor tyrosine kinases, cytokine receptors, and antigen receptors in addition to integrins [21, 25]. In addition to localizing to focal adhesions, SFKs are also found at the plasma membrane, as they are membrane associated through myristoylation, palmitoylation and polybasic motifs.

Given the outlined roles of FAK and SFKs, it is not surprising that these kinases regulate cell migration in normal and cancerous cells. Specifically, FAK regulates FA turnover during migration. Mouse embryonic fibroblasts have more adhesions and migrate more slowly in the absence of FAK [26]. More detailed mechanistic studies found that loss of FAK inhibits FA turnover and that phosphorylation of FAK at Y397 and Y576 is required for FA disassembly, as mutating these sites stabilizes adhesions [27-29]. Src kinase activity also regulates FA turnover, as inhibiting Src kinase activity by expressing a non-enzymatic mutant of Src or treatment with an inhibitor decreased the rate of FA disassembly [29]. FA turnover is defective in fibroblasts lacking

SFKs [29, 30]. Both FAK and Src are frequently upregulated or highly activated in different types of cancer, which has led to both kinases being targets for cancer therapies [31-34].

1.2.2 *pY-Cas signaling*

p130Cas (Cas) is a Src substrate that is tyrosine phosphorylated in response to adhesion. Cas was first identified as a tyrosine phosphorylated protein from v-Src and v-Crk transformed [35]. Since then, Cas signaling has been extensively studied and has been shown to regulate many processes including cell adhesion, migration and membrane ruffling.

Cas acts as a scaffold protein in FAs with a structure that provides many binding sites for signaling proteins [36, 37]. Cas has an N-terminal SH3 domain and a C-terminal focal adhesion targeting (FAT) domain, which are linked by a central domain. The central region contains 15 repeated YxVP sequences, a four-helix bundle, and Src binding sequences, PXXP and YDYV. The 15 repeats are highly phosphorylated at the tyrosine residues by Src after Src binding to Cas. These phosphorylated repeats provide binding sites for several signaling proteins that promote adhesion, migration and membrane ruffling.

pY-Cas binding partner, Crk (and its paralog, CrkL), regulates downstream signaling to promote membrane ruffling. Membrane ruffling is regulated by small GTPase, Rac1, which promotes the polymerization of branched actin networks, as previously described. Membrane ruffling occurs when a network of recently polymerized actin filaments form broad protrusions and has been shown to require Rac1 in a broad range of cell types [38, 39]. Upstream of Rac1, pY-Cas is bound by Crk through an SH2 domain. Crk is then bound by DOCK180, which associates with and activates Rac1 [40]. The pY-Cas-Crk-DOCK180-Rac1 signaling pathway requires Cas tyrosine phosphorylation by Src, the pY-Cas/Crk complex formation, DOCK180 binding Crk and DOCK180 binding Rac1 [40-43]. Disruption of any of these interactions inhibits membrane ruffling. Thus, tyrosine phosphorylation of the central domain of Cas by Src kinase is the driving factor in stimulating membrane ruffling (Figure 1.2).

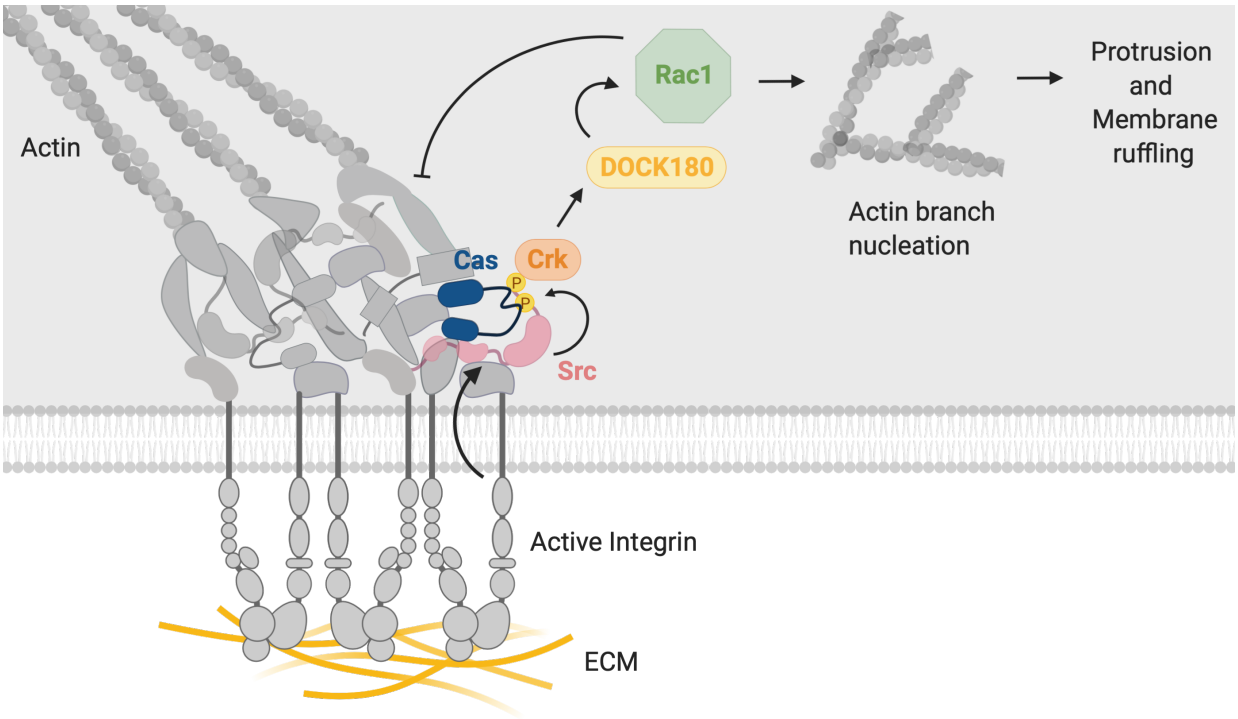

Figure 1.2 pY-Cas promotes membrane ruffling. Tyrosine kinase, Src, is activated in response to adhesion and binds and phosphorylates Cas in the Cas central domain. These pY sites provide binding sites for Crk, which is then bound by DOCK180. DOCK180 activates small GTPase, Rac1, which promotes nucleation and polymerization of branched actin networks. Actin polymerization drives membrane protrusion and membrane ruffling. Rac1 activity also inhibits the formation of FAs. Figure created with BioRender.com.

1.3 BCAR3

In addition to being regulated by Src and binding Crk, Cas also interacts with a protein called breast cancer anti-estrogen resistance 3 (BCAR3; AND-34; NSP2). BCAR3 is an FA protein which was first identified in a screen to identify genes that confer antiestrogen resistance in a hormone-dependent breast cancer cell line [44]. Insertional mutagenesis was used in the screen to integrate retroviruses randomly into the genome to truncate or alter expression of genes. The BCAR3 gene was identified from a tamoxifen-resistant clone and follow up experiments determined that overexpression of BCAR3 can induce antiestrogen resistance. Nevertheless, the role of BCAR3 in cancer is unclear.

1.3.1 *Role of BCAR3 in cancer*

The original cloning of BCAR3 as conferring antiestrogen resistance suggested that it would promote cancer phenotypes. Indeed, BCAR3 protein levels in different breast cancer cell lines correlate with breast cancer progression. Both MCF7, which is a noninvasive ER-positive cell line, and T47D, which is a moderately invasive ER-positive cell line, have low levels of BCAR3, while MDA-MB-231 and BT549, which are ER-negative cell lines often used to represent very aggressive, metastatic breast cancer, express much higher levels of BCAR3 [45]. Staining for BCAR3 in normal and tumor breast tissue sections shows increased BCAR3 protein levels in several subtypes of breast tumor [46]. Further, BCAR3 increases migration and invasion of cancer cells in vitro, consistent with increased malignancy in vivo. Overexpression of BCAR3 in the relatively nonmobile and noninvasive breast cancer cell lines promotes migration, while depleting BCAR3 in the highly migratory and invasive breast cancer cell lines inhibits migration [45]. These data suggest a model in which overexpression of BCAR3 in breast cancer cells relative to normal cells promotes the increased migratory and invasive phenotypes of cancer cells.

While the bulk of the in vitro experiments studying the role of BCAR3 in migration support a model in which BCAR3 promotes migratory and invasive phenotypes in cancer cells, several recent studies have found that BCAR3 expression is correlated to favorable outcomes. Specifically, BCAR3 can be used as a prognostic factor in multiple myeloma, where high mRNA expression of BCAR3 predicted better prognoses and low expression at the time of diagnosis predicted earlier relapse [47]. Additionally, low mRNA expression of BCAR3 in primary breast cancer cells is correlated with worse metastasis-free survival and relapse-free survival and loss of heterozygosity of *BCAR3* alleles is correlated with lymph node invasion [48]. This patient data suggests that high BCAR3 expression is beneficial and could contribute to better disease outcomes, which conflicts with the in vitro studies that suggest that high BCAR3 levels would contribute to worse outcomes. However, the patient data uses BCAR3 mRNA expression levels and the studies using breast cancer cell lines looked at BCAR3 protein levels. Additionally, these studies do not account for differences in regulation and phosphorylation in breast tumors that may contribute to disease progression and survival. A phosphoproteomic study found differential phosphorylation of BCAR3 and Cas in basal compared to luminal breast cancer cell lines, where phosphorylation

of BCAR3 and Cas is increased in the basal subtype [49]. Therefore, further investigation of BCAR3 regulation is needed to understand the role of BCAR3 in disease progression.

1.3.2 *BCAR3 structure and family*

BCAR3 belongs to the novel SH2-containing family of protein (NSP), whose members share structural domains. NSP proteins NSP1, SHEP1 (NSP3; CHAT), and BCAR3 contain an SH2 domain, a domain that shares sequence with the CDC25 homology domain found in Ras guanine nucleotide exchange factors, and a proline/serine rich domain that links these domains together [37]. BCAR3 can bind EGFR and PTPα through its SH2 domain [50-52]. The C-terminal CDC25 homology domain of BCAR3 has a structure that does not facilitate enzymatic activity [53], but does bind to FA protein Cas to form a signaling node in FAs [37]. Given the domains and sequence motifs found in BCAR3, there are likely many other binding partners that have not yet been identified.

1.3.3 *Molecular mechanism of BCAR3 in cell migration, FA dynamics and protrusive activity*

The role of BCAR3 in migration has been extensively studied in breast cancer cell lines. When detecting BCAR3 protein levels in several breast cancer cell lines, it was observed that BCAR3 protein levels seem to correlate with early and late stages of breast cancer progression. Both MCF7, which is a noninvasive ER-positive cell line, and T47D, which is a moderately invasive ER-positive cell line, have low levels of BCAR3. MDA-MB-231 and BT549 are ER-negative cell lines often used to represent very aggressive, metastatic breast cancer and express much higher levels of BCAR3 [45]. Further, overexpression of BCAR3 in the relatively nonmobile and noninvasive breast cancer cell lines promotes migration and depleting BCAR3 in the highly migratory and invasive breast cancer cell lines inhibits migration [45]. These data suggest a model in which overexpression of BCAR3 in breast cancer cells relative to normal cells promotes the increased migratory and invasive phenotypes of cancer cells.

One mechanism through which BCAR3 regulates migration is through its regulation of FA turnover. Depleting BCAR3 in aggressive breast cancer cells, BT549 cells, increases the length of

adhesions after spreading on fibronectin [54]. Longer adhesions suggest a possible defect in FA turnover, as adhesions may be unable to disassemble properly. More specifically, groups have studied FA turnover more directly by fluorescently labeling an FA protein such as vinculin and using TIRF microscopy to measure assembly and disassembly rates. Knocking down BCAR3 in BT549 cells reduced the percentage of adhesions undergoing disassembly and increased the percentage of static adhesions. FA assembly was not affected by BCAR3 knockdown [54]. This study suggests that BCAR3 regulates migration by promoting FA disassembly.

In addition to FA dynamics, BCAR3 also regulates membrane protrusions and cell spreading. Knocking down BCAR3 in BT549 cells reduced the average protrusion area and time to the maximum membrane extension [54]. Conversely, overexpressing BCAR3 in MCF7 cells and NIH 3T3 cells increased the average protrusive area [54] and membrane ruffling [55], respectively. These results collectively suggest that BCAR3 promotes membrane protrusion. Additionally, BCAR3 promotes efficient cell spreading, as depleting BCAR3 in breast cancer cells delays adherence and spreading [56].

BCAR3 promotes migration and membrane protrusion through activation of Rac1. Knocking down BCAR3 in breast cancer cells reduced the amount of active GTP-bound Rac1, but had no effect on total Rac1 levels. When constitutively expressed Rac1 was expressed in BCAR3-depleted cells, this rescued the loss of protrusions observed when BCAR3 was knocked down [54]. Additionally, overexpression of BCAR3 in human embryonic kidney cells increased levels of active Cdc42 and Rac1 [55]. In order to identify which functional domains are required for BCAR3-induced activation of Rac1, deletion and point mutants of BCAR3 were expressed and active Rac was measured. A functional SH2 domain and C-terminal CDC25 homology domain are required for BCAR3-induced activation of Rac1 [57]. In addition to activating Rac1, there is evidence that RhoA and its downstream signaling molecules are more active in the absence of BCAR3 [54].

Downstream of activated Rac1, BCAR3 has been shown to regulate actin cytoskeletal remodeling in breast cancer cells and mouse embryonic fibroblasts. Knocking down BCAR3 in breast cancer cells resulted in the formation of prominent stress fibers [54], while increasing expression in mouse

embryonic fibroblasts reduced the number of actin stress fibers with the remaining stress fibers being less organized [55].

Collectively, studies investigating migratory roles of BCAR3 suggest that BCAR3 regulates FA disassembly, membrane protrusiveness and actin rearrangement to promote migration. This is achieved in part through activation of GTPases, Rac1 and Cdc42.

1.3.4 *BCAR3 and Cas form a signaling complex in FAs*

BCAR3 is bound by FA adaptor protein, Cas, across a range of cell types [46, 58]. In fact, serial immunoprecipitation experiments revealed that most BCAR3 is in complex with Cas in breast cancer cells, although there is free, BCAR3-dissociated Cas [46]. Additionally, BCAR3 is coexpressed with Cas in human breast tumors [46]. Because of the documented BCAR3-Cas interaction and the known roles of Cas and BCAR3 in FAs, possible cooperation between BCAR3 and Cas has been extensively studied. Indeed, the Cas gene was identified in the same screen for antiestrogen effects as BCAR3, leading to its alternative name as BCAR1 [44].

Early work demonstrated that BCAR3 enhances Cas-mediated Src kinase activity. Knocking down BCAR3 in breast cancer cells and mouse embryonic fibroblasts reduced Src autophosphorylation at Y419, which is used as a marker of Src activity, but did not change overall levels of Src [52, 56]. Inversely, overexpression of BCAR3 can induce Src activity [56]. The regulation of Src activity by BCAR3 is mediated by Cas, as coexpression of Src and Cas enhance phosphorylation of Src substrates paxillin and Src itself and coexpression AND-34 (BCAR3) in addition to Cas and Src increased phosphorylation above that seen in the first condition. Importantly, AND-34 and Src overexpression without Cas did not induce phosphorylation of Src substrates, suggesting that BCAR3 activates Src kinase through Cas [58]. Additional studies suggest that Cas-Src association and BCAR3-Cas association are both required for this BCAR3-dependent enhancement of Cas-mediated Src activity [56, 59].

Activation of Src kinase through Cas and BCAR3 promotes tyrosine phosphorylation of Cas [56], which activates signaling pathways that regulate FA disassembly and cytoskeleton remodeling. As

one would expect given the role of BCAR3 in promoting pY-Cas, overexpression of BCAR3 increased Cas binding to Crk, an adaptor protein crucial for Cas signaling [54]. Further, BCAR3-Cas association is required for this effect, as transfecting breast cancer cells with wildtype but not a Cas-binding mutant of BCAR3 increased levels of Src pY416 [59]. These studies suggest a model in which BCAR3 regulates cell motility by promoting tyrosine phosphorylation of Cas and Cas downstream signaling (Figure 1.3).

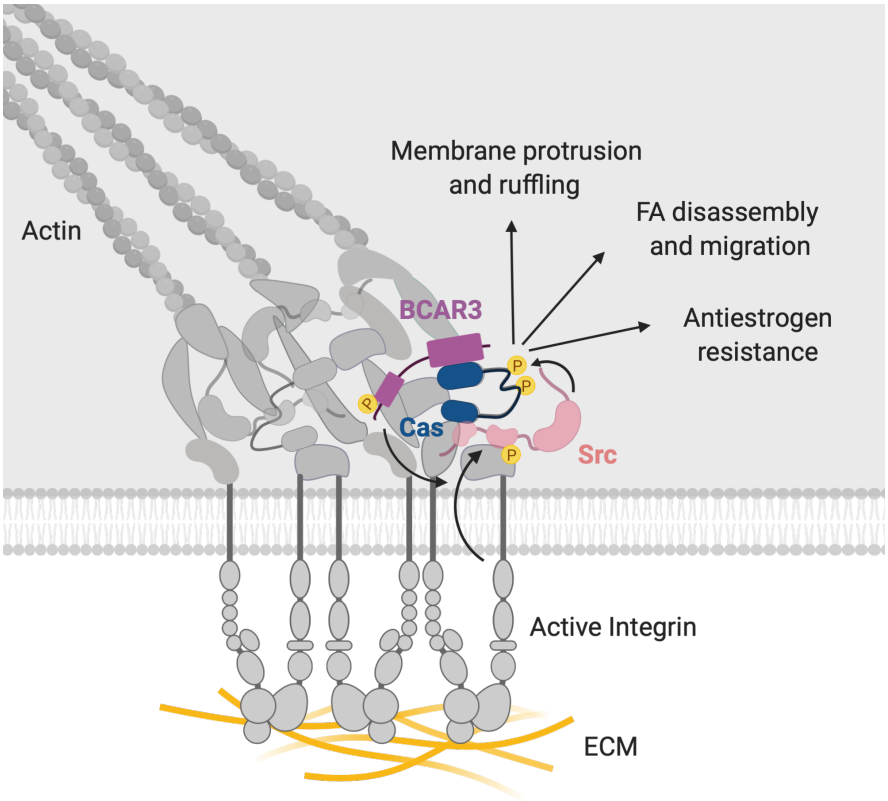

Figure 1.3 BCAR3-Cas form a signaling node in adhesions. BCAR3 association with Cas is required for efficient activation of Src kinase and Src-mediated tyrosine phosphorylation of Cas in the Cas central domain. BCAR3-Cas binding is also required for mechanisms downstream of pY-Cas, including membrane ruffling through activation of Rac1, FA disassembly, migration and antiestrogen resistance. Figure created with BioRender.com.

Experiments using the mutant BCAR3 that cannot bind Cas have shown that most functions of BCAR3 previously identified require BCAR3-Cas association. BCAR3-Cas association is required to induce membrane ruffling, for efficient FA disassembly, migration, BCAR3-mediated

Cas phosphorylation and Src kinase activity, antiestrogen resistance, and BCAR3-mediated activation of Rac1 [46, 59] (Figure 1.3). Because BCAR3 binding to Cas is required for the known functions of BCAR3, questions are raised about whether BCAR3 has any Cas-independent functions or if the only function of BCAR3 is to promote Cas signaling.

1.3.5 *Regulation of BCAR3*

While the roles of BCAR3 in regulating cell motility and Cas signaling have been well studied, how BCAR3 itself is regulated is not well understood.

Little is known about how BCAR3 is phosphorylated or which sites regulate its signaling or bind to other proteins. Preliminary experiments in fibroblasts demonstrated that AND-34 can be tyrosine phosphorylated in response to adhesion to serum growth factors or adhesion to matrix protein [60]. However, no work has identified specific phosphorylated residues or detailed their roles in different signaling pathways or the upstream stimuli. We know from large mass spectrometry screens that BCAR3 is phosphorylated in many cancers and cell types [49, 61], but detailed mechanistic studies have not been conducted. The role of BCAR3 phosphorylation in its regulation and signaling is of active interest.

Thus far, only one direct mechanism of regulation of BCAR3 has been identified and detailed. BCAR3 can be inhibited by TGFβ through proteasomal degradation. As BCAR3 inhibits Smad-dependent cell migration in breast cancer cells, this regulation of BCAR3 is part of a positive feedback loop [48]. Further investigation is required to understand other mechanisms of BCAR3 regulation.

1.3.6 *BCAR3 in growth factor signaling*

There is evidence that several of the downstream roles of BCAR3 are stimulated upstream by different growth factors. For example, BCAR3 works within insulin signaling. Membrane ruffling stimulated by insulin requires BCAR3 [62], although the mechanism through which BCAR3 promotes membrane ruffling is unknown. In addition to insulin signaling, there is evidence that BCAR3 works downstream of EGF stimulation. BCAR3 is required for the actin cytoskeletal remodeling that follows EGF stimulation in breast cancer cells [54] and EGF-stimulated

membrane ruffling and dissolution of stress fibers [45]. Depletion of BCAR3 disrupts the ability of breast cancer cells to sense their environment, as knocking down BCAR3 inhibits migration of breast cancer cells toward EGF [45]. Additionally, knocking down BCAR3 decreases EGF-dependent Cas tyrosine phosphorylation [45]. Given that BCAR3 can bind the EGF receptor through its SH2 domain [50, 51], it is not surprising that BCAR3 can work downstream of EGF stimulation to regulate migration and actin remodeling. While these studies provide preliminary evidence that BCAR3 and some of its roles are regulated by EGF, there are still a lot of mechanistic questions to be addressed. BCAR3 binding to EGFR has not been widely documented like BCAR3-Cas binding. Additionally, specific residues in BCAR3 that are phosphorylated following EGF stimulation, nor the kinse(s) that directly phosphorylate BCAR3, have not been identified.

1.4 CRL5-SOCS E3 LIGASE

A major mechanism of negative regulation of cellular protein is ubiquitin-mediated proteasomal degradation. In contrast to quickly reversible phosphorylation by protein phosphatases, ubiquitination, while also reversible by deubiquitinating enzymes, often results in irreversible degradation of the targeted protein [63, 64]. Thus, a signal can be limited or silenced for a period of time as the pool of protein is depleted before the being activated again.

Ubiquitination occurs primarily on the side chain ε-amino groups of lysine residues and is added by a three step enzyme cascade that requires ubiquitin activating, conjugating and ligase enzymes. First, ATP is used to add ubiquitin to a cysteine residue on a ubiquitin-activating enzyme (E1). Next, the ubiquitin is transferred from the charged E1 to a cysteine residue on an ubiquitin-conjugating enzyme (E2). In the last step, a ubiquitin-ligase (E3) that is bound to a substrate is bound by the charged E2 [65-67]. Importantly, specificity is conferred through the E3 ligases, which recognize and bind specific target proteins. Many E3 ligases are members of the really interesting new gene (RING) family of E3 ubiquitin ligases, which facilitate the transfer of ubiquitin directly from the E2 to the substrate [68]. Lysine residues of substrates can be modified by one ubiquitin (monoubiquitination) or additional ubiquitin molecules can be added to the seven lysine residues in ubiquitin to form a chain (polyubiquitination) [69]. The type of ubiquitin linkage directs the downstream function of the modification, although not all of the linkage-specific

functions are well worked out. It is well established that K11-linked and K48-linked polyubiquitin chains target the substrate for degradation by the 26S proteasome [70, 71].

1.4.1 *CRL5-SOCS E3 ubiquitin ligase*

To date, there are only two families of E3 ubiquitin ligases that ubiquitinate tyrosine phosphorylated proteins, the Cbl family comprising Cbl/Cbl-b/Cbl-c, and the family of cullin-RING-ligase 5 (CRL5) complexes with substrate adaptors from the suppressor of cytokine signaling (SOCS) family [72]. Here I focus on CRL5-SOCS E3 ligases. Cullin-RING-ligases are multi-subunit E3 ubiquitin ligases. The scaffold protein that forms the backbone of the complex is the cullin protein. A RING protein, either Rbx1 or Rbx2, that binds a ubiquitin-charged E2 protein binds to one end of the cullin scaffold while substrate receptor proteins bind the other end. CRLs are activated when a ubiquitin-like protein, Nedd8, is transferred to the complex. CRL E3 ubiquitin ligases include CRL1, CRL2, CRL3, CRL4A, CRL4B, and CRL5 [73, 74].

CRL5 recruits SOCS box domain-containing substrate adaptor proteins through Elongin B/C, which links Cul5 to the substrate-bound adaptor. Nine different families comprising more than forty proteins have a SOCS box, each family targeting substrates using different binding motifs and domains. One such family is the SOCS family, of which there are eight members, SOCS1-7 and CisH. Each SOCS protein has an SH2 domain that binds to phosphorylated tyrosine residues and an N-terminal region with variable sequence and unknown structure [75]. While SOCS receptors could bind substrates through the N-terminus, there are many examples of SOCS proteins binding to substrates through their SH2 domain. Thus, CRL5-SOCS E3 ligases can specifically target phosphorylated substrates for degradation.

1.4.2 *CRL5 inhibits cell transformation*

Work from our lab shows that CRL5 inhibits transformation in normal mammary epithelial cells, as depleting Cul5 stimulates EGF-independent growth, migration and membrane ruffling. CRL5 function with SOCS2, SOCS4, SOCS5, and SOCS6 to inhibit these processes, as knocking down these four SOCS in combination recapitulates the increase in migration and EGF-independent growth we observed when Cul5 alone is knocked down [76]. CRL5 inhibits migration not only of

epithelial cells, but also of neurons in the developing brain [77]. In addition to suppressing transformation of MCF10A cells, CRL5 also regulates Src family kinase activity in both MCF10A cells and mouse embryonic fibroblasts (MEFs) [76, 78]. Knocking down Cul5 in MCF10A cells increases Src activity [76] and knocking down Cul5 in MEFs increases levels of activated, but not inactivated, Src protein [78]. The increased Src activity in Cul5-deficient MCF10A cells is required for the transformed phenotypes [76].

Our work suggests that CRL5 with SOCS2, SOCS4, SOCS5, and SOCS6 inhibits epithelial cell transformation by regulating the turnover of pY-proteins [76]. Cas turnover is regulated by CRL5-SOCS6. SOCS6 specifically targets pY-Cas in FAs at the leading edge of migrating cells to regulate FA turnover and membrane ruffling [76, 79]. We are interested in identifying substrates of these SOCS proteins that regulate Cul5-mediated phenotypes in MCF10A cells.

This dissertation provides a detailed study of a novel CRL5-SOCS substrate, BCAR3, and the first identification of a biological role for a specific site of phosphorylation in BCAR3. This study provides new insight into Cas phosphorylation and activity at the leading edge of migrating cells. Additionally, I investigate how focal adhesion structure is maintained over time.

Chapter 2. A REGULATORY CIRCUIT AT THE LEADING EDGE OF MIGRATING CELLS

2.1 INTRODUCTION

Cell motility is an essential component in processes such as embryogenesis, tissue repair and cancer metastasis. Migrating cells must push through densely packed extracellular matrix (ECM), which cells bind through transmembrane receptors called integrins. At the cell front, integrin ligation induces transient clusters of activated integrins, called focal complexes (FXs), stimulates Src-family protein-tyrosine kinases (SFKs) and Rac1 GTP loading, and induces actin polymerization, which pushes the leading edge forwards, manifested in two-dimensional culture as membrane ruffles or lamellipodia [11, 12, 80, 81]. Rearward flowing actin interacts with proteins associated with the activated integrin tails, including talin and vinculin, deforming those proteins, opening binding sites for additional cytoskeletal proteins, and activating focal adhesion kinase (FAK) and Rho [13, 14, 82-84]. Together, the physical forces and biochemical activities of Src, FAK and GTPases combine to stabilize and grow clusters of integrins and many different structural signaling and adaptor proteins to form focal adhesions (FAs) that anchor actin stress fibers. Myosin motors generate force on the stress fibers and behind the nucleus to move the cell body forwards, disassembling the FAs under the cell body. In this model of cell migration, integrins and their associated FX and FA complexes in distinct parts of the migrating cell must be differentially regulated, highlighting the importance of regulating each adhesion component properly.

The activities of SFKs and FAK are critical transducers of integrin signals. These kinases phosphorylate several FX and FA proteins, which regulate assembly and disassembly of adhesion complexes. Loss of FAK inhibits FA turnover [27]. Specifically, FAK phosphorylation at Y397 and Y576 is required for FA disassembly and mutating these sites stabilizes adhesions and alters association/dissociation of FAK with adhesions [28, 29]. Src kinase activity is required for efficient FA disassembly, as expression of a non-enzymatic mutant of Src or treatment with a Src inhibitor decreased disassembly rate [29]. SFK Fyn is important for leading edge movement and is activated by a protein tyrosine phosphatase, RPTPA [85, 86]. Src substrate and FA adaptor

proteins p130Cas (Cas) and paxillin are tyrosine-phosphorylated in response to adhesion, which provide binding sites for adaptor protein Crk, activate GTPases, stimulate membrane ruffling and increase FA disassembly [29, 35, 42, 43, 87-89].

Adaptor molecule Breast Cancer Antiestrogen Resistance 3 (BCAR3; AND-34; NSP2) forms an important signaling node with Cas (BCAR1), whose tyrosine phosphorylation has been shown to regulate FA disassembly and migration [45, 52, 58, 59]. BCAR3-Cas association increases Src kinase activity, Src-Cas association and Cas tyrosine phosphorylation by Src [56]. BCAR3 was first identified in a screen to identify genes that confer antiestrogen resistance when overexpressed [44]. Like other members of the novel SH2-domain containing protein family (NSP), BCAR3 contains an N-terminal SH2 domain and a C-terminal non-enzymatic GEF-like domain that shares homology to the family of Cdc25 Ras GEFs [37]. This C-terminal domain of BCAR3 binds the C-terminal focal adhesion targeting (FAT) domain of Cas [53].

Studies using breast cancer cell lines have shown that BCAR3-Cas interaction is required for efficient migration and invasion of breast cancer cells [46, 54]. Additionally, high levels of BCAR3 protein are associated with aggressive breast cancer phenotypes. Overexpression of BCAR3 in non-metastatic breast cancer lines increased migration and invasion [45]. While in vitro experiments using cell lines suggest that BCAR3 promotes FA disassembly, migration and invasion, patient data suggests that BCAR3 expression correlates with favorable outcomes in several diseases, including breast cancer and multiple myeloma [47, 48]. These studies do not identify any form of BCAR3 regulation, which could provide important insight that resolves these seemingly contradictory findings. Therefore, further investigation of BCAR3 is needed to understand its role in different mechanisms of migration, invasion and disease progression.

While BCAR3 has been studied in the context of cell motility and its role in promoting Cas signaling, little is known about how BCAR3 is regulated and how it contributes to these broader signaling pathways. An early study showed that tyrosine phosphorylation of AND-34 (another name for BCAR3) in 3T3 cells can be stimulated by serum and adhesion to fibronectin, although specific sites of phosphorylation were not investigated [60]. In breast cancer cell lines, stimulation with TGFß decreases BCAR3 protein levels dependent on the proteasome, but the study did not

provide a specific mechanism of BCAR3 regulation [48]. Therefore, there is still much to be learned about mechanisms of BCAR3 phosphorylation and the signaling that regulates it.

We became interested in BCAR3 while studying the role of a multi-subunit cullin-RING-ligase (CRL), CRL5, in inhibiting epithelial cell transformation. Previous work from our group showed that disrupting CRL5 function stimulates growth factor-independent growth, migration, membrane ruffling, and formation of transformed acini in a normal mammary cell line [76]. Our work suggests that CRL5 suppresses epithelial cell transformation through several pathways by regulating the turnover of different proteins involved in migratory phenotypes. In a previous study, we found that Cas turnover is regulated by CRL5 and CRL5 adaptor protein, SOCS6. SH2 domain-containing SOCS6 targets tyrosine phosphorylated (pY) Cas in FAs at the leading edge of the cell but not the rear. This regulates FA assembly and disassembly and leading edge ruffling [76, 79].

BCAR3 was identified in a screen to identify additional substrates of CRL5 that may contribute to the cellular transformation observed in the absence of functional CRL5 [90]. Using phosphoproteomics, we identified two BCAR3 phosphopeptides that are increased in cells without functional CRL5, suggesting that BCAR3 may be a substrate of CRL5. Here we provide evidence that pY-BCAR3 turnover is directly regulated by CRL5-SOCS6 and that phosphorylation is also needed for BCAR3 to function in membrane dynamics and cell migration.

2.2 RESULTS

2.2.1 *BCAR3 is a substrate of CRL5*

Previous work in the lab has focused on identifying substrates of the E3 ubiquitin ligase, CRL5. We conducted a phosphoproteomic screen to identify phosphopeptides that are increased in Cul5-deficient MCF10A cells. BCAR3 pY117 and pY266 were increased in Cul5-deficient cells relative to control cells, suggesting BCAR3 phosphorylation or protein abundance is negatively regulated by CRL5 [90].

Having identified BCAR3 as a possible substrate of CRL5, I set out to validate that CRL5 directly regulates BCAR3. The experimental setup of the phosphoproteomic screen introduces several

possible explanations for the increase in BCAR3 phosphopeptides in the absence of Cul5 other than CRL5 directly regulating BCAR3. One possibility is that knocking down Cul5 increases kinase activity in the cells, resulting in increased pY independent of direct ligase activity. In fact, we have published evidence that knocking down Cul5 consistently increases Src activity, which was identified by measuring levels of autophosphorylation at Y416 [76, 78]. Therefore, increased Src kinase activity could be causing the increase in BCAR3 phosphopeptides rather than a lack of CRL5-mediated BCAR3 turnover.

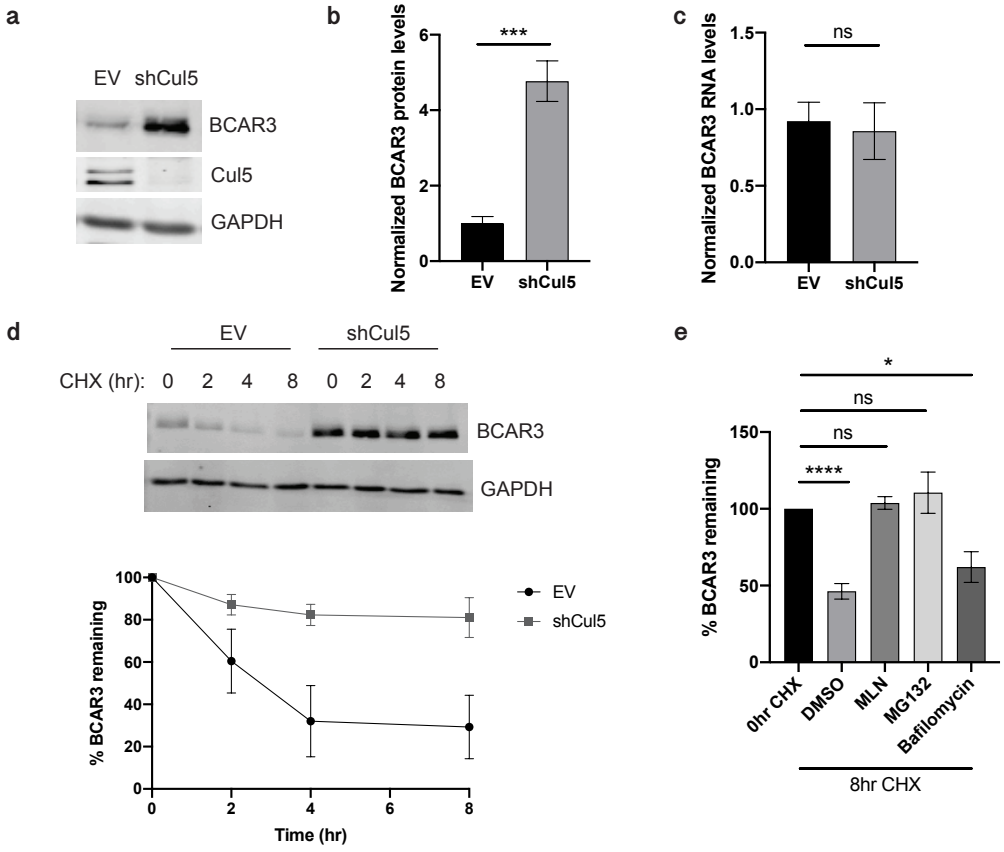

Figure 2.1. BCAR3 protein level and stability are increased in Cul5-deficient cells. (a) Western blot and (b) quantification of BCAR3 protein levels in MCF10A EV and shCul5 cells. GAPDH used as a loading control. Student's t-test: $p < 0.001$, n=3. (c) qPCR was used to identify RNA levels of BCAR3 in EV and shCul5 cells. Student's t-test: $p > 0.05$, n=3. (d) MCF10A control and Cul5-deficient cells were treated with cycloheximide (CHX) for 0, 2, 4, and 8 hours. Upper and lower panels show a representative Western blot and quantification of 3 independent experiments. (e) MCF10A cells were treated with CHX for 8 hours and either MLN4924 (cullin neddylation inhibitor), MG132 (proteasome inhibitor) or bafilomycin A1 (lysosome inhibitor). One-way ANOVA: *$p < 0.05$; ****$p < 0.0001$.

To test whether BCAR3 protein levels are regulated by CRL5, I used RNA interference to knockdown Cul5 in MCF10A cells, as previously described [76], and monitored BCAR3 protein abundance using Western blotting (Figure 2.1a,b). I found that BCAR3 protein is increased in Cul5-deficient cells. The increase in BCAR3 protein levels when Cul5 is knocked down could be a result of increased transcription under these conditions. However, BCAR3 RNA levels measured by qPCR were unchanged in Cul5-deficient cells relative to control cells (Figure 2.1c). These results suggest that CRL5 regulates BCAR3 protein post-transcriptionally.

Having determined that CRL5 regulates BCAR3 protein but not RNA levels, we tested whether CRL5 regulates BCAR3 protein stability. We hypothesized that inhibiting ligase activity of CRL5 would stabilize BCAR3 since it could not be ubiquitinated by CRL5 and targeted for proteasomal degradation. BCAR3 turnover was measured using a cycloheximide chase assay, where new protein synthesis is inhibited by cycloheximide and the remaining pool of cellular proteins is degraded over time. Over an 8 hour time course, BCAR3 is more stable in Cul5-deficient cells than in control cells (Figure 2.1d). Since many biological assays utilized in the lab are done in a low serum, EGF-free assay media, I also measured BCAR3 stability in assay media and found that BCAR3 is stabilized in Cul5-deficient cells under these conditions as well (Supplement Figure 1). Additionally, BCAR3 turnover was inhibited by MLN4924, a cullin neddylation inhibitor, suggesting that a functional cullin RING ligase is required for BCAR3 turnover (Figure 2.1e). Inhibition of BCAR3 turnover by MG132, a proteasomal inhibitor, and not bafilomycin, a lysosomal inhibitor (Figure 2.1e), suggests that BCAR3 is targeted for proteasomal degradation.

Taken together, these data are consistent with the hypothesis that BCAR3 is targeted for proteasomal degradation by CRL5.

2.2.2 *pY-BCAR3 binds and is regulated by SOCS6, independent of Cas*

CRL5 can bind targets through eight different pY-dependent SOCS proteins or many alternative pY-independent adaptors. In order to test whether a member of the SOCS protein family could bind BCAR3, I transiently expressed T7-tagged SOCS proteins in HeLa cells and immunoprecipitated after treatment with pervanadate, which inhibits pY phosphatases. Western

blots for endogenous BCAR3 show BCAR3 is specifically co-immunoprecipitated with SOCS6 and no other SOCS protein (Figure 2.2a). As expected, Cas also bound specifically to SOCS6 (Figure 2.2a) [76]. To test whether BCAR3 degradation is mediated by SOCS6, I transiently knocked down SOCS6 in MCF10A cells with siRNA and observed an increase in BCAR3 protein level similar to the increase observed when Cul5 is knocked down (Figure 2.2b). Additionally, cycloheximide chase experiments in SOCS6-deficient cells demonstrate that BCAR3 is more stable in the absence of SOCS6 (Figure 2.2c). Collectively, these experiments suggest that CRL5-dependent turnover of BCAR3 is mediated by SOCS6.

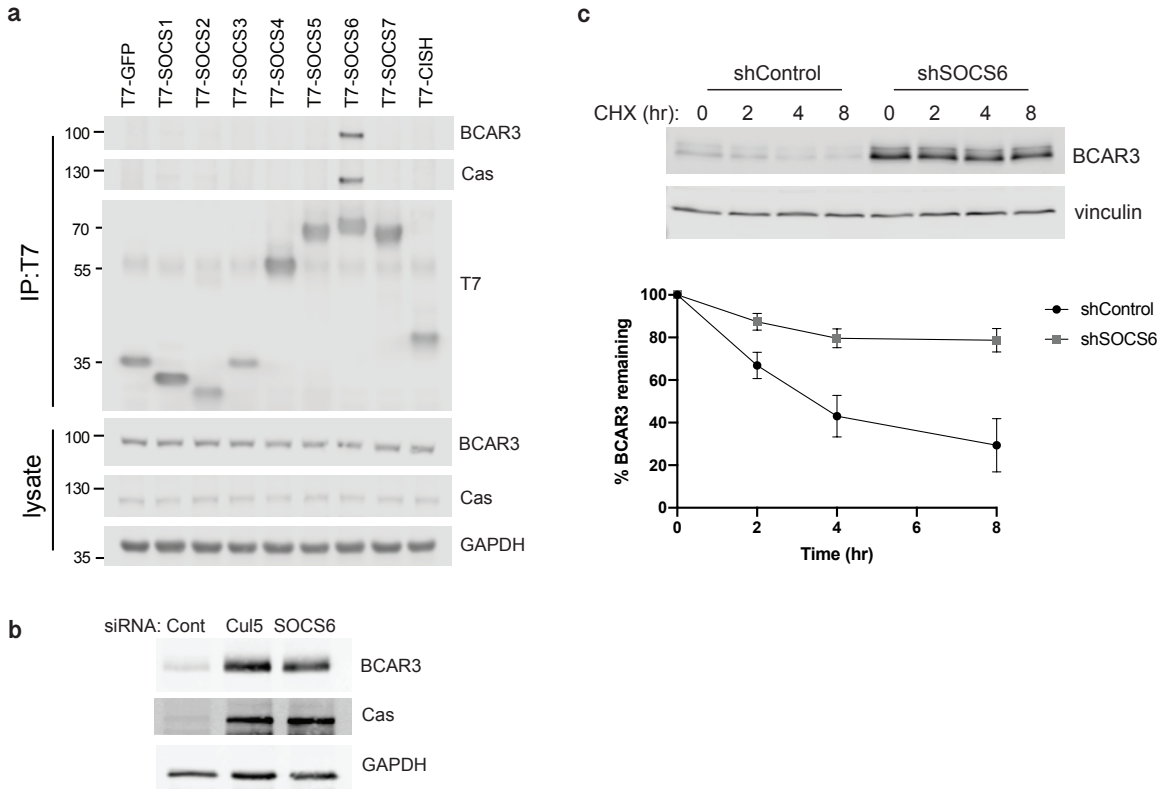

Figure 2.2. SOCS6 binds and regulates the turnover of BCAR3. (a) HeLa cells were transfected with control vector or T7-tagged SOCS proteins. The transfected cells were treated with pervanadate and lysed. Lysates were immunoprecipitated with anti-T7 antibody and immunoblotted with anti-BCAR3 and anti-Cas. (b) MCF10A cells were transfected with control siRNA or siRNA against Cul5 or SOCS6 and lysed for Western blotting. (c) MCF10A control and SOCS6-deficient cells were treated with cycloheximide (CHX) for 0, 2, 4, and 8 hours. Upper and lower panels show a representative Western blot and quantification of 3 independent experiments.

Regulation of BCAR3 by CRL5-SOCS6 is not unique to MCF10A cells. Knocking down Cul5 and SOCS6 in U2OS cells significantly increases levels of BCAR3 protein, in both growth media and EGF-free assay media. However, BCAR3 is not regulated by CRL5-SOCS6 in HeLa cells, as knocking down Cul5 or SOCS6 does not increase BCAR3 protein levels. In contrast, Cas protein levels are increased following knock down of Cul5 or SOCS6 in HeLa cells, suggesting that BCAR3 and Cas turnover occurs by distinct mechanisms (Supplement Figure 2).

The interaction between BCAR3 and SOCS6 is particularly interesting for several reasons. First, we have previously documented a role of CRL5-SOCS6 in inhibiting pY-Cas to regulate membrane ruffling [76]. Cas is a focal adhesion protein, like BCAR3, and has been extensively studied for its role as a scaffolding and signaling protein in focal adhesions [35, 41, 91-94]. Second, BCAR3 and Cas are binding partners and form a signaling node [46, 53, 60, 95]. Since both BCAR3 and Cas are bound by and regulated by SOCS6, co-localize in focal adhesions [45, 46] and co-immunoprecipitate with each other in several cell types [46, 59], my data are consistent with several possible mechanisms of regulation (Figure 2.3a). One possibility is that SOCS6 binds directly to BCAR3 and binds Cas separately. Alternatively, SOCS6 could bind BCAR3 indirectly through its interaction with Cas. A third possibility is that SOCS6 binds Cas indirectly through BCAR3. A model in which Cas is bound directly by SOCS6 is preferred, as we identified pY664 as a binding site for SOCS6 in Cas [76].

To determine whether Cas mediates BCAR3-SOCS6 interaction, I employed several different strategies. First, I used a mutant of BCAR3 that cannot bind to Cas to determine if BCAR3 can still interact with SOCS6 when the BCAR3-Cas association is broken. This mutant of BCAR3, BCAR3 EE, was identified by another group [59] and has two point mutations, L744E and R748E, that prevent binding to Cas. I confirmed that BCAR3 EE does not bind Cas by immunoprecipitating SNAP-V5-BCAR3 WT and EE and probing Cas (Figure 2.3b). Despite not binding to Cas, BCAR3 EE can still bind to SOCS6 (Figure 2.3b), suggesting that Cas is not required for that interaction. Second, I tested whether BCAR3-SOCS6 association remains intact when Cas is knocked down. I transfected HeLa cells with 3xFlag-mBCAR3 and T7-SOCS6 following treatment with either control siRNA or siRNA against Cas. The results showed that

BCAR3 binds SOCS6 when Cas is knocked down (Figure 2.3c). Collectively, these data suggest that BCAR3-SOCS6 binding is independent of BCAR3 binding to Cas.

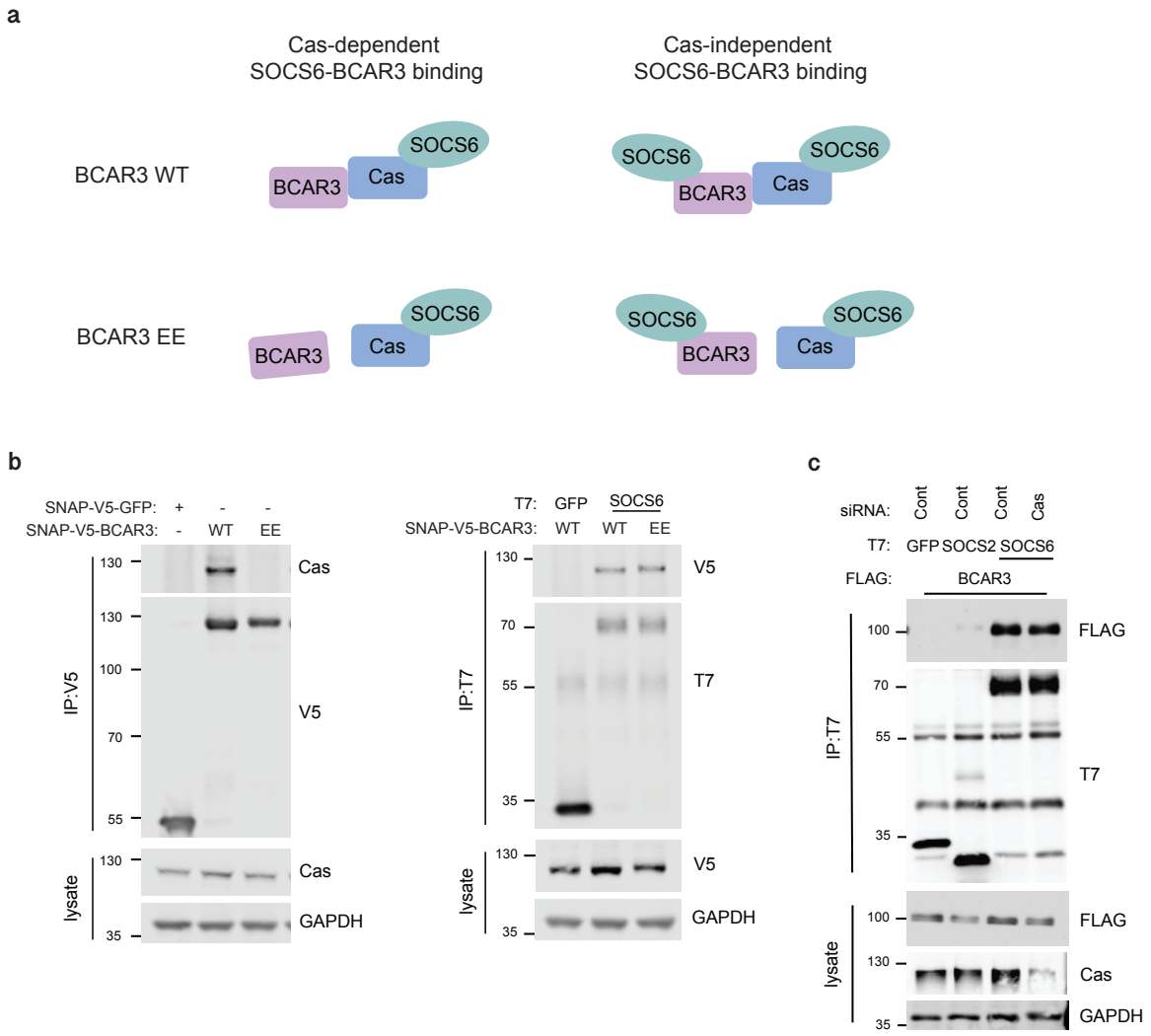

Figure 2.3. BCAR3-SOCS6 binding is independent of BCAR3 binding to Cas. (a) Diagram of possible SOCS6, BCAR3, and Cas binding. (b) HeLa cells were transfected with control vector, SNAP-V5-BCAR3 WT or SNAP-V5-BCAR3 EE and lysed. Lysates were immunoprecipitated with anti-V5 antibody and immunoblotted with anti-Cas. HeLa cells were transfected with control vector or T7-SOCS6 and SNAP-V5-BCAR3 WT or SNAP-V5-BCAR3 EE. The transfected cells were treated with pervanadate and lysed. Lysates were immunoprecipitated with anti-T7 antibody and immunoblotted with anti-V5. (c) HeLa cells were treated with siRNA against Cas or control siRNA and transfected with T7-SOCS6 and 3xFLAG-BCAR3. Lysates were immunoprecipitated with anti-T7 antibody and immunoblotted with anti-FLAG and anti-Cas.

2.2.3 *BCAR3-SOCS6 binding and BCAR3 turnover require pY*

Both SOCS6 and BCAR3 contain SH2 domains, so their binding could be mediated by pY-SH2 domain interaction. In support of this possibility, I found that treatment with pervanadate, which inhibits phosphotyrosine phosphatases, increases BCAR3-SOCS6 association (Figure 2.4a). This result suggests that increasing tyrosine phosphorylation increases binding of SOCS6 to BCAR3, with either SOCS6 SH2 binding pY-BCAR3 or BCAR3 SH2 binding pY-SOCS6. To determine if pY-BCAR3 is bound by the SOCS6 SH2 domain, I tested the effect of disrupting the SOCS6 SH2 domain by deletion (ΔC) or point mutation (R407K) on binding to BCAR3 (Figure 2.4b). The results showed that neither T7-SOCS6 ΔC nor R407K can bind to endogenous BCAR3 (Figure 2.4c), suggesting that BCAR3-SOCS6 association requires a functional SOCS6 SH2 domain. Collectively, these data suggest that pY-BCAR3 is bound by the SOCS6 SH2 domain.

To determine which BCAR3 tyrosine site is required for SOCS6 binding, we identified known sites of BCAR3 tyrosine phosphorylation through PhosphoSite, which compiles protein phosphorylation information from high and low throughput sources of data [61]. According to PhosphoSite, mouse and human BCAR3 Y42, Y117, Y212, Y266 and Y429 were phosphorylated in at least 25 screens [61]. I tested whether one of these residues may be required for SOCS6 binding to BCAR3 by mutating all 5 tyrosine residues to phenylalanine (BCAR3 F5), which cannot be phosphorylated (Figure 2.4d). Using co-immunoprecipitation, I found that BCAR3 F5 has significantly reduced binding to SOCS6 compared to wildtype BCAR3 (Figure 2.4e), suggesting that one or more of those sites is required for efficient BCAR3-SOCS6 binding. When I mutated each tyrosine to phenylalanine individually (Figure 2.4d), I found that only Y117 is necessary for BCAR3 association with SOCS6 (Figure 2.4e). Mutating the F117 residue in the F5 mutant back to a tyrosine (BCAR3 F4, Figure 2.4d) rescued BCAR3 binding to SOCS6 (Figure 2.4f), demonstrating that Y117 is sufficient for BCAR3-SOCS6 association. These data support a model in which BCAR3 is phosphorylated at Y117 and bound at this site by SOCS6 through its SH2 domain.

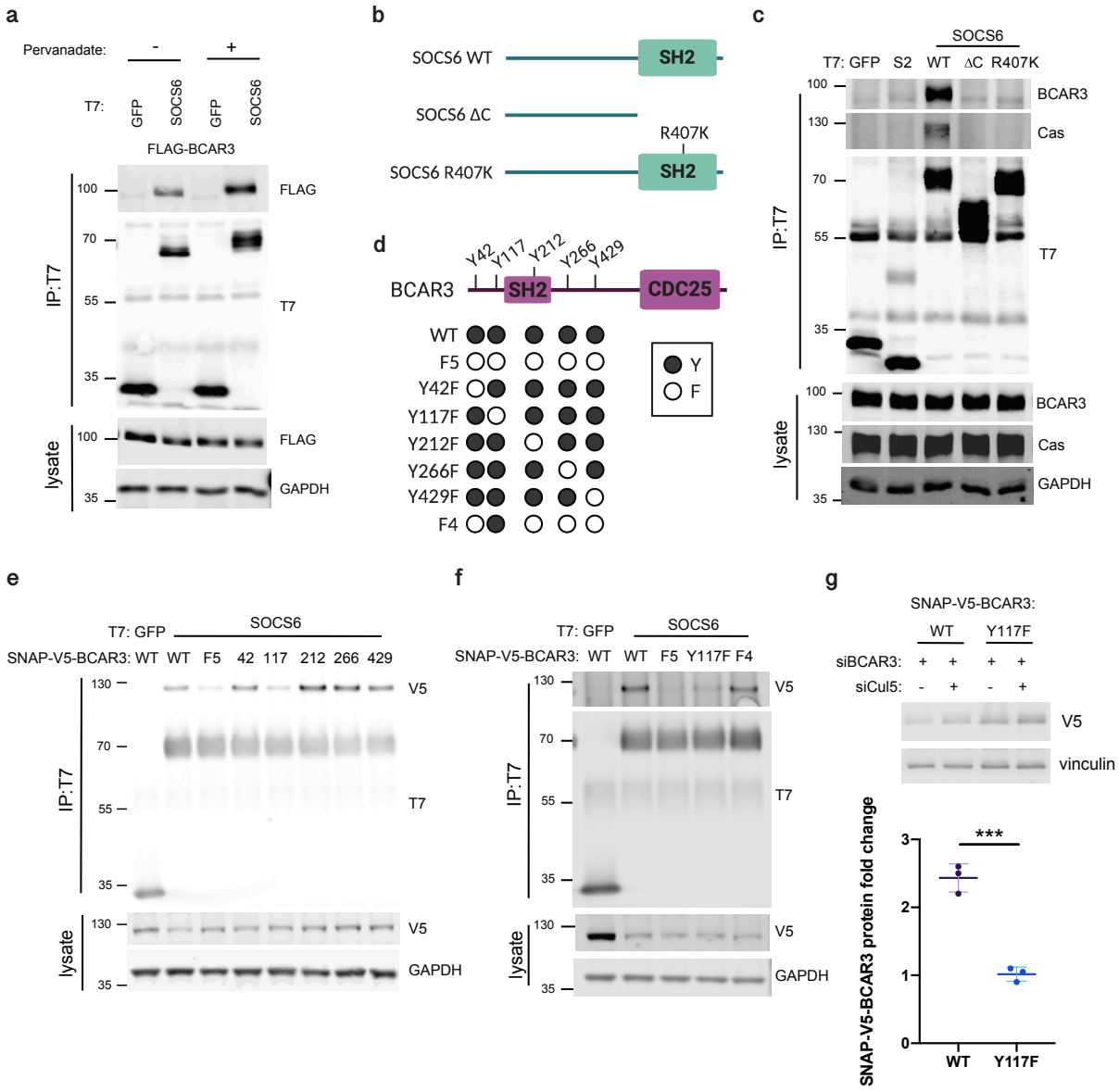

Figure 2.4. BCAR3-SOCS6 binding and BCAR3 turnover require pY. (a) HeLa cells were transfected with T7-GFP or T7-SOCS6 and 3xFLAG-BCAR3 and treated with pervanadate or vehicle. Lysates were immunoprecipitated with anti-T7 antibody. (b) Schematic of SOCS6 WT, ΔC, and R407K mutants. (c) HeLa cells were transfected with control vector and T7-tagged SOCS constructs, treated with pervanadate and lysed. Cell lysates were immunoprecipitated with anti-T7 antibody and immunoblotted with anti-BCAR3. (d) Schematic of BCAR3 WT and BCAR3 mutants. Tyrosine residues Y42, Y117, Y212, Y266 and Y429 were identified through PhosphoSite as sites that are phosphorylated across a range of tissues and cellular conditions. (e) HeLa cells were transfected with T7-GFP or T7-SOCS6 and V5-BCAR3 WT or tyrosine point mutants. Transfected cells were treated with pervanadate and lysed. Lysates were immunoprecipitated with anti-T7 antibody and immunoblotted with anti-V5. (f) HeLa cells were transfected with T7-GFP or T7-SOCS6 and V5-BCAR3 WT or tyrosine point

mutants. Transfected cells were treated with pervanadate and lysed. Lysates were immunoprecipitated with anti-T7 antibody and immunoblotted with anti-V5. (g) Dox-inducible MCF10A cell lines that express SNAP-V5-BCAR3 WT and Y117F when treated with doxycycline were transfected with siRNA against BCAR3 to knockdown endogenous BCAR3 and control siRNA or siRNA against Cul5, treated with dox and lysed. Western blots were probed with anti-V5 and anti-vinculin. SNAP-V5-BCAR3 levels were quantified from the Western blots, normalized to levels of vinculin, and use to calculate a fold change in BCAR3 protein levels in Cul5-deficient cells divided by levels in Cul5-containing cells. Student's t-test: ***p = 0.0005, n=3.

Because I found that BCAR3 pY117 is necessary for SOCS6 binding in HeLa cells (Figure 2.4e) and I also found that BCAR3 is not regulated by CRL5-SOCS6 in HeLa cells (Supplement Figure 2), I wanted to confirm that BCAR3 is phosphorylated at Y117 in HeLa cells. Further, as I previously found that increasing cellular pY by treating cells with pervanadate increases BCAR3-SOCS6 association (Figure 2.4a), I also wanted to determine whether treatment with pervanadate increases pY117. In collaboration with Ho-Tak Lau and Shao-En Ong at the University of Washington, I used phosphopeptide-mass spectrometry to identify phosphorylation of SNAP-V5-BCAR3 in HeLa cells. Specifically, I transiently transfected SNAP-V5-BCAR3 into HeLa cells, treated with pervanadate for 30 minutes and lysed cells for immunoprecipitation with V5 antibody. Immunoprecipitated samples were run on a gel and stained with SimplySafe blue stain (Supplement Figure 3a). Western blotting of the samples shows an increase in pY after pervanadate treatment, identified by probing with anti-pY monoclonal 4G10 (Supplement Figure 3b). The SNAP-V5-BCAR3-containing bands were cut from the gel and analyzed using phosphopeptide-mass spectrometry. Phosphorylation of BCAR3 at Y117 in HeLa cells was detected with and without pervanadate treatment and treatment with pervanadate dramatically increases pY117 (Supplement Figure 3c). This result is consistent with my biochemistry data in Figure 2.4. While no additional tyrosine residues were detectably phosphorylated in the absence of pervanadate, BCAR3 pY42, pY266 and pY341 were detected in the pervanadate-treated sample (Supplement Figure 3d). Further attempts to identify physiological stimuli that would increase BCAR3 phosphorylation in MCF10A cells in the absence of pervanadate using this method were unfortunately unsuccessful. I also attempted, but was unable, to generate phosphopeptide antibodies that could detect BCAR3 pY117 by Western blotting.

Because BCAR3 Y117F cannot be bound by SOCS6, I hypothesized that the stability of BCAR3 Y117F would not be regulated by Cul5. I tested this hypothesis by knocking down Cul5 in MCF10A cells expressing either SNAP-V5-BCAR3 WT or Y117F. Knocking down Cul5 increased levels of BCAR3 WT, but not Y117F (Figure 2.4g), confirming that BCAR3 Y117F is not regulated by CRL5.

2.2.4 *BCAR3 regulates single-cell migration, invasion and collective migration*

To test whether BCAR3 regulates migration of normal epithelial cells, as reported for breast cancer cells and mouse fibroblasts [45, 46, 52, 58], I used siRNA to knock down BCAR3 in MCF10A cells and assayed single-cell migration and invasion into Matrigel using modified Boyden chambers, with EGF as a chemoattractant (Figure 2.5b,c). BCAR3 was needed for single-cell migration and invasion in these assays. Depleting cells of Cul5 increased single-cell migration, as reported previously [76], but had little effect on Matrigel invasion towards EGF, consistent with the non-invasive morphology of Cul5-depleted MCF10A cell acini cultured in Matrigel [76]. BCAR3 was required for the migration and invasion of Cul5-containing and Cul5-depleted cells (Figure 2.5b,c), suggesting that BCAR3 regulates single-cell migration and invasion in a Cul5-independent mechanism. BCAR3 was also required for migration and invasion of MCF10A cell clones in which the *bcar3* gene was disrupted using Crispr/Cas9 technology (Supplement Figure 4). Thus, BCAR3 is important for individual cell migration and invasion towards EGF regardless of Cul5 activity.

In contrast, when I measured collective migration of MCF10As in a scratch-wound assay in the absence of EGF, I found that BCAR3 was only required for migration when Cul5 was absent (Figure 2.5d). This epistatic relationship is consistent with CRL5 targeting BCAR3 for degradation to suppress BCAR3-dependent migration. EGF overcomes this regulation, presumably by stimulating parallel mechanisms (see below, Figure2.7e, left, for a diagram). Inspection of the wound edge revealed that BCAR3 is also needed for the increased membrane ruffling and lamellipodium length of Cul5-depleted cells (Figure 2.5e-g). Thus, BCAR3 is necessary for increased membrane ruffling, lamellipodia length, and migration of Cul5-deficient cells when EGF

is absent. However, these results do not show whether increased levels of BCAR3 are sufficient to stimulate these events, as other CRL5-regulated proteins, such as Cas, may also be necessary.

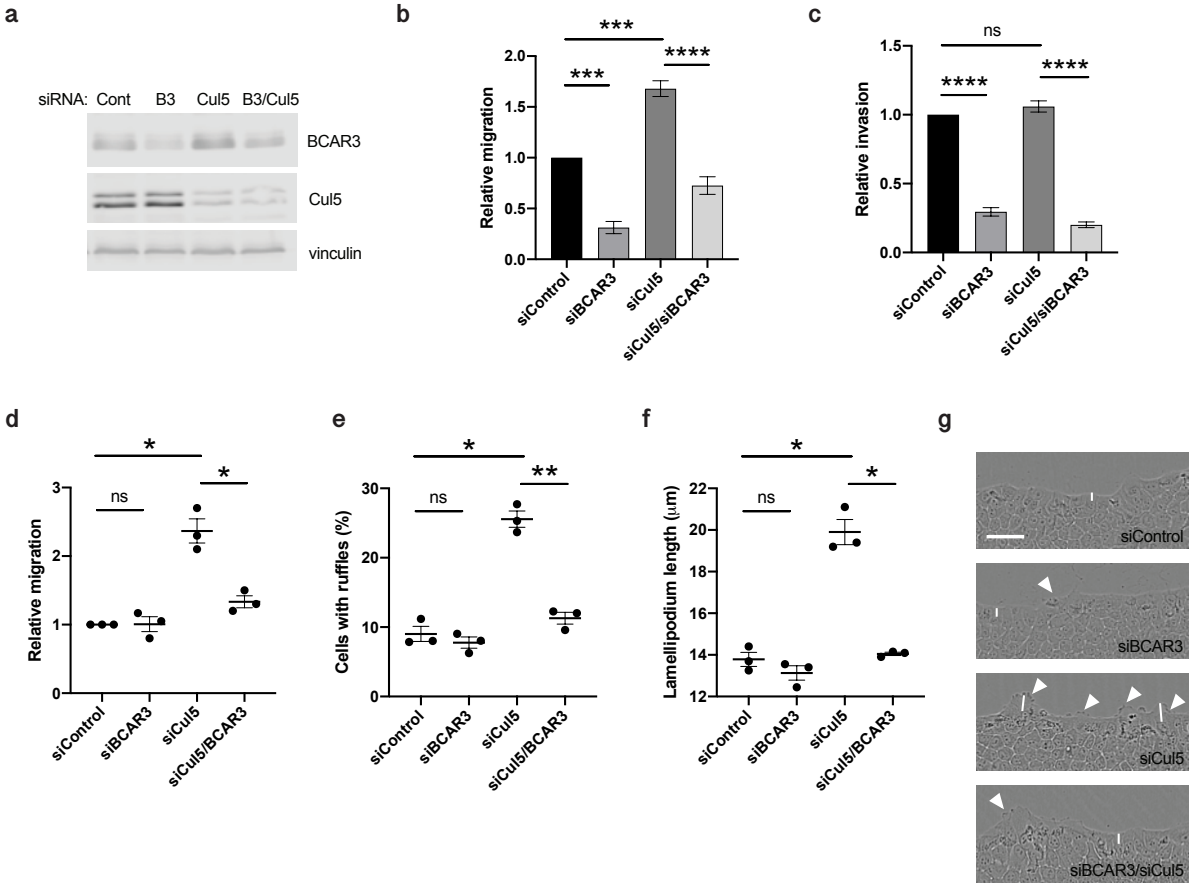

Figure 2.5 BCAR3 regulates single-cell migration, invasion and collective migration. (a) Western blot of siRNA treated cells. (b) MCF10A cells were transfected with control siRNA or siRNA against BCAR3 or Cul5. Single cell migration was assayed using a Boyden chamber assay, where siRNA-treated cells were placed in the upper chamber in EGF-free assay media and EGF-containing growth media was placed in the bottom chamber. Mean and SEM; n=3. ***p<0.0005 and ****p<0.0001 by One-way ANOVA. (c) MCF10A cells were transfected with control siRNA or siRNA against BCAR3 or Cul5. Invasion through Matrigel was assayed using a transwell insert coated with Matrigel, where siRNA-treated cells were placed in the upper chamber in EGF-free assay media and EGF-containing growth media was placed in the bottom chamber. Mean and SEM; n=3. ****p<0.0001 by One-way ANOVA. (d) Dox-inducible SNAP-V5-GFP MCF10A cells were transfected with control siRNA or siRNA against BCAR3 or Cul5. Cells were plated and allowed to grow to confluence, placed in EGF-free media and scratched. Relative migration was measured after 24hrs. Mean and SEM; n=3. *p<0.05 by One-way ANOVA. (e) Images of the scratch wounds after 6 hours of migration were used to count the percentage of ruffling cells. Mean and SEM of >250 cells per condition from n=3 experiments. *p<0.05 and **p<0.005 by One-way ANOVA. (f) Images of the

scratch wounds after 6 hours of migration were used to measure the length of the lamellipodia. Mean and SEM of 50 cells per condition from n=3 experiments. *p<0.05 by One-way ANOVA. (g) Representative images of scratch wounds after 6 hours of migration. Arrows indicate membrane ruffles and lines indicate lamellipodia measurements. Scale bar = 100μm.

2.2.5 *BCAR3 Y117 is required for BCAR3-induced membrane ruffling*

To test whether increased levels of BCAR3 in Cul5-deficient cells are sufficient to stimulate cell membrane protrusions or migration, I generated MCF10A cell lines in which epitope-tagged wildtype or mutant BCAR3 is expressed from a Doxycycline (DOX)-regulated promoter. I first infected MCF10A cells with lentivirus expressing the reverse Tet transactivator (rTTA), followed by infection with another lentivirus containing the Tet operator and SNAP-V5-hBCAR3. SNAP is a DNA repair protein, O^6-alkylguanine-DNA alkyltransferase, that reacts with benzyl guanine derivatives to form covalent adducts [96], and V5 is a synthetic peptide sequence for which mouse and rabbit antibodies are available. Following antibiotic selection for stably transduced cells, I induced with DOX and used cell-permeable fluorescent SNAP ligands [97] to sort the cells by flow cytometry (Supplement Figure 5). Even though I grew the lines in the absence of DOX, the lines were unstable, perhaps due to selection against expression of rTTA or silencing of the integrated proviruses. Although silencing of the integrated proviruses seems unlikely, as further antibiotic selection did not stabilize the cell lines. Nevertheless, by using cells within a few passages of sorting, I was able to measure migration and other phenotypes.

Induction of wildtype BCAR3 expression stimulated membrane ruffling in a dose-dependent fashion (Figure 2.6a,b). Ruffling was increased approximately two-fold at 10 ng/ml DOX, which approximately doubled the quantity of BCAR3 in the cells (see below, Figure 2.7a). However, expression of BCAR3 did not stimulate cell migration (Figure 2.6c). This suggests that the increased level of BCAR3 in Cul5-depleted cells is not only necessary (Fig 2.5e) but also sufficient to increase ruffling, in the absence of other changes. However, increased levels of BCAR3 do not account for the increased migration of Cul5-deficient cells, suggesting that increased levels of other Cul5 targets, such as Cas, are also needed to increase migration when Cul5 is absent (Figure 2.7e, left).

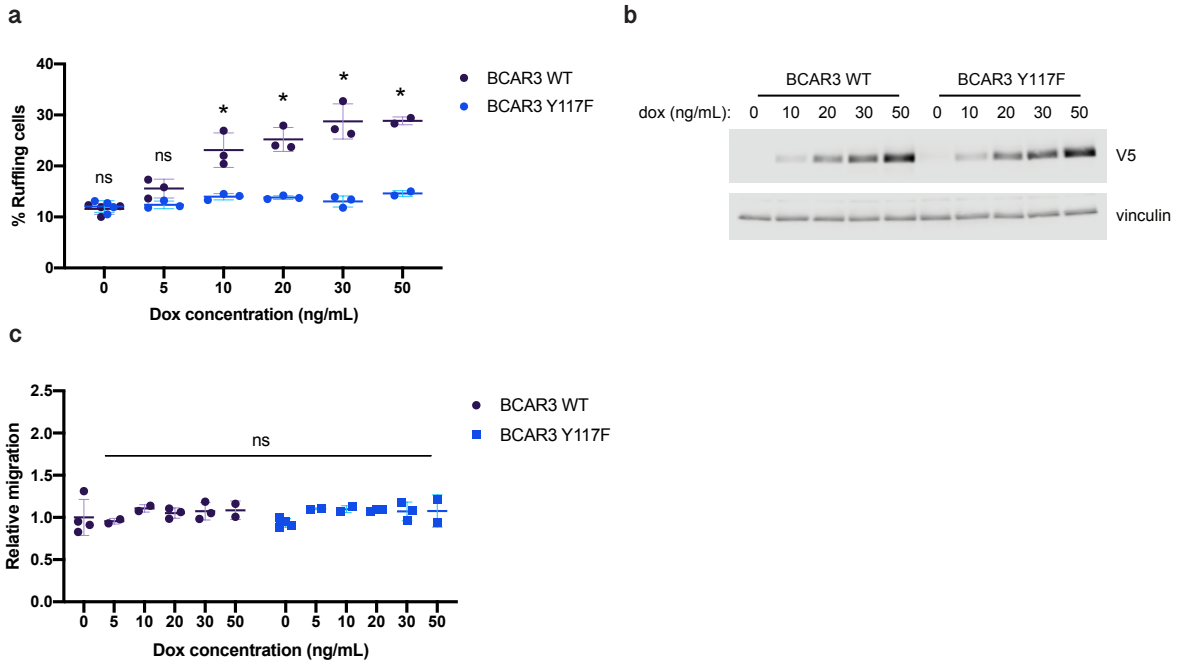

Figure 2.6. BCAR3 Y117 is required for BCAR3-induced membrane ruffling. (a) Dox-inducible SNAP-V5-BCAR3 WT and Y117F MCF10A cells were plated for migration assays and treated with 0, 5, 10, 20, 30, or 50 ng/mL dox. Once confluent monolayers were formed, cells were put in EGF-free media, scratched and allowed to migrate. Images of the scratch wounds after 6 hours of migration were used to count the percentage of ruffling cells. Mean and SEM. *$p<0.05$ by multiple t-tests. (b) Western blot of dox-treated cells used in the migration and ruffling assays. (c) Dox-inducible SNAP-V5-BCAR3 WT and Y117F MCF10A cells were plated for migration assays and treated with 0, 5, 10, 20, 30, or 50 ng/mL dox. Once confluent monolayers were formed, cells were put in EGF-free media, scratched and allowed to migrate. Relative migration was measured after 12 hours. Mean and SEM. $p>0.05$ by multiple t-tests.

Since mutation of Y117 in BCAR3 stabilizes BCAR3 from Cul5-dependent degradation (Figure 2.4g), we had expected the Y117F mutant to be more active than wildtype. Remarkably, Y117F BCAR3 was not more active but was unable to induce ruffling (Fig 2.6a,b). This suggests that, in addition to being the target for SOCS6 binding and degradation by the CRL5-SOCS6 complex, pY117 is also required for overexpressed BCAR3 to stimulate membrane ruffling (Figure 2.7e).

2.2.6 *BCAR3 Y117 is required to rescue Cul5-inhibited membrane ruffling and migration*

To test whether BCAR3, expressed at normal level, also requires Y117 to regulate ruffling and migration in Cul5-deficient cells, I inhibited expression of endogenous BCAR3 with siRNA while

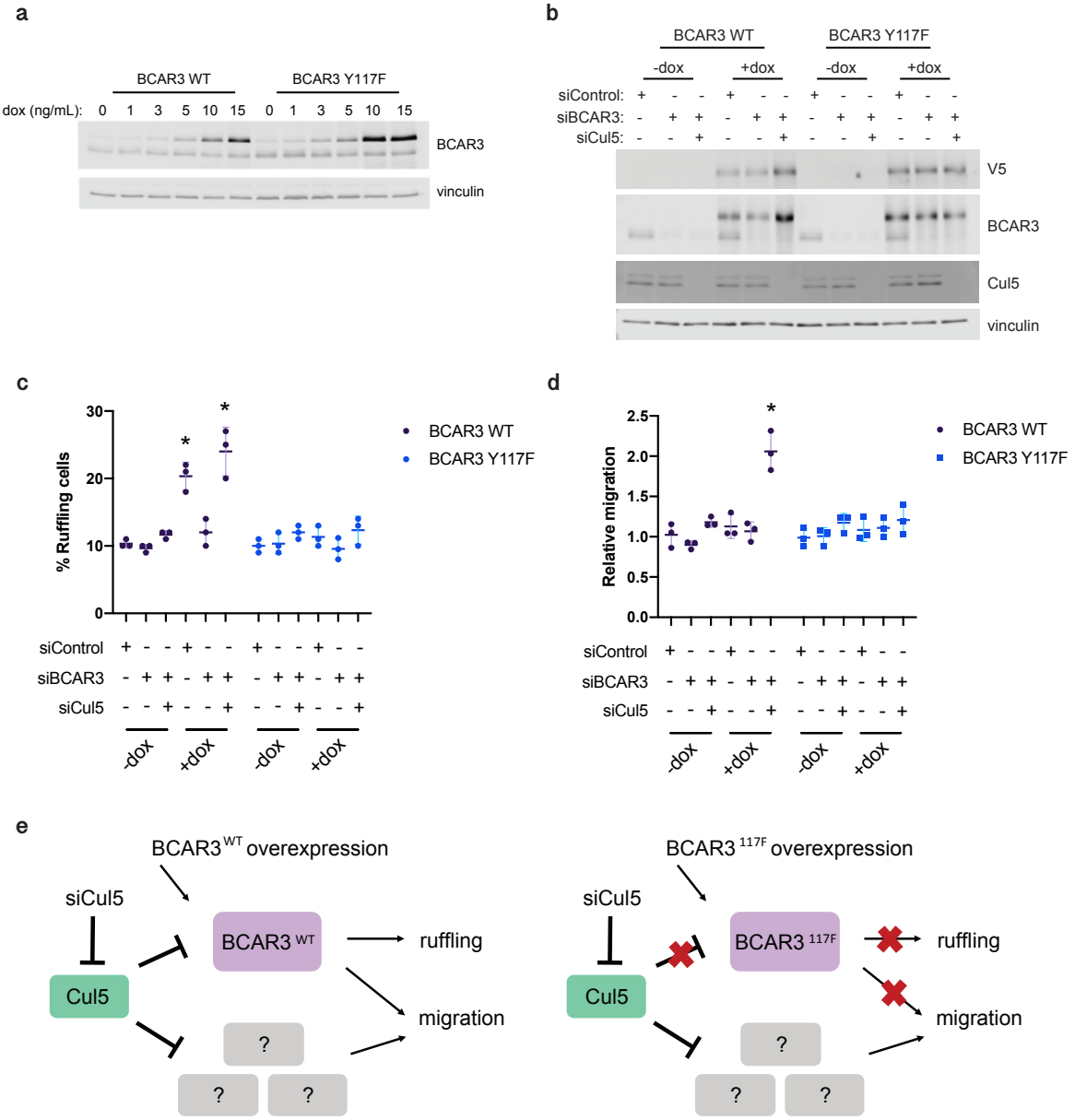

Figure 2.7. BCAR3 Y117 is required to rescue Cul5-inhibited membrane ruffling and migration. (a) Dox-inducible SNAP-V5-BCAR3 WT and Y117F MCF10A cells were treated with a range of concentrations of dox (ng/mL) and lysates were run for Western blotting and probed for BCAR3 to detect endogenous and induced BCAR3. (b) Western blot of siRNA-treated, dox-treated cells used in the migration assay. SNAP-V5-BCAR3 WT and Y117F cells were treated with control siRNA or siRNA against Cul5 or the 3'UTR of BCAR3 and treated with 10ng/mL dox. Once confluent monolayers were formed, cells were put in EGF-free media, scratched and allowed to migrate. (c) Images of the scratch wounds after 6 hours of migration were used to count the percentage of ruffling cells. Mean and SEM. *$p<0.05$ by multiple t-tests. (d) Relative migration was measured after 12 hours. Mean and SEM. *$p<0.05$ by multiple t-tests. (e) Diagram of CRL5-mediated regulation of membrane ruffling and migration through BCAR3 Y117.

inducing expression of wildtype or mutant SNAP-V5-BCAR3 with 10 ng/ml DOX. Under these conditions, SNAP-V5-BCAR3 is expressed at the same level as endogenous BCAR3 in cells treated with control siRNA (Figure 2.7a,b). Wildtype SNAP-V5-BCAR3 supported basal ruffling and migration when endogenous BCAR3 was depleted, and supported increased ruffling and migration when Cul5 and BCAR3 were both depleted (Figure 2.7c,d). The percent ruffling cells was approximately proportional to the quantity of BCAR3 present (endogenous BCAR3 plus SNAP-V5-BCAR3, Figure 2.7c). Expression of wildtype SNAP-V5-BCAR3 also substituted for endogenous BCAR3 to support the increased migration of Cul5-deficient cells (Figure 2.7d), consistent with the model that Cul5 regulates ruffling through BCAR3 but regulates migration through BCAR3 and other proteins. Remarkably, BCAR3 Y117F was inactive in both these rescue assays (Figure 2.7c,d), as expression of SNAP-V5-BCAR3 Y117F did not support the increased membrane ruffling or migration of Cul5-deficient, BCAR3-deficient cells. These data support a model in which BCAR3 Y117 is required for the proper function of BCAR3 to regulate membrane ruffling and migration through CRL5-SOCS6 (Figure 2.7e).

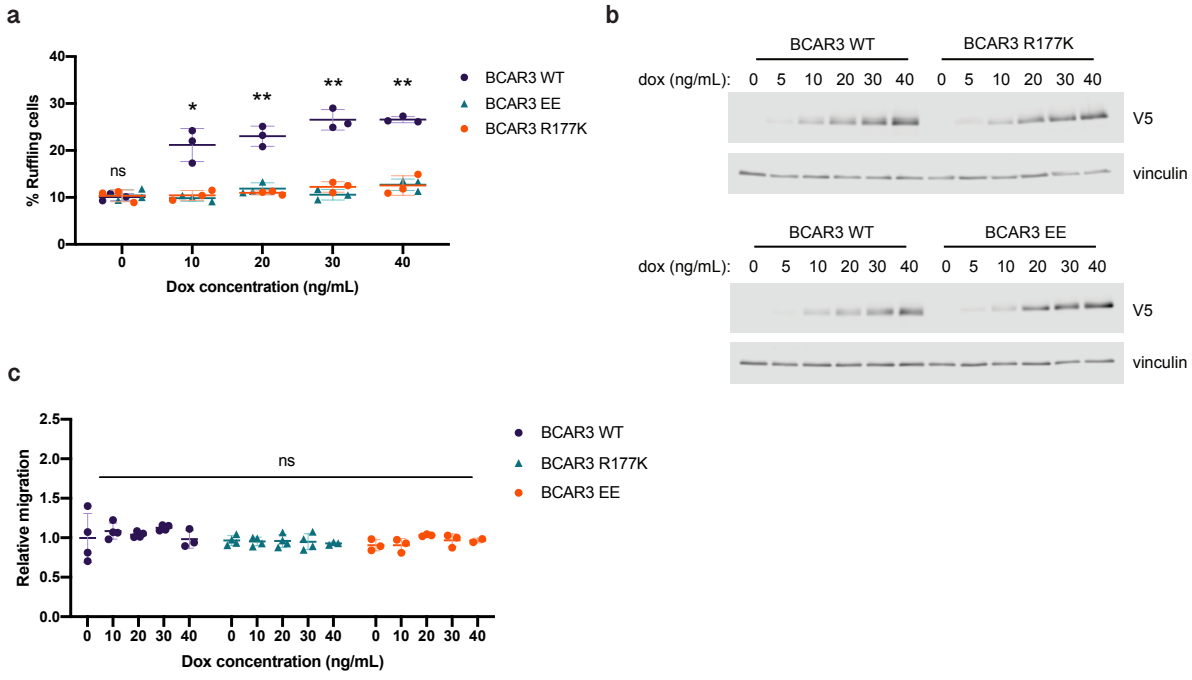

Figure 2.8. BCAR3 SH2 domain and Cas-binding site are required for BCAR3-induced membrane ruffling. (a) Dox-inducible SNAP-V5-BCAR3 WT, R177K, and EE MCF10A cells were plated for migration assays and treated with 0, 10, 20, 30, or 40 ng/mL dox. Once confluent monolayers were formed, cells were put in EGF-free media, scratched and allowed to migrate. Images of the scratch wounds after 6 hours of migration were used to count the percentage of ruffling cells. Mean and SEM. *p<0.05 and

**p<0.005 by multiple t-tests. (b) Western blot of dox-treated cells used in the migration assay. (c) Dox-inducible SNAP-V5-BCAR3 WT, R177K, and EE MCF10A cells were plated for migration assays and treated with 0, 10, 20, 30, or 40 ng/mL dox. Once confluent monolayers were formed, cells were put in EGF-free media, scratched and allowed to migrate. Relative migration was measured after 12 hours. Mean and SEM. p>0.05 by multiple t-tests.

2.2.7 *BCAR3 SH2 and Cas-binding site are required for BCAR3-dependent membrane ruffling and cell migration*

Because Cas binding to BCAR3 is required for many BCAR3 functions [46, 59] and the BCAR3 SH2 domain is required to confer antiestrogen resistance and activate Rac in some cell types [57], I wanted to determine whether the BCAR3 Cas-binding site and SH2 domain are required for BCAR3-mediated ruffling and migration.

I first tested whether the BCAR3 SH2 domain and Cas-binding sites are required to stimulate BCAR3-mediated membrane ruffling and found that the SH2 domain mutant (R177K) and the Cas-binding mutant (EE) are unable to induce membrane ruffling (Figure 2.8a,b). These mutants were also unable to stimulate migration (Figure 2.8c), as we expected due to our previous results showing that BCAR3 is not sufficient to induce migration (Figure 2.6c).

To test whether BCAR3, expressed at normal level, also requires the BCAR3 SH2 domain and Cas-binding site to regulate ruffling and migration in Cul5-deficient cells, I induced expression of the BCAR3 R177K and EE mutants in the absence of endogenous BCAR3 and conducted ruffling and migration experiments. While wildtype BCAR3 supported the increased migration and membrane ruffling of Cul5-deficient cells, we did not observe increased membrane ruffling or migration in Cul5-deficient cells when BCAR3 R177K and EE were expressed in place of endogenous BCAR3 (Figure 2.9a-c). These data suggest that the BCAR3 SH2 domain and Cas-binding site are required for BCAR3 function in regulating membrane ruffling and migration (Figure 2.9d).

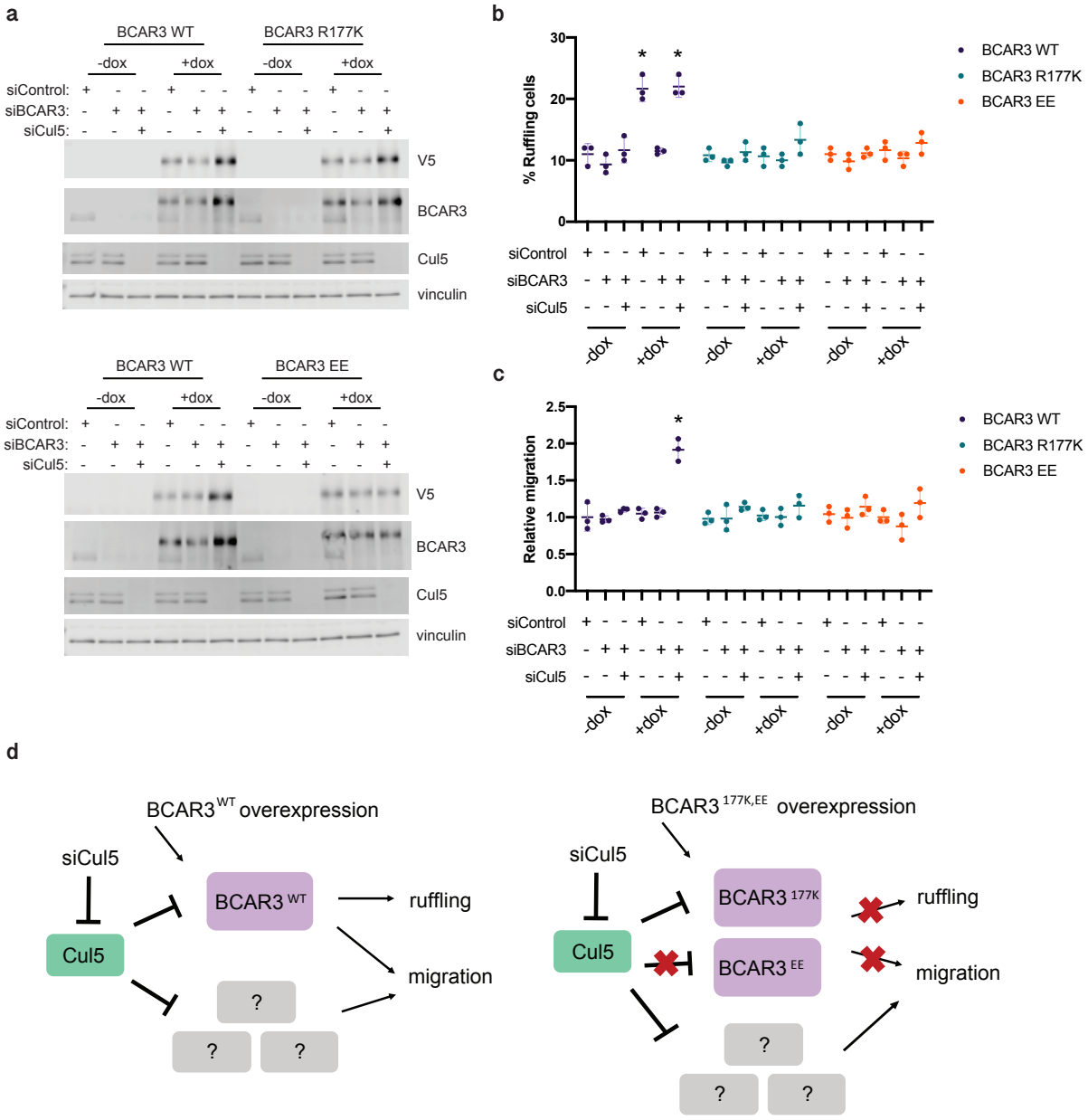

Figure 2.9. BCAR3 SH2 domain and Cas-binding site are required to rescue Cul5-inhibited membrane ruffling and migration. (a) Western blots of siRNA-treated, dox-treated cells used in the migration assay. SNAP-V5-BCAR3 WT, R177K and EE MCF10A cells were treated with control siRNA or siRNA against Cul5 or the 3'UTR of BCAR3 and treated with 10ng/mL dox. Once confluent monolayers were formed, cells were put in EGF-free media, scratched and allowed to migrate. (b) Images of the scratch wounds after 6 hours of migration were used to count the percentage of ruffling cells. Mean and SEM. *p<0.05 by multiple t-tests. (c) Relative migration was measured after 12 hours. Mean and SEM. *p<0.05 by multiple t-tests. (d) Diagram of the regulation of membrane ruffling and migration through BCAR3 177 and Cas-binding.

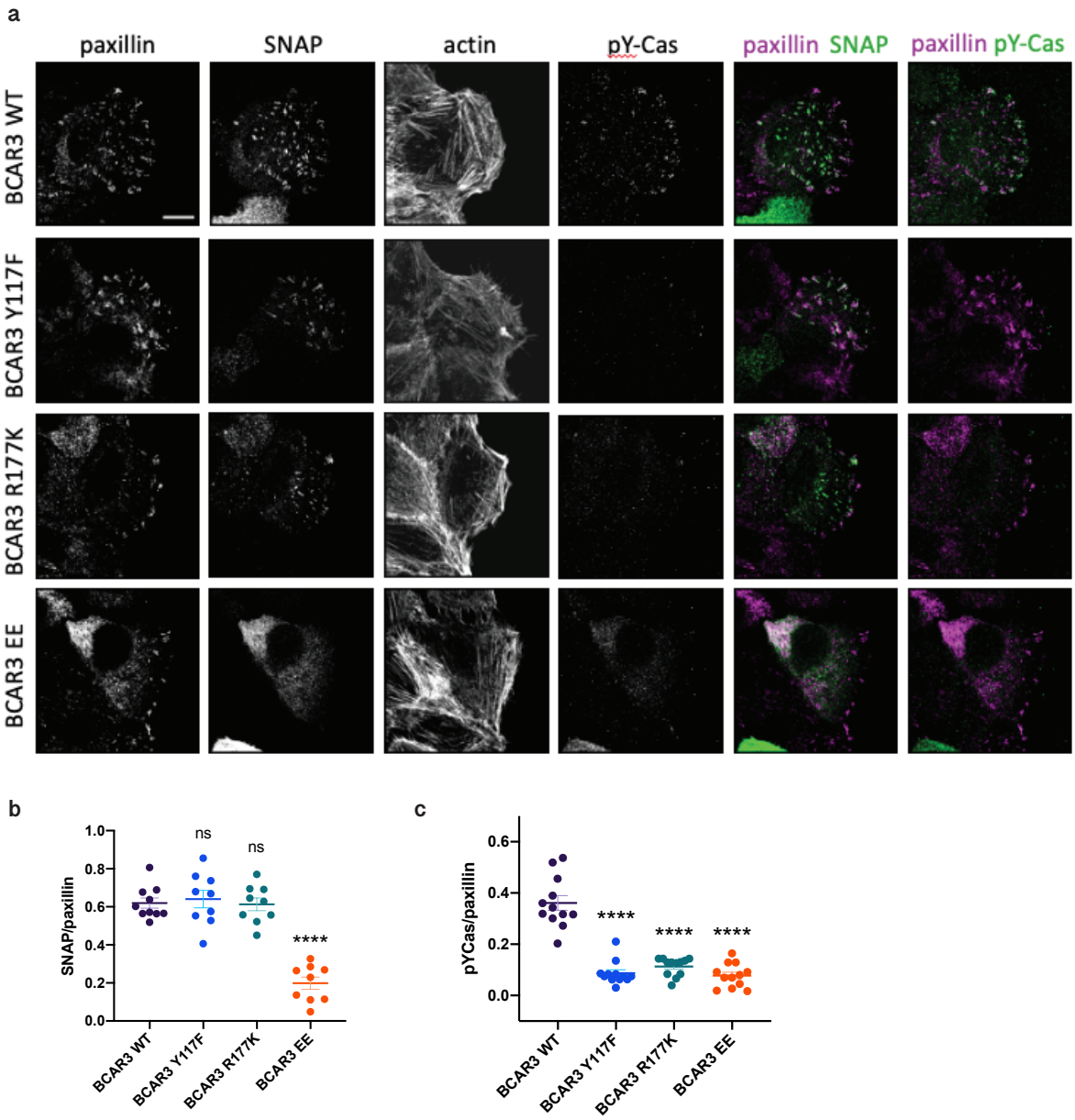

Figure 2.10. Cas recruits BCAR3 to FX/FAs, where BCAR3 stimulates Cas phosphorylation dependent on BCAR3 Y117 and SH2 domain. (a) Dox-inducible SNAP-V5-BCAR3 MCF10A cells were treated with siRNA against the 3'UTR of BCAR3, plated on glass coverslips and treated with 10ng/mL dox. Once confluent monolayers were formed, cells were put in EGF-free media, scratched and allowed to migrate. Cells were treated with cpJF549-SNAP ligand, fixed and stained for adhesion marker paxillin, pY165-Cas and actin. Images are maximum intensity of multiple z-stacks. Scale bar = 10μm. (b) Quantification of the mean fluorescence intensity of SNAP-BCAR3 and paxillin in adhesion sites at the leading edge, normalized to intensity at the base of the cell. Mean and SEM. ****p<0.0001 by One-way ANOVA. (c) Quantification of the integrated intensity of pY165-Cas and paxillin in adhesion sites at the leading edge. Mean and SEM. ****p<0.0001 by One-way ANOVA.

2.2.8 *Cas recruits BCAR3 to FX/FAs, where BCAR3 stimulates Cas phosphorylation, dependent on BCAR3 Y117 and SH2 interactions*

The identification of BCAR3 Y117, SH2 domain and Cas-binding site as sites required for BCAR3 function raises the question of how these sites function in the regulation of membrane ruffling and migration. As BCAR3-Cas binding is required for many functions of BCAR3 [46, 59], I tested whether the BCAR3 mutants could bind Cas. BCAR3 EE does not bind Cas, as expected (Figure 2.3b), however BCAR3 Y117F and R177K do bind Cas (Supplement Figure 6), suggesting that the loss of function of these two mutants is not due to an inability to bind Cas.

As explained above, lamellipodium protrusion and leading edge ruffling involve integrin activation in FXs and SFK-dependent activation of Rac through phosphorylation of Cas and other proteins [29, 35, 42, 43, 87-89]. BCAR3 and Cas both localize to contact sites of breast cancer cells and mouse fibroblasts [46, 52]. Therefore, it is possible that BCAR3 regulates Cas in FXs. We attempted to detect BCAR3 using immunofluorescence with commercial rabbit and mouse antibodies. Signals were weak but we could confirm endogenous BCAR3 co-localizing with FA marker vinculin at the leading edge of migrating cells and near the edge of spread cells (Supplement Figure 7). Staining intensity increased when wildtype SNAP-V5-BCAR3 expression was induced and V5 staining colocalized with FAK, suggesting correct localization of the tagged protein (Supplement Figure 7). Because the antibodies were insensitive, we used cell permeable (cp) JF549SNAP ligand to label expressed SNAP-V5-BCAR3 [97]. Cells were depleted of endogenous BCAR3 using RNAi, wildtype or mutant SNAP-V5-BCAR3 was induced, cells were allowed to reach confluence and then migrate in EGF-free media into a scratch wound. SNAP-V5-BCAR3, paxillin and filamentous actin were then visualized using deconvolution microscopy. Mean fluorescence intensity of paxillin and BCAR3 in FX/FA regions at the leading edge were normalized for intensity in the cell rear, and the ratio of BCAR3 to paxillin in FX/FAs was determined. Under these conditions, both endogenous and Y117F mutant BCAR3 localize to FX/FAs (Figure 2.10a,b).

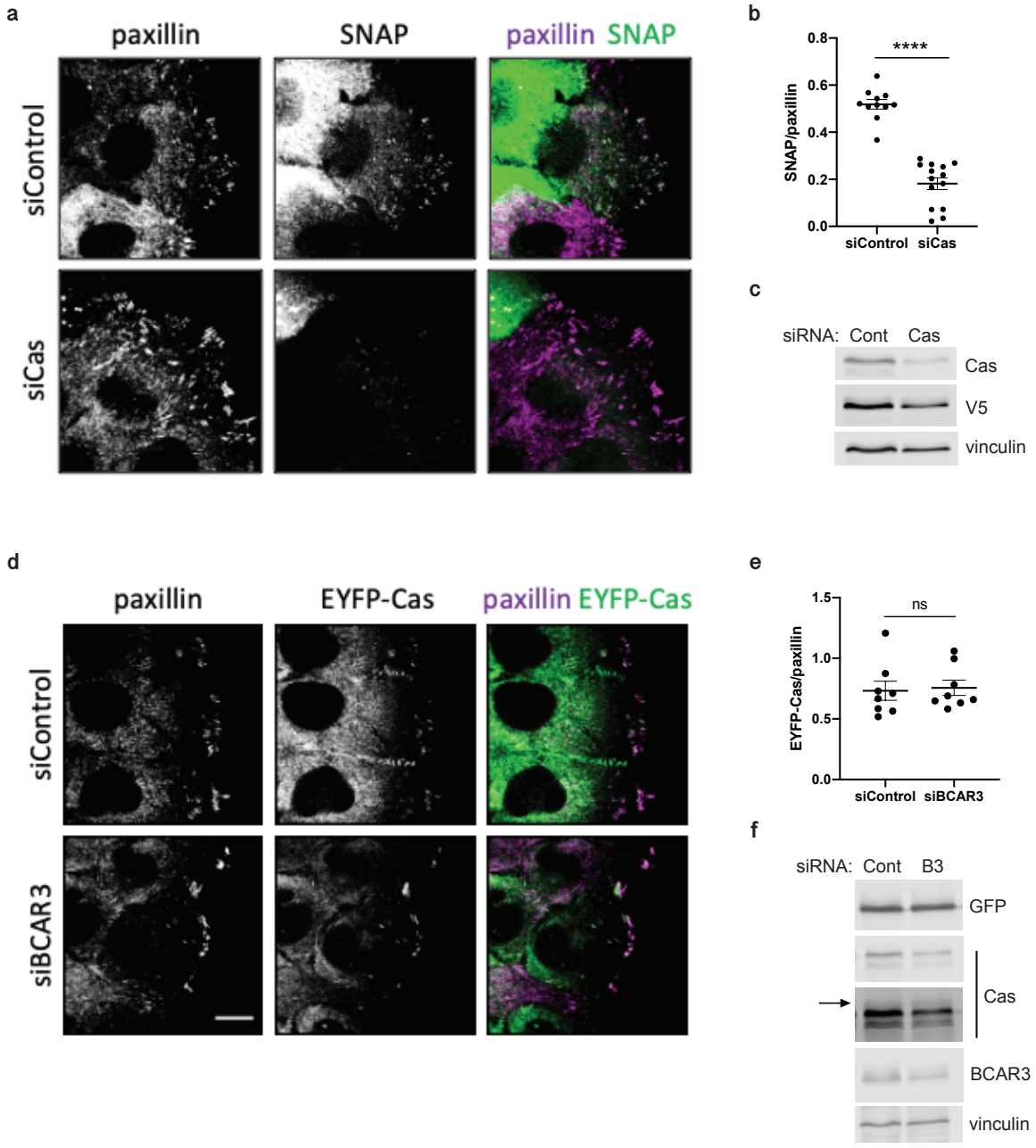

Figure 2.11. Cas is required for BCAR3 localization to FAs, but BCAR3 is not required for Cas localization to FAs. (a) Dox-inducible SNAP-V5-BCAR3 WT MCF10A cells were treated with siRNA against Cas, plated on glass coverslips and treated with 10ng/mL dox. Once confluent monolayers were formed, cells were put in EGF-free media, scratched and allowed to migrate. Cells were treated with cpJF549-SNAP ligand, fixed and stained for adhesion marker paxillin. Images are maximum intensity of multiple z-stacks. (b) Quantification of the mean fluorescence intensity of SNAP-BCAR3 and paxillin in adhesion sites at the leading edge, normalized to intensity at the base of the cell. Mean and SEM. ****$p<0.0001$ by unpaired t-test. (c) Western blot of cell lysates. (d) MCF10A cells expressing low levels of EYFP-Cas were treated with

siRNA against BCAR3 and plated on glass coverslips. Once confluent monolayers were formed, cells were put in EGF-free media, scratched, allowed to migrate, fixed and stained for adhesion marker paxillin. Images are maximum intensity of multiple z-stacks. Scale bar = 10μm. (e) Quantification of the mean fluorescence intensity of EYFP-Cas and paxillin in adhesion sites at the leading edge, normalized to intensity at the base of the cell. Mean and SEM. $p>0.05$ by unpaired t-test. (f) Western blot of cell lysates.

Previous studies have indicated that mutation of LxxE and RxxE in the CDC25H domain of BCAR3 did not inhibit BCAR3 localization of over-expressed BCAR3 to Cas-containing adhesions [46], suggesting that Cas is not required for BCAR3 localization. However, I found that SNAP-V5-BCAR3 did not localize to FX/FAs at the leading edge of migrating cells from which Cas had been depleted using RNAi (Figure 2.11a,b), as detected using cpJF549SNAP ligand and paxillin antibodies. Correspondingly, mutation of LxxE and RxxE in SNAP-V5-BCAR3 EE inhibited localization to FA/FXs at the leading edge of migrating cells (Figure 2.10a,b). Thus, when expressed at physiological levels, BCAR3 localization to adhesions requires binding to Cas.

Cas localization to membrane ruffles and vinculin-containing adhesions was reported to require BCAR3 [45, 98]. However, I found that depleting BCAR3 from MCF10A cells did not prevent Cas localization to FAs, as detected using YFP-Cas expressed at low level relative to endogenous Cas (Figure 2.11d,e). Thus, when BCAR3 and Cas are expressed at physiological levels, Cas localizes to FX/FAs independent of BCAR3, but BCAR3 localization requires Cas.

We next tested whether BCAR3 Y117 is needed for Cas phosphorylation in FX/FAs, using antibodies to pY165, one of the repeated YxxP motifs in Cas that bind Crk. As expected, Cas was phosphorylated in FX/FAs of cells expressing wildtype SNAP-V5-BCAR3. However, unexpectedly, Cas was not phosphorylated in cells expressing Y117F, R177K or EE mutants of SNAP-V5-BCAR3, suggesting that BCAR3 not only has to be bound to Cas but also needs to be phosphorylated at Y117 and interact with proteins through its SH2 domain in order for Cas phosphorylation to occur (Figure 2.10a,c). The phosphorylation of Cas in FX/FAs correlates with the rescue of ruffling (Figures 2.7c and 2.9b). Taken together with the known importance of Cas pYxxP motifs to stimulate membrane ruffling [42, 43, 87], this suggests that BCAR3 binding to Cas in FX/FAs activates Cas phosphorylation to drive ruffling (Figure 2.12).

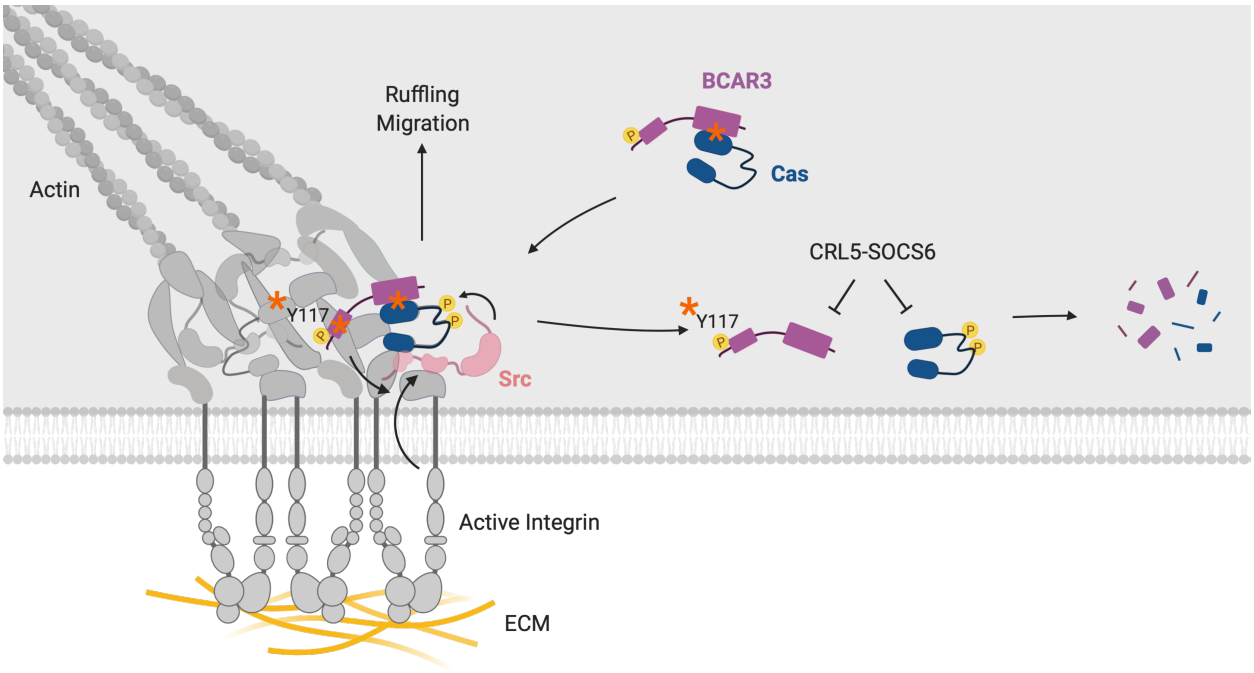

Figure 2.12. Model of the regulatory circuit. BCAR3 is recruited to adhesion sites by binding Cas. Once in adhesions, BCAR3 promotes tyrosine phosphorylation of Cas through a mechanism that requires BCAR3 Y117, SH2 domain and Cas-binding site. I hypothesize that BCAR3 promotes pY-Cas through activation of Src kinase in a mechanism that requires these BCAR3 sites. pY-Cas then promotes membrane ruffing. pY117-BCAR3 and pY-Cas are then targeted independently for proteasomal degradation by CRL5-SOCS6. Thus, this regulatory circuit inhibits BCAR3-mediated pY-Cas signaling at the leading edge of migrating cells. ★ indicates required BCAR3 sites at each step in the model. Image created with BioRender.com.

2.3 Discussion

Our results support a model in which BCAR3 is recruited to FX/FAs near the leading edge of migrating cells by binding to Cas through its CDC25H domain. BCAR3 may be complexed with Cas in the cytosol and recruited jointly, or Cas may localize followed by BCAR3 later. Once in FXs, BCAR3 promotes Cas phosphorylation in a mechanism that requires the SH2 domain and Y117 phosphorylation. We do not know which kinase phosphorylates BCAR3, nor whether phosphorylation occurs before or after BCAR3 enters the FX. Following activation by BCAR3, Cas phosphorylation then drives membrane ruffling by well-documented mechanisms involving Crk, DOCK180 and Rac [29, 35, 42, 43, 87-89]. Thus, BCAR3 provides a critical switch to activate

Cas. Following phosphorylation at Y117, BCAR3 now becomes a target for degradation, by binding to SOCS6 and the CRL5 E3 ubiquitin ligase. At the same time, pY-Cas is degraded by the same mechanism. This terminates signaling until new Cas and BCAR3 molecules are recruited from the cytosol.

2.3.1 *A single site for BCAR3 function and degradation*

Our data suggest that phosphorylation of BCAR3 at a single site is required both for BCAR3 function in membrane ruffling and cell migration and also for BCAR3 degradation. This means that BCAR3 activation by phosphorylation at this site also limits the duration of activity, constituting a built-in negative feedback loop. One possibility is that pY117 induces a conformation change in BCAR3, exposing or altering other domains to regulate Cas phosphorylation. An alternative possibility is that BCAR3 pY117 binds a downstream effector protein that regulates Cas, but the identity of that protein is unclear. Membrane ruffling occurs in the absence of SOCS6 and therefore SOCS6 is not a candidate for pY117-dependent signaling. This situation for BCAR3 resembles Dab1 phosphorylation at sites that bind a related SOCS protein, SOCS7, to target Dab1 for CRL5-dependent degradation and also bind PI3' kinase and Src to generate downstream signals [77]. However, the situation with Cas is slightly different. The site in Cas that binds SOCS6 and is needed for degradation is not critical for phosphorylation of other sites that generate downstream signals, allowing some disconnect between activity and degradation [76]. As a result, mutation of the SOCS-binding site in Cas generates a gain-of-function mutant.

2.3.2 *Implications for Cas*

Our results add new complexity to Cas regulation. Cas phosphorylation requires SFK activity, and in some cell types, FAK activity. However, the requirement for FAK activity may be simply due to FAK's role in SFK activation [99]. Src phosphorylates Cas efficiently in vitro, raising the question of why Cas phosphorylation in vivo requires BCAR3. One possibility is that BCAR3 helps activate SFKs in FXs. Over-expression and knockdown of BCAR3 increases and decreases Src autophosphorylation, respectively [52, 56, 58]. This effect may not be evident in vitro. Indeed,

the BCAR3 SH2 domain binds a pY789 in RPTPa, forming a complex together with Cas [52]. Since RPTPa is able to activate SFKs by dephosphorylating a C-terminal inhibitory tyrosine residue [85, 86], the role of BCAR3 in the phosphorylation of Cas may primarily be the activation of SFKs through RPTPa.

This work also addresses Cas localization to adhesions, which requires both its SH3 domain, which can bind to FA proteins vinculin and FAK, as well as its C-terminal CCCH or FAT domain, which binds paxillin, BCAR3 and other proteins [100-103]. Our data suggest that BCAR3 binding is not needed for Cas to localize properly, leaving open the question of which other proteins recruit Cas to FXs.

2.3.3 *Differences from published work*

Similar to what was observed in breast cancer cells [46, 59], our results confirm that BCAR3 binding to Cas is required for its migratory functions in normal breast cells. However, we see differences in localization requirements for BCAR3 and Cas. While previous studies that have investigated BCAR3 and Cas localization in cancer cells have relied on overexpression, we examined their localization in normal cells using endogenous expression levels. Overexpression can drive binding interactions that do not occur at physiological expression levels and our results show that overexpression creates gain of function effects. Opposite to previous work [45, 46, 98], we found that Cas is required for BCAR3 localization to adhesion sites, but Cas localization is independent of BCAR3. Whether these differences are due to the difference in cell type, expression levels or some other variable is unclear.

2.3.5 *Relation to cancer*

Our finding that BCAR3 is subject to complex post-translational regulation may be helpful in reconciling the cell culture observations that BCAR3 over-expression increases transformed phenotypes with the patient data showing that high levels of BCAR3 correlate with favorable patient outcomes and vice versa [47, 48, 58]. It is possible that changes in BCAR3 protein stability or phosphorylation state influence BCAR3 activity in patients, but that these regulations at the

protein level are not accounted for when looking at mRNA expression and making conclusions about outcomes. In fact, staining tumor tissues shows that BCAR3 protein is higher in many breast tumors relative to normal breast tissue [46], suggesting that BCAR3 protein is higher in breast cancer cells and may be mis-regulated. Additionally, BCAR3, Cas and other Src substrates are phosphorylated at higher levels in basal breast cancer cells relative to luminal breast cancer cells [49], contributing to the hypothesis that mis-regulation of BCAR3 may contribute to disease progression.

2.3.6 *Remaining questions*

The biggest outstanding question is which kinase and upstream stimuli lead to phosphorylation at BCAR3 Y117. BCAR3 is tyrosine phosphorylated in response to serum and adhesion [60]. Additionally, BCAR3 binds EGFR through its SH2 domain [50, 51] and regulates EGF-stimulated and insulin-stimulated membrane ruffling [45, 62]. These studies provide potential candidate stimuli that need to be investigated further. Whether BCAR3 Y117 is phosphorylated in the cytosol or adhesion sites is also unclear. Attempts to label pY117-BCAR3 using a polyclonal rabbit antibody raised against a pY117 peptide were unsuccessful due to a lack of specificity of the antibody.

This is the first study to identify and detail the role of a specific phosphorylation site in BCAR3. As such, little is known about the regulation, signaling and downstream function of other BCAR3 phosphorylation sites. Identifying these sites of phosphorylation and mapping their signaling pathways would provide novel insight into the function and regulation of BCAR3.

Chapter 3. REGULATION OF FOCAL ADHESION PROETIN EXCHANGE

3.1 INTRODUCTION

Focal adhesions (FAs) are large multi-protein complexes that couple the intracellular contractile actin cytoskeleton with the extracellular matrix. The protein network that makes up an adhesion is molecularly complex and is composed of many different structural, signaling and adaptor proteins. As each focal adhesion protein has multiple possible binding partners, the network of interactions is highly complex and the composition of adhesions across cell types can vary.

Many studies have demonstrated that focal adhesion proteins have dynamic properties in which proteins continuously associate with and disassociate from the adhesion, resulting in the exchange of adhesion-bound protein with cytoplasmic protein [104-108]. Interestingly, measuring the dynamics of focal adhesion proteins can provide novel insight into their molecular roles within the adhesion. Groups have shown that known structural proteins such as vinculin and talin are much less mobile than FAK and Cas, which serve as signaling and adaptor molecules [104]. These basic experiments looking at the mobility of each FA protein have been built on to investigate more complex questions. For example, there have long been questions about how a cell senses extracellular physical forces and converts them into biochemical signals. By studying the exchange of FA proteins when substrate stiffness is modulated, groups have identified mechanosensitive proteins and learned more about their signaling [104-108]. While the exchange of signaling proteins such as FAK are unaffected by changes in extracellular stiffness, the mobility of vinculin and talin are altered when ECM stiffness is changed. This suggests that vinculin and talin serve a role in detecting extracellular signals. Further, inhibiting FAK and Src kinase activity inhibited the ability of tensin, but not vinculin, to sense changes in matrix stiffness [104]. Thus, studying the dynamic exchange of FA proteins is a powerful tool that can be used to better understand molecular signaling in FAs.

The dynamic exchange of focal adhesion proteins can be measured using a technique called fluorescence recovery after photobleaching (FRAP). First developed in the 1970s, FRAP can be

used to study protein movement by measuring fluorescence recovery in an area where fluorescence had previously been bleached. More specifically, fluorescent molecules are photobleached by a high intensity laser beam in a specific area or compartment of the cell. The photobleaching is irreversible and therefore the recovery fluorescence in the bleached area is due to the exchange of non-bleached molecules from surrounding areas, replacing the bleached molecules that left that area. Following photobleaching, fluorescence intensity in the photobleached area is measured over time, typically measured for 2 minutes or so. Common measurements taken using FRAP data include the mobile fraction (the fraction of molecules that exchange), the immobile fraction (the fraction of proteins that don't exchange) and the half-life (the time it takes to recover half of the maximum recovered intensity) [109, 110]. By fluorescently labeling your protein of interest, you can study the mobility of specific proteins in different cellular compartments.

FRAP has been used to study the mobility of FA proteins in adhesions. Studies have shown that there are several subpopulations of focal adhesion proteins whose dynamics are distinct from one another. Early FRAP experiments classified focal adhesion proteins as either "mobile" or "immobile," which was characterized by whether these proteins exchanged and were replaced by fluorescent protein from the cytoplasm. Most focal adhesion proteins have mobile fractions ranging from 40-80%, indicating that there is a sizable population of protein that does not exchange and is immobile [104-108].

More recent studies have found that FA protein exchange is more complex than initially thought. Using computer simulations and mathematical modeling in addition to FRAP studies, one group showed that vinculin and paxillin have four subpopulations whose dynamics are distinct from one another. These subpopulations include a rapidly diffusing cytoplasmic population, an immobile population bound to the FA, an exchanging population that can associate with the FA, and a "juxtamembrane" population that surrounds the FA and diffuses at a reduced rate [105]. The characterization of subpopulations of FA proteins beyond the mobile and immobile populations reveals there is more to learn about the dynamics of FA proteins and how they contribute to FA structure.

While the literature classifies the population of FA protein that does not exchange with cytoplasmic protein as immobile, these proteins were only immobile during the short timeframe of the FRAP experiment. This leaves open the possibility that this subpopulation could exchange much more slowly, but is not detected because fluorescence recovery is usually measured for a couple minutes after photobleaching. In fact, no studies have extended the FRAP timepoints beyond a couple of minutes to see if these proteins are truly immobile.

I became interested in the slow exchanging and immobile subpopulations of FA proteins because the rapidly exchanging subpopulation only associates with the adhesion for a short amount of time ranging from a fraction of a second to several seconds and is therefore unlikely to play an important role in regulating adhesion dynamics. Rapidly exchanging proteins have a high off-rate because they are not integrated into the focal adhesion structure. In the short time a rapidly-exchanging protein is associated with the adhesion, it seems unlikely that it could be phosphorylated or be able to contribute to the molecular signaling that regulates FA dynamics. The "immobile" population of FA proteins is integrated into the structure of the adhesion and associates with the adhesion long enough to be regulated (for example, phosphorylated) and contribute to signaling that regulates FA turnover. I hypothesize that rapidly exchanging proteins don't associate with the adhesion long enough to regulate FA dynamics and that the immobile, or slow-exchanging, proteins are able to regulate FA dynamics because of their increased association with the adhesion.

In support of this hypothesis, we have shown that proteolysis regulates focal adhesion dynamics. Specifically, we showed that the E3 ubiquitin ligase CRL5-SOCS6 inhibits FA turnover at the leading edge of migrating cells by targeting pY-Cas in leading edge adhesions for proteasomal degradation [79]. While is it not understood how long this process takes, we believe that this mechanism of regulating FA turnover works on a longer timescale than the few seconds a rapidly-exchanging protein associates with the adhesion.

Based on what is known about FA protein exchange and the role of proteolysis in regulating FA dynamics, I sought to test the following model. I hypothesize that the rapid population of Cas is not anchored to the adhesion structure and can therefore not undergo phosphorylation and does not regulate FA dynamics. Conversely, I hypothesize that the "immobile" population of Cas can

be phosphorylated because of its long association with the adhesion. In this model, the immobile population is not truly immobile but rather exchanges slowly, as it is targeted by SOCS6-CRL5 and replaced by cytoplasmic Cas on a slow time course that has not been previously measured (Figure 3.1).

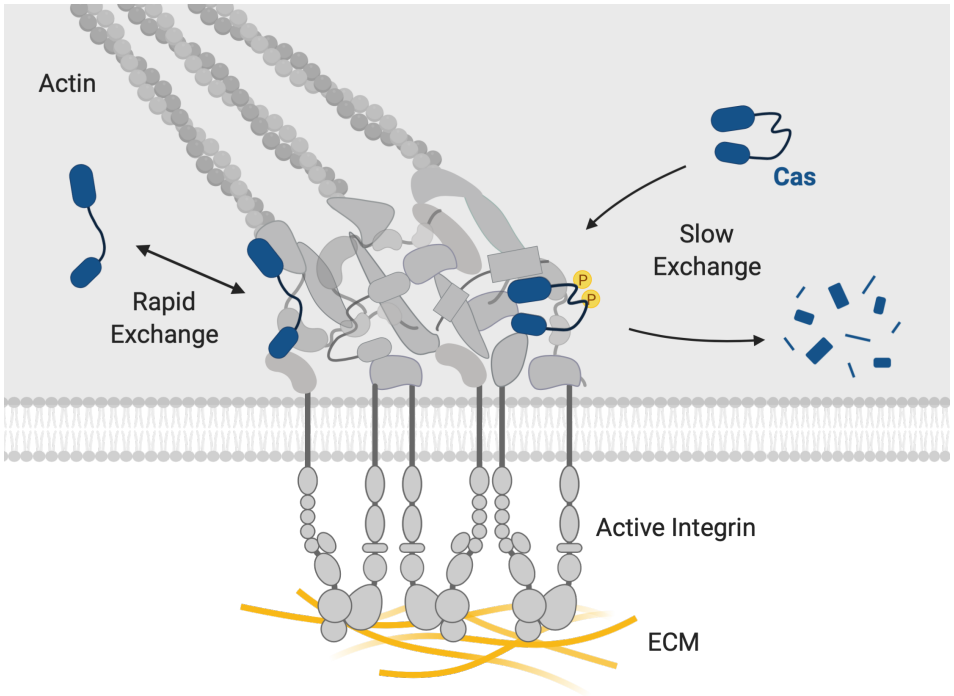

Figure 3.1. Model of slow Cas exchange in focal adhesions. In this model, there are two dynamically distinct subpopulations of Cas. A population of Cas rapidly exchanges with cytoplasmic Cas. A different population of Cas is anchored to the adhesion and can therefore be phosphorylated to regulate downstream signaling and be targeted by CRL5-SOCS6. Turnover over pY-Cas, which is then replaced with cytoplasmic Cas, happens on a longer timescale. Image created with BioRender.com.

3.2 Results

3.2.1 *Vinculin has rapid and slow exchanging, not immobile, subpopulations*

In order to test my hypothesis that focal adhesion proteins have a slow-exchanging population that is not truly immobile, I made an MCF10A cell line that stably expresses EYFP-vinculin to use in FRAP experiments. Several studies have measured vinculin exchange over a recovery of 2-6

minutes after bleaching in a range of cells, including HeLa cells, U2OS cells and mouse embryonic fibroblasts. These studies have shown that vinculin has a mobile, rapidly exchanging population of 40-60% over these short recovery periods [104-108]. While these groups looked at vinculin exchange in plated cells, I was interested in understanding vinculin exchange under conditions where migration has been stimulated. To do this, I allowed MCF10A EYFP-vinculin cells to grow to confluence, put the cells in low serum, EGF-free assay media, and one day later wounded the monolayer. FRAP studies were conducted 7 hours after scratching to allow migration to occur and I measured vinculin exchange in FAs at the leading edge of the migrating cells. Measuring exchange for 2 minutes, I found that vinculin has a rapidly-exchanging population that makes up roughly ~50-60% of the vinculin in the adhesion (Fig 3.2a-c). These results are consistent with previous studies [104-108].

Next, I wanted to extend the time over which fluorescence recovery was measured after bleaching in order to determine if all of the vinculin molecules eventually leave the adhesion and become replaced with fluorescent vinculin from the cytoplasm. I made several attempts to measure vinculin exchange in migrating cells for 60 minutes, however several factors prevented the collection and analysis of these data. Despite a perfect focus application on the microscope, the cells would sometimes drift out of focus over time. However, this problem could be overcome with some troubleshooting. More challenging and impeding was the extreme changes in the size and shape of the FAs over time, which presented problems in the analysis and interpretation of the FRAP data. Given these challenges, I measured vinculin exchange for 60 minutes under conditions where migration was not directly stimulated and cells were sparsely plated. I found that the fluorescence intensity completely recovered to the intensity before bleaching after an average of 30 minutes and then plateaued, suggesting that all vinculin molecules had exchanged with fluorescent vinculin in the cytoplasm (Fig 3.2d-f). While complete fluorescence recovery occurred over a wide range of times (Fig 3.2g), 81% of the adhesions measured reached the initial intensity in the time frame measured and the other 19% reached >90% recovery. Taken together, these data suggest that the populations of FA proteins previously thought to be immobile may slowly exchange with cytoplasmic protein over minutes or hours. Further studies of other FA proteins would confirm whether this occurs broadly in the FA structure or if it is unique to vinculin.

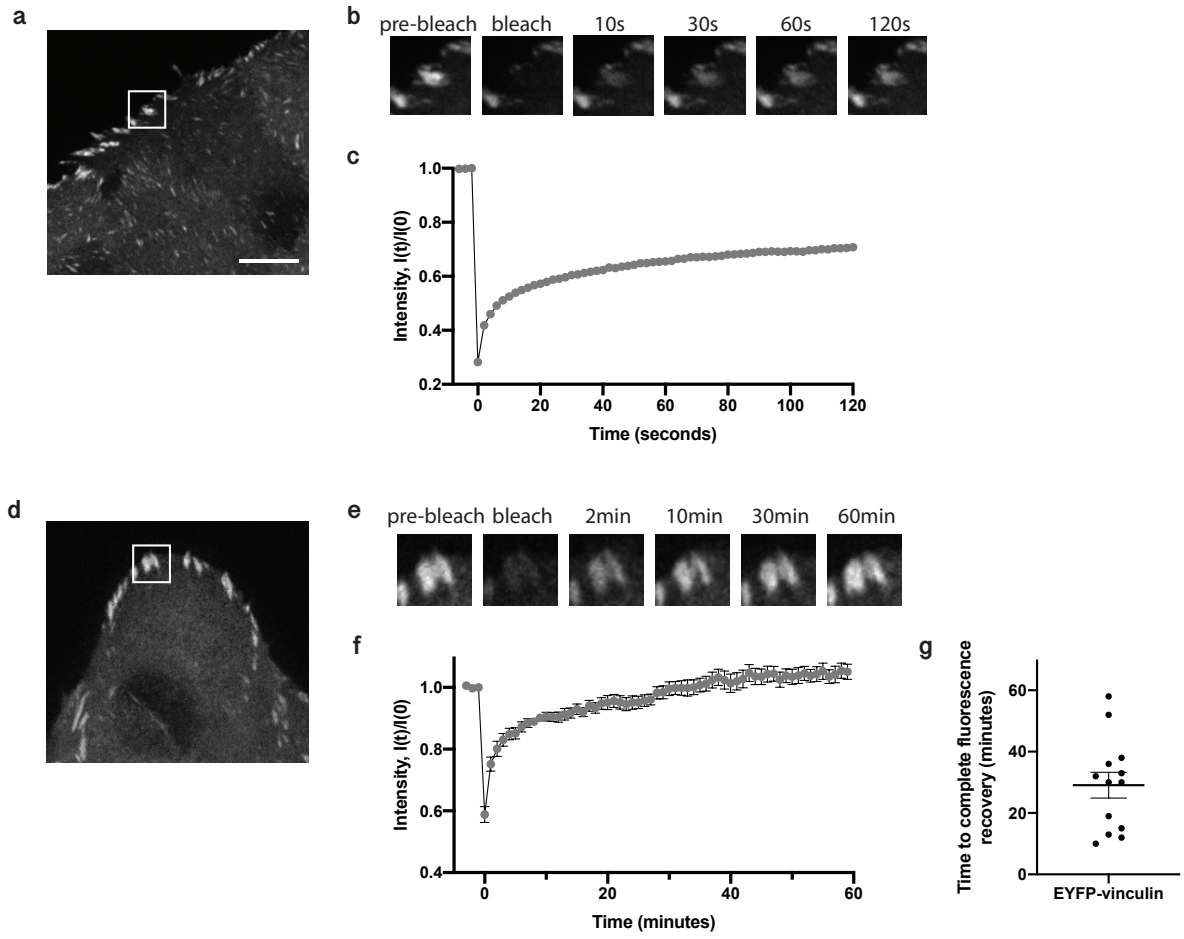

Figure 3.2. Vinculin has rapid and slow exchanging, not immobile, subpopulations. (a) MCF10A cells expressing EYFP-vinculin were grown to confluence, scratched and allowed to migrate for 7 hours. The boxed FA was bleached using a 405nm laser. Scale bar = 10μm. (b) Time course of the fluorescence recovery of the bleached adhesion. (c) Fluorescence recovery curve; mean and SEM of normalized intensities of 46 adhesions. (d) MCF10A cells expressing EYFP-vinculin were plated sparsely. The boxed adhesions were bleached using a 405nm laser. (e) Time course of the fluorescence recovery of the bleached adhesions. (f) Fluorescence recovery curve; mean and SEM of normalized intensities of 16 adhesions. (g) Time to complete fluorescence recovery, I(0), for 13 adhesions.

In an effort to more closely study this specific subpopulation of slow-exchanging protein in FAs, I worked to optimize techniques that would allow me to directly visualize these proteins. While FRAP allowed me to study exchange of FA proteins with cytoplasmic protein, the protein population of interest is bleached and the exchange is inferred by the increase of fluorescence. We are unable to visualize and track the photobleached population after bleaching. Therefore, I worked

to optimize photoconversion experiments, where the protein of interest is labeled with a green fluorescent tag that converts to a red fluorescent state after irradiation with UV light. Specifically, I chose the photoconvertible protein mEos2 (and variant mEos3.2) because it is monomeric, stable and bright. Additionally, studies have shown that the function of many different proteins has not been detectably disrupted when tagged with monomeric tags like mEos [111, 112]. Tagging FA proteins with a photoconvertible tag would allow me to directly track proteins leaving the adhesion because I can convert the color of adhesion proteins from green to red and leave all other protein green. Then protein leaving the adhesion can be visualized by a loss of red signal and an increase in green signal. I made constructs to express mEos2-Cas and mEos3.2-Cas in cells and tested the photoconversion on multiple microscopes. First, I transiently transfected mEos2-Cas into HeLa cells and tested photoconversion of adhesion-associated Cas in a Spinning Disk microscope. Following irradiation of a small area containing adhesions, the fluorescent tag in this area did convert to red but the green fluorescence intensity across the cell significantly increased (Supplement Figure 8a). This dramatic increase in green signal would interfere with analysis of the data. I also tested photoconversion setting on a Zeiss confocal microscope and saw nice conversion to red without the increase in green signal (Supplement Figure 8b). However, this microscope also comes with limitations, such as slower imaging and worse resolution than the Spinning disk. Further optimization and use of this approach could give us insight into the movement of the slow-exchanging population of FA proteins.

3.2.2 *Rapid Cas exchange from focal adhesions is not regulated by CRL5*

Having established that vinculin has a subpopulation that exchanges slowly, I next wanted to investigate whether Cas has a similar subpopulation that is regulated by CRL5. Given the model in which tyrosine phosphorylated Cas is integrated in the adhesion structure and removed for ubiquitination by CRL5-SOCS6 and proteasomal degradation, I hypothesized that rapid exchange of Cas is not regulated by CRL5. I tested this by transiently knocking down Cul5 in MCF10A EYFP-Cas cells using RNA interference and used FRAP to monitor Cas exchange from adhesions for 2 minutes. As an additional negative control, I did parallel FRAP experiments measuring vinculin exchange in the same conditions. Since vinculin is not regulated by CRL5, I hypothesized that knocking down Cul5 would not affect the rapid or slow exchange of vinculin. I found that

knocking down Cul5 does not change the exchange of the rapid populations of either Cas or vinculin (Fig 3.3). This was determined using two metrics. First, the percentage of protein that exchanged over the 2 minutes, or the mobile fraction, did not change in the absence of Cul5 (Fig 3.3b,e). Second, the time it takes to recover half of the maximum recovered fluorescence, or $\tau_{1/2}$, also did not change when Cul5 was knocked down (Fig 3.3c,f). These data show that the population of Cas that exchanges rapidly with cytoplasmic protein is not regulated by CRL5-SOCS6.

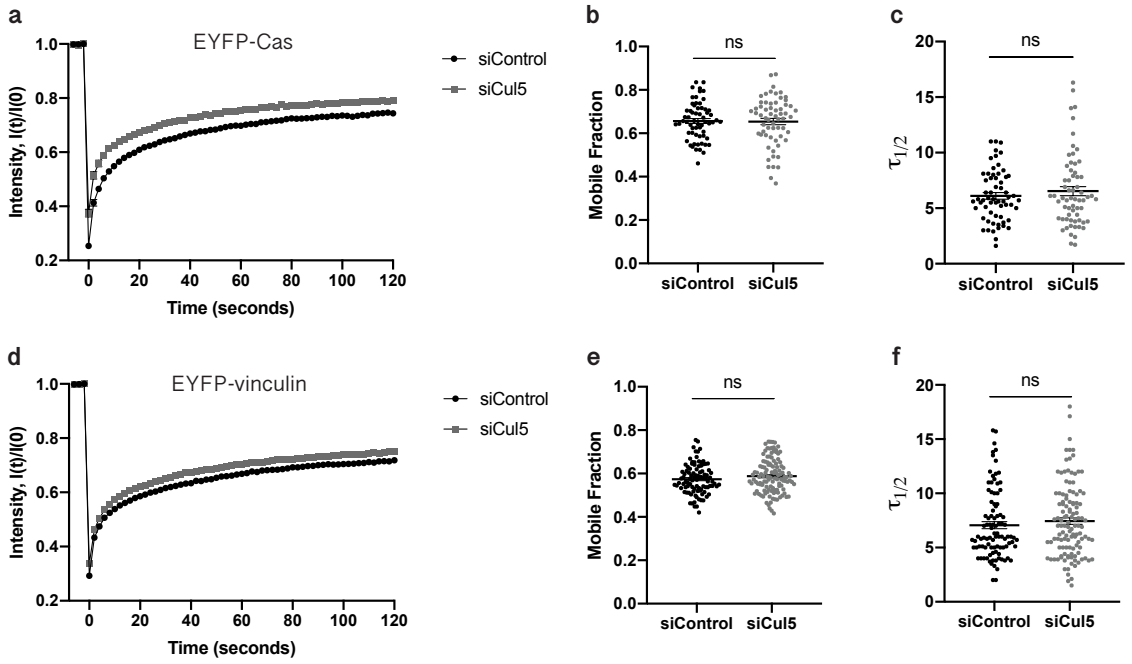

Figure 3.3. Rapid Cas exchange is not regulated by CRL5. (a) MCF10A cells expressing EYFP-Cas were treated with control siRNA or siRNA against Cul5, grown to confluence, scratched and allowed to migrate for 7 hours. Fluorescence recovery curve; mean and SEM of normalized intensities of at least 60 adhesions. (b) Mobile fraction and (c) half recovery time of EYFP-Cas in FAs of migrating cells; mean and SEM of least 60 adhesions per condition; Unpaired t-test p=0.8875 and p=0.4029. (d) MCF10A cells expressing EYFP-vinculin were treated with control siRNA or siRNA against Cul5, grown to confluence, scratched and allowed to migrate for 7 hours. Fluorescence recovery curve; mean and SEM of normalized intensities of at least 95 adhesions. (b) Mobile fraction and (c) half recovery time of EYFP-vinculin in FAs of migrating cells; mean and SEM of least 95 adhesions per condition; Unpaired t-test p=0.1741 and p=0.3989.

I next sought to determine whether a slow-exchanging population of Cas is regulated by CRL5 by knocking down Cul5 and extending the FRAP experiments to 60 minutes. I hypothesized that knocking down Cul5 would decrease the percentage of Cas that exchanges, as pY-Cas would not

be inhibited by CRL5 and would therefore remain in the adhesion. The exchange of vinculin would not change in the absence of Cul5. Unfortunately, I was unable to complete these experiments because the analysis was complicated by changes in FA size and shape, as previously discussed.

3.2.3 *BCAR3 regulates Cas exchange in focal adhesions*

When I first became interested in the dynamics of Cas in FAs, I sought to understand the role of its binding partner BCAR3 in regulating Cas exchange. Since Cas and BCAR3 form a signaling node in FAs [53] and BCAR3 promotes tyrosine phosphorylation of Cas by Src [56, 59], I hypothesized that BCAR3 regulates Cas exchange. Specifically, I proposed a model in which unphosphorylated Cas freely associates and dissociates from FAs by binding BCAR3 and its N-terminal binding partner, FAK. When bound to both FAK and BCAR3, Cas is anchored to the adhesion and phosphorylated by Src. Signaling downstream of pY-Cas stimulates FA disassembly, which is inhibited at the leading edge of migrating cells by CRL5-SOCS6.

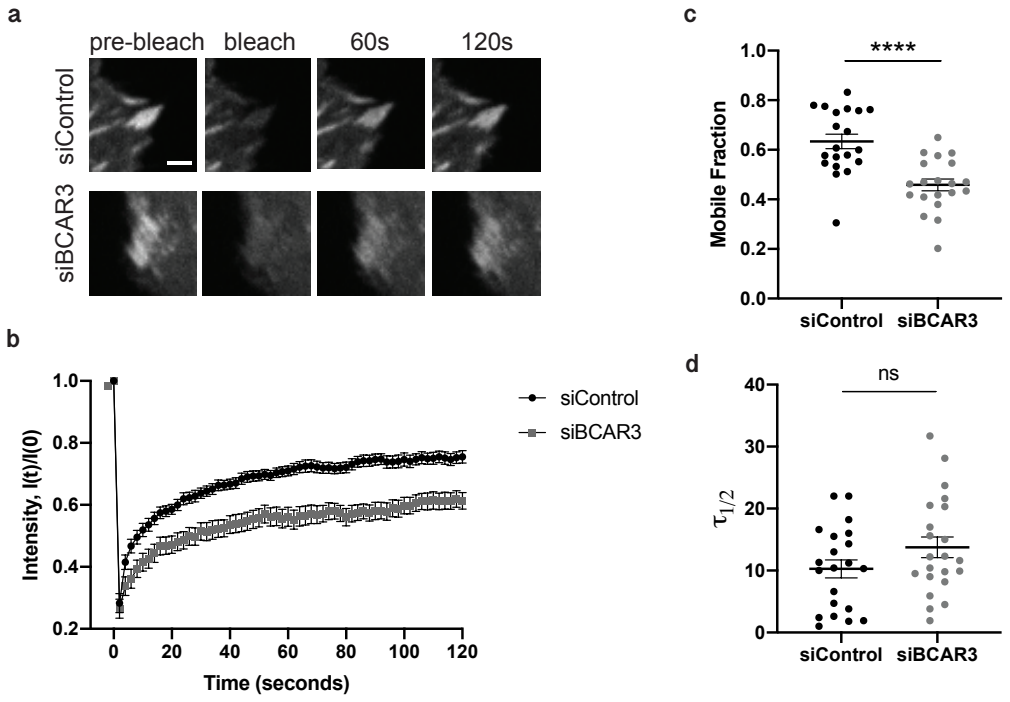

Figure 3.4. BCAR3 regulates Cas exchange in focal adhesions. (a) MCF10A cells expressing EYFP-Cas were treated with control siRNA or siRNA against BCAR3 and plated sparsely. Timecourse images of EYFP-Cas-containing adhesions treated with siControl and siBCAR3 before and after photo-bleaching. Scale bar = 2μm. (b) Fluorescence recovery curve; mean and SEM of normalized intensities of at least 20

adhesions per condition. (c) Mobile fraction and (d) half recovery time of EYFP-Cas; mean and SEM of least 20 adhesions per condition; Unpaired t-test ****$p<0.0001$ and $p=0.1268$.

In order to test my hypothesis that BCAR3 helps anchor Cas to FAs to promote phosphorylation of Cas, I made an MCF10A cell line that stably expresses EYFP-Cas to use in FRAP experiments and measured Cas exchange following transient knockdown of BCAR3 in sparsely plated cells. I hypothesized that knocking down BCAR3 would increase the mobile fraction of Cas, as losing a binding partner would prevent Cas from anchoring to the adhesion. Surprisingly, I found that knocking down BCAR3 significantly decreased the mobile fraction of Cas and had no effect on the half-life (Fig 3.4a-d).

3.3 DISCUSSION

My data suggest that populations of FA proteins previously thought to be immobile may exchange slowly with cytoplasmic protein. Because I only studied the slow exchange of vinculin over long time course FRAP experiments, further research is required to determine if other FA proteins also have a slow-exchanging population. I'm particularly interested in the possibility of a subpopulation of Cas that exchanges slowly and in identifying how this subpopulation is regulated.

In order to continue this project and answer these open questions, challenges involved in measuring and analyzing fluorescence recovery over long periods of time need to be overcome. One challenge of analyzing long timescale FRAP data collected from migrating cells is that focal adhesions restructure over time, changing both size and shape. This structural reorganization is enhanced (accelerated) in migrating cells, where adhesions are less stable and turnover to promote movement. For this reason, most experiments examining the exchange of focal adhesion proteins are done on cells plated in dishes where migration has not been stimulated and focal adhesions are somewhat stable. In fact, one study investigating the dynamics of paxillin and vinculin justify their choice of cell type (HeLa cells) and short FRAP timescale (up to 2-3 minutes) by pointing out that the focal adhesions would not restructure over the course of the experiment [105]. Changes in size and shape of the adhesions complicates the analysis of the fluorescence recovery. If an adhesion grows in size over the course of the experiment, should the percent recovery still be calculated

using the initial fluorescence intensity before photobleaching? Under this scenario, the fluorescence intensity of a fully recovered adhesion would be higher than the initial intensity. The established analysis methods for FRAP do not account for changes in these variables. Therefore, using these methods would artificially inflate the total percent recovery and half recovery time. In addition to measuring protein exchange, we would also be measuring the addition of new fluorescent proteins. Due to these complications, I was unable to convincingly analyze protein dynamics in the focal adhesions of migrating cells over long periods of time.

To more closely characterize the slow-exchanging population of FA protein, mathematical modeling and curve fitting needs to be used and novel models may need to be developed. The most simple model, where there is one binding state, fits the normalized FRAP data to an exponential equation. In a more complicated model where there are two binding states, normalized FRAP data may be fit to a double exponential equation. A model for multiple, sequential binding sites where an initial binding interaction is required for subsequent binding events has not yet been developed [113]. Given that FRAP experiments measuring fluorescence recovery over 60 minutes has never been done, more advanced modeling and collaboration is required to understand the slow-exchanging population of vinculin I identified.

The identification of a slow-exchanging population of vinculin raises interesting questions about possible differences of exchange in FAs in different cellular locations and whether this population is found in a specific section of individual FAs. Given my observation that different FAs reached total fluorescence recovery of EYFP-vinculin anywhere from 10 to >60 minutes, it is possible that differences in FA location and cell-cell contact could contribute to the regulation of FA dynamics. In fact, a recent study showed that FA protein dynamics can change depending on FA location relative to the cell edge and on whether the FA is parallel to or pointing to the cell edge [108]. Additionally, photoconversion experiments much like I previously described have demonstrated that FA proteins can be labeled and observed leaving adhesions, with the remaining protein forming clusters in the FA [108]. Utilizing photoconversion experiments such as these could provide insight into the spatial position of the slow-exchanging population within the adhesion and whether this is regulated by the position of the FA in the cell.

Chapter 4. CONCLUSIONS AND FUTURE DIRECTIONS

This dissertation details a novel mechanism of BCAR3 regulation, where pY117-BCAR3 is targeted for proteasomal degradation by the E3 ubiquitin ligase, CRL5-SOCS6. In addition, BCAR3 Y117 is required for BCAR3-induced membrane ruffling and for BCAR3 to support the increased membrane ruffling and migration observed in Cul5-deficient cells. This result was surprising, as we hypothesized that the increased abundance of BCAR3 Y117F would result in a gain of function phenotype, and suggests that BCAR3 Y117 is required both for function and turnover of BCAR3. As such, this work is the first to identify a biological role for a specific phosphorylation site in BCAR3.

In addition to BCAR3 Y117, the BCAR3 SH2 domain and Cas-binding site are required for BCAR3-induced membrane ruffling and to rescue the increased membrane ruffling and migration of Cul5-deficient cells. These sites are also required for efficient BCAR3-mediated Cas phosphorylation in leading edge adhesions.

Collectively, my work supports a model in which Cas recruits BCAR3 to adhesion sites, where BCAR3 stimulates Cas tyrosine phosphorylation dependent on BCAR3 Y117 and BCAR3 SH2 domain. Overall, my results provide new insights into BCAR3 protein expression, degradation and phosphorylation, and Cas phosphorylation and activity to induce leading edge protrusion in migrating cells.

4.1 MECHANISMS REGULATING BCAR3 PROTEIN EXPRESSION

Despite many studies detailing the biological functions of BCAR3 [44-46, 50, 52, 54-56, 58, 59, 98, 114-117], how BCAR3 expression is regulated is not well understood. RNA levels vary in different tissues and across different cancer cell lines and patient samples, suggesting transcriptional regulation. In addition to direct transcriptional regulation, BCAR3 RNA levels may be regulated by microRNAs (miRs), as BCAR3 expression is inhibited by miR-126-5p in endometrial cells, which acts as a regulator of cell migration and invasion [118]. My studies and the work of others also demonstrate the importance of the regulation of BCAR3 protein levels and stability. A previous study showed that TGFβ stimulates proteasomal degradation of BCAR3 [48],

although the details of this mechanism have not been worked out. Further studies may reveal additional mechanisms through which BCAR3 is regulated and how these mechanisms modulate BCAR3 expression or function. Indeed, while investigating CRL5-mediated turnover of BCAR3, I discovered two more possible CRL5-independent mechanisms of BCAR3 turnover.

First, BCAR3 is degraded by an unidentified factor found in the MCF10A growth media, independent of Cul5. When protein synthesis was stopped replacing the conditioned media with fresh media containing cycloheximide, BCAR3 was consistently degraded in both control and Cul5-deficient cells (Supplement Figure 9). Subsequent experiments revealed that adding cycloheximide directly to the media already on the cells resulted in stabilization of BCAR3 in the absence of Cul5, as previously discussed (Figure 2.1d). This surprising result suggests that additional stimulation with some factor that had been depleted activates the degradation of BCAR3 independent of CRL5. Possible stimuli include EGF, insulin, hydrocortisone, cholera toxin or a component in horse serum. Follow up experiments to identify the factor did not yield conclusive results (data not shown).

Second, I found that Cas protects BCAR3 from CRL5-independent degradation. BCAR3 and Cas stabilize each other in breast cancer cells [59] and I observed a similar relationship in normal breast cells (Supplement Figure 10). When Cas is knocked down using RNAi, BCAR3 protein levels are reduced in control and Cul5-deficient cells, suggesting that BCAR3 is destabilized in the absence of Cas regardless of the presence of CRL5 (Supplement Figure 10b). Details of this mechanism are not understood. BCAR3/Cas stabilization in breast cancer cells requires their association [59], so it is possible that uncoupling of BCAR3 from Cas reveals site(s) required for their turnover or induces conformational changes that do so.

Although I was unable to work out the mechanisms of these two CRL5-independent mechanisms of BCAR3 degradation, it would be interesting to identify how these pathways fit into the context of CRL5-dependent BCAR3 turnover and its role in regulating membrane ruffling and migration. Given the increased migration and invasion in breast cancer cell lines relative to the normal breast epithelial cells in this study, it would be interesting to determine whether mis-regulation of these mechanisms contributes to the enhanced migratory phenotypes in breast cancer.

4.2 BCAR3 PHOSPHORYLATION

This work identified BCAR3 Y117 as a site required for CRL5-mediated turnover and function of BCAR3 and suggests that phosphorylation at this site is crucial. Despite many attempts to use mass spectrometry to identify which kinase or extracellular stimuli is responsible for phosphorylation of Y117 or other BCAR3 tyrosine sites, I was unsuccessful. Therefore, we do not know whether phosphorylation occurs in adhesions or in the cytosol, or whether it is catalyzed by integrin-linked kinases, such as SFKs or FAK, or growth factor receptors. If growth factor receptors are responsible, BCAR3 may provide a mechanism to only allow integrin-dependent Cas phosphorylation when growth factors are present.

Previous studies in the literature and some of my own work provide insight into possible signals that stimulate BCAR3 phosphorylation, which we are actively investigating. An early study showed that BCAR3 is tyrosine phosphorylated in response to serum and adhesion [60]. In addition to studies that directly investigate BCAR3 phosphorylation, looking for binding partners and known functional roles in different signaling pathways can also provide potential candidates to investigate. BCAR3 binds EGFR through its SH2 domain [50, 51] and regulates EGF-stimulated membrane ruffling [45]. BCAR3 also regulates insulin-stimulated membrane ruffling [62]. Additionally, my work has shown that stimulation of MCF10A cells with EGF/insulin or EGF alone promote phosphorylation of BCAR3, indicated by the band shift following stimulation (Supplement Figure 11). Given that EGF and insulin are components of MCF10A media that stimulate unknown sites of BCAR3 phosphorylation and that BCAR3 regulates cell spreading and adhesions [46, 54, 56], we are currently investigating whether adhesion, EGF or insulin stimulate BCAR3 pY at Y117. Since little is known about the regulation and function of other BCAR3 phosphorylation sites, we are also interested in following up on any other sites that come up in these experiments.

4.3 HOW BCAR3 PROMOTES CAS PHOSPHORYLATION

This work identified novel sites of BCAR3 that are required to promote Cas phosphorylation. While previous work demonstrated the importance of BCAR3-Cas binding for BCAR3-mediated

Cas phosphorylation [59], the role of BCAR3 Y117 and SH2 domain has not been established. How BCAR3 Y117 and SH2 domain regulate Cas phosphorylation remains unclear.

It is possible that pY117 BCAR3 regulates Src activity on Cas, as BCAR3 has also been shown to regulate Src kinase activity [52, 56, 58]. While it is unknown how BCAR3 regulates Src activity, it is possible that the mechanism involves the protein tyrosine phosphatase, PTPα, which is a known Src activator [85, 86]. Previous work identified PTPα as a BCAR3 binding partner. Interestingly, the BCAR3-PTPα interaction is mediated by pY789 PTPα and the BCAR3 SH2 domain [52], which could explain my result that the BCAR3 SH2 domain is required to promote Cas phosphorylation at leading edge adhesions. Given these studies, a possible model of BCAR3 regulation of Src kinase activity and pY-Cas could be BCAR3 SH2 domain-mediated BCAR3-PTPα association activates Src kinase.

In the future, it would be interesting to investigate the role of PTPα in this model. By knocking down PTPα in MCF10A cells and examining the effect on Cas phosphorylation, I could determine whether PTPα contributes to the regulatory pathway I've identified. In addition to the published work suggesting that PTPα binds BCAR3 and is required for BCAR3 localization to adhesion sites [52], unpublished work from our lab provides evidence that PTPα may be regulated by CRL5. PTPα may work downstream of SOCS2 [90] and overexpressed PTPα protein levels may be regulated by CRL5. While detecting endogenous PTPα using available antibodies has been challenging, further investigation of the role of PTPα in this regulatory mechanism could provide insight into how BCAR3 regulates Cas phosphorylation.

My finding that knocking down BCAR3 decreases the mobile population of Cas in adhesions could be consistent with the requirement of BCAR3 for Cas phosphorylation, as Cas phosphorylation and recruitment of CRL5-SOCS6 is required for Cas removal from adhesions [79]. However, this result is difficult to interpret because I was unable to measure Cas exchange over a long time course to examine the slow-exchanging population. A study examining Cas exchange in the presence and absence of Cul5 over a long time course would clarify whether slow Cas exchange is regulated by CRL5. In addition to experiments using RNAi, measuring Cas exchange in cells where endogenous BCAR3 has been replaced with the BCAR3 mutants used in this study, which

I have shown inhibit phosphorylation of Cas, could provide us with insight into how Cas leaves adhesions.

Chapter 5. MATERIALS AND METHODS

5.1 PLASMIDS

pMXpuroII and pMXpuroII-shCul5 plasmids were made as previously described [76].

pLKO.1-nontarget small hairpin RNA (shRNA) control vector (SHC002) and pLKO.1-shSOCS6 (TRCN0000284351) were purchased (Sigma Aldrich).

pCAG-T7-mSOCS1, pCAG-T7-mSOCS2, pCAG-T7-mSOCS3, pCAG-T7-mSOCS4, pCAG-T7-mSOCS5, pCAG-T7-mSOCS6, pCAG-T7-mSOCS7, and pCAG-T7-mCisH were made as previously described [76, 77]. All pCAG-T7-SOCS plasmids used in this work have LC-QQ mutations to prevent binding to CRL5, which were made as previously described [90]. pCAG-T7-mSOCS6 R407K was made as previously described [79]. pCAG-T7-mSOCS6 ΔC was made by PCR amplifying codons 1-381 of mSOCS6 using 5' primer complementary to the T7 tag and a 3' primer that inserts a stop codon after codon 381 followed by a NotI site. The PCR product was inserted into pCAG-T7-SOCS6 by BamH1/NotI restriction digest and ligation.

pCMV-SPORT6-mBCAR3 was purchased from the Harvard Plasmid Database (MmCD00318547). pcDNA5-3xFlag-mBCAR3 FRT/TO was made by Gateway cloning. mBCAR3 was PCR amplified with flanking attB sites from pCMV-SPORT6-mBCAR3 and inserted into pDONR221 with a BP reaction (Thermo Fisher Scientific). pDEST-5'-3xFlag-pcDNA FRT/TO was a gift from Anne-Claude Gingras [90]. pDONR221-mBCAR3 was moved into pDEST-5'-3xFlag-pcDNA FRT/TO with a LR reaction (Thermo Fisher Scientific).

pLX304-hBCAR3-V5 was obtained from the Patrick Paddison lab [119]. pLX304-hBCAR3-F5-V5 was made by Gibson Assembly (NEB). A gBlock containing BCAR3 Y42F, Y117F, Y212F, Y266F and Y429F mutations was assembled into pLX304-hBCAR3-V5.

rtTA-N144 (Plasmid #66810) and pLenti-CMV-TRE3G-eGFP Blast (Plasmid #27568) were purchased (Addgene).

pLenti-TRE3G-SNAP-V5-hBCAR3 was made by Jason Berndt as follows. A gBlock containing sequence for SNAP-V5 tags was inserted into pLTRE3G-eGFP at the AgeI restriction site using Gibson Assembly (NEB) to make pLTRE3G-SNAP-V5-eGFP. hBCAR3 was PCR amplified with flanking AgeI and XbaI sites and inserted into AgeI and XbaI-digested pLTRE3G-SNAP-V5-eGFP to make pLTRE3G-SNAP-V5-hBCAR3.

pLTRE3G-SNAP-V5-hBCAR3 Y266F and pLTRE3G-SNAP-V5-hBCAR3 R177K were made by site-directed mutagenesis. pLTRE3G-SNAP-V5-hBCAR3 Y42F, pLTRE3G-SNAP-V5-hBCAR3 Y212F, pLTRE3G-SNAP-V5-hBCAR3 Y429F, and pLTRE3G-SNAP-V5-hBCAR3 EE were made by Jason Berndt using site-directed mutagenesis. pLTRE3G-SNAP-V5-hBCAR3 Y117F was made by Gibson Assembly (NEB). A gBlock containing the BCAR3 Y117F mutation was assembled into pLTRE3G-SNAP-V5-hBCAR3 WT. pLTRE3G-SNAP-V5-hBCAR3 F5 was made by BamHI restriction digest of pLTRE3G-SNAP-V5-hBCAR3 Y42F and pLX304-hBCAR3-F5-V5 and ligation of the hBCAR3 5F fragment into BamHI-digested pLTRE3G-SNAP-V5-hBCAR3 WT. pLTRE3G-SNAP-V5-hBCAR3 F4 was made by PshAI restriction digest of pLTRE3G-SNAP-V5-hBCAR3 WT and pLTRE3G-SNAP-V5-hBCAR3 F5, followed by ligation of the hBCAR3 Y117F fragment from the WT plasmid into the PshAI-digested F5 plasmid.

pMSCVpuro-EYFP-vinculin was made as previously described [79]. pMSCVpuro-EYFP-Cas was made as previously described [76].

5.2 CELL LINES

MCF10A cells were cultured in DMEM/F12 (Thermo Fisher Scientific) supplemented with 5% horse serum (Thermo Fisher Scientific), 0.1 μg/ml cholera toxin (EMD Millipore), 10 μg/ml insulin (Thermo Fisher Scientific), 0.5 μg/ml hydrocortisone (Sigma-Aldrich), and 20 ng/ml EGF (Thermo Fisher Scientific). Indicated experiments used assay media (DMEM/F12, 2% horse serum, 0.1 μg/ml cholera toxin, 10 μg/ml insulin, 0.5 μg/ml hydrocortisone, and 0 ng/ml EGF). The cells were passaged using 0.02% trypsin in PBS/EDTA. Trypsin was inactivated with an equal

volume of DMEM/10% FBS and cells were harvested by centrifugation before resuspending in growth media. HeLa, U2OS, and 293T cells were grown in DMEM/10% FBS and passaged with trypsin as above.

MCF10A EV and shCul5 cells were made as previously described [76]. MCF10A shControl and shSOCS6 cells were made by Carissa Pilling. Viruses containing pLKO.1-control and pLKO.1-shSOCS6 were packaged using HEK 293T cells and MCF10A cells were infected. Stable cell lines were selected using 4µg/mL puromycin.

BCAR3 KO MCF10A cells were made by Jason Berndt as follows. Early passage MCF10A cells were serially diluted and subclones were grown and characterized. Clone J8 was selected because cell morphology matched MCF10A parental cells. The J8 clonal cell line was infected with CRISPR plasmid, pLCRISPRv2, containing either empty vector or guide RNA against BCAR3. pLCRISPRv2-sgRNA-hBCAR3 were made by cloning annealed oligos (5'-CACCGTCAGAGAGCTACCTGCCGAT-3' or 5'-CACCGCCCGAAACATACCAATCGGC-3') into the BsmBI site of pLCRISPRv2. Potential knockouts were isolated by single cell expansion. Validation of BCAR3 knockout was done through gDNA isolation, PCR, and sequencing, as well as Western blotting.

MCF10A dox-inducible SNAP-V5 BCAR3 cells were made with help from Laura Arguedas-Jimenez. Viruses containing rtTA-N144 were packaged using 293T cells and used to infect MCF10A cells. A stable line was selected using 50µg/mL hygromycin. The MCF10A cell line stably expressing rtTA was then infected with viruses containing one of the pLTRE3G-SNAP-V5 constructs (pLTRE3G-SNAP-V5-eGFP, pLTRE3G-SNAP-V5-BCAR3 WT, pLTRE3G-SNAP-V5-BCAR3 Y42F, pLTRE3G-SNAP-V5-BCAR3 Y117F, pLTRE3G-SNAP-V5-BCAR3 Y212F, pLTRE3G-SNAP-V5-BCAR3 Y266F, pLTRE3G-SNAP-V5-BCAR3 Y429F, pLTRE3G-SNAP-V5-BCAR3 F5, pLTRE3G-SNAP-V5-BCAR3 F4, pLTRE3G-SNAP-V5-BCAR3 R177K, or pLTRE3G-SNAP-V5-BCAR3 EE). Stable lines were selected using 10µg/mL blasticidin. Each cell line was hygromycin resistant and blasticidin resistant, however not all cells within each line expressed the SNAP-V5-containing construct following induction with 50-100ng/mL dox for 48-72 hours (determined by immunofluorescence). To remove non-inducible cells, dox-treated cells

were treated with 100nM JaneliaFluor cp646-SNAP-ligand (Lavis Lab, Janelia Farms) [97] for 1 hour, washed three times with PBS, incubated in ligand-free growth media for an hour and positive cells were sorted and harvested by FACS using the APC channel to detect JF cp646.

MCF10A cells stably expressing EYFP-vinculin were made as previously described [79]. MCF10A cells stably expressing EYFP-Cas were made by retrovirus infection with pMSCV-EYFP-Cas and selected with 2μg/mL puromycin. Low-expressing cells compatible with microscopy experiments were sorted and harvested by FACS.

5.3 ANTIBODIES

Antibodies used in this dissertation: rabbit anti-BCAR3, rabbit anti-V5 (Bethyl); mouse anti-Cas, mouse anti-paxillin (BD Biosciences); rabbit anti-BCAR3, rabbit anti-pY165-Cas (Cell Signaling Technology); rabbit anti-Cullin5 (Abcam); rabbit anti-Cas, rabbit anti-FAK, rabbit anti-GAPDH (Santa Cruz Biotechnology); mouse anti-vinculin, rabbit anti-FLAG, mouse anti-FLAG (Sigma); mouse anti-T7 tag (EMD Biosciences); mouse anti-V5 (Invitrogen); 4G10 (Bio X Cell).

5.4 REAGENTS

Reagents used in this dissertation: cycloheximide (Sigma), epidermal growth factor (Invitrogen), MLN4924 (Active Biochem), MG132 (Fisher Scientific), bafilomycin A, doxycycline (Fisher Scientific).

5.5 siRNA TRANSFECTION

MCF10A cells were trypsinized and plated in a 12-well plate right before transfection such that cells would be 50% confluent after attaching. A mixture of 50 pmol siRNA, 1.25μl Lipofectamine 2000 (Invitrogen) and Optimem (Invitrogen) was added to the newly plated MCF10A cells and left on overnight. The next day the media was changed to fresh growth media. A second siRNA transfection was done 48 hours after the first transfection using the same protocol scaled up to use a 6-well dish (125 pmol siRNA).

HeLa and U2OS cells were plated in a 12-well plate the day before transfection such that cells were 50% confluent at the time of transfection. A mixture of 50 pmol siRNA, 2.5µl oligofectamine (Invitrogen) and Optimem was added to directly to the cells after two washes with PBS. After 4 hours, Optimem with 20% FBS was added to the cells. The next day, cells were split into 6-well dishes with fresh growth media. A second siRNA transfection was done 48 hours after the first transfection using the same protocol scaled up to use a 6-well dish (125 pmol siRNA).

Cells were either lysed or assays were performed 48 hours after the second transfection.

Table 5.1 siRNA Sequences

siRNA	Target Sequence	Source	Notes
Control siRNA	5'-AATTCTCCCGAACGTGTCACGT-3'	Qiagen	
SOCS6 siRNA Pool	5'-TAGAATCGTGAATTGACATAA-3' 5'-CAGCTGCGATATCAACGGTGA-3' 5'-TTGATCTAATTGAGCATTCAA-3' 5'-CGGGTACAAATTGGCATAACA-3'	Qiagen	
Cul5 siRNA Pool	5'-GACACGACGTCTTATATTA-3' 5'-CGTCTAATCTGTTAAAGAA-3' 5'-GATGATACGGCTTTGCTAA-3' 5'-GTTCAACTACGAATACTAA-3'	GE Dharmacon	
BCAR1 siRNA Pool	5'-AAGCAGTTTGAACGACTGGAA-3' 5'-CTGGATGGAGGACTATGACTA-3' 5'-CAGCATCACGCGGCAGGGCAA-3' 5'-CAACCTGACCACACTGACCAA-3'	Qiagen	
BCAR3 siRNA Pool	5'-CCGGAACTCTGGCGTCAACTA-3' 5'-CCGAGCGGCCACTCTGAGTAA-3' 5'-GCCCAACGAGTTTGAGTCAAA-3' 5'-AAGGTATCAGTTATATGATAT-3'	Qiagen	
BCAR3 siRNA	5'-GGUAACUACUGCUAAUGUUTT-3'	Life Technologies	Targets 3'UTR

5.6 QPCR

An RNeasy Plus Mini kit (Qiagen) was used to extract RNA and an iScript reverse transcription supermix (BioRad) was used to make cDNA. cDNA abundance was measured using an iTaq

Universal SYBR Green Supermix kit (BioRad) using primers listed in Table 5.2. Samples were run on the QuantStudio 5 Real-Time PCR System.

Table 5.2 qPCR Primers

Primer	Sequence
BCAR3 forward	5' – AATCGCTTCTCCAAACAGAGC – 3'
BCAR3 reverse	5' – ATTCACCGGCATGTTTCTGG – 3'
Cul5 forward	5' – TTTTATGCGCCCGATTGTTTTG – 3'
Cul5 reverse	5' – TTGCTGGGCCTTTATCATCCC – 3'
GAPDH forward	5' – CAGCCTCAAGATCATCAGCA – 3'
GAPDH reverse	5' – TGTGGTCATGAGTCCTTCCA – 3'

5.7 Cell lysis and Western blotting

Cells were washed three times in phosphate-buffered saline (PBS) before lysis. Cells were lysed in X-100 buffer (1% Triton X-100, 150mM NaCl, 10mM HEPES pH 7.4, 2mM EDTA, 50mM NaF) or RIPA buffer (1% Triton X-100, 0.1% SDS, 20mM Tris-HCl pH 7.4, 150mM NaCl, 5mM EDTA, 5mM EGTA, 1% sodium deoxycholate) with fresh protease inhibitors (10ug/mL Aprotinin, 1mM PMSF, 1mM Sodium Vanadate) added before use.

Lysates were boiled in 1xSDS sample buffer, resolved by SDS-PAGE using 10% polyacrylamide gels, and transferred onto nitrocellulose membrane. The membrane was blocked in Odyssey blocking buffer (TBS) (LICOR) with 5% BSA for phosphotyrosine antibodies or 5% non-fat dry milk for all other antibodies. Following blocking, the membrane was probed with a primary antibody followed by IRDye 800CW goat anti-rabbit or 680RD goat anti-mouse conjugated secondary antibodies. Membranes were visualized using the Odyssey Infrared Imaging System (LICOR).

5.8 DNA transfections and Immunoprecipitation

HeLa cells were plated in 6-well plates the day before transfection such that cells were 50% confluent on the day of transfection. A mixture made of DNA, Lipofectamine 2000 (Thermo Fisher

Scientific) and Optimem (Invitrogen) was made according to manufacture protocol, added to the cells and removed after 5 hours.

Between 24-48 hours after transfection, immunoprecipitation experiments were conducted. For indicated experiments, cells were incubated with 1mM sodium pervanadate for 30 minutes. Cells were lysed on ice in X-100 buffer (1% Triton X-100, 150mM NaCl, 10mM HEPES pH 7.4, 2mM EDTA, 50mM NaF) and fresh protease inhibitors (10ug/mL Aprotinin, 1mM PMSF, 1mM Sodium Vanadate). Lysates were cleared by centrifugation for 10 minutes at 14,000 g. Lysates were rotated with 1µg antibody at 4°C for 3 hours, after which Protein A/G plus agarose beads (Santa Cruz Biotechnology) were added for 1 hour at 4°C. Centrifugation was used to pellet the beads at the bottom of the tube and the beads were washed three times with lysis buffer. The beads were resuspended in SDS sample buffer, boiled, lightly mixed to release bound protein and centrifuged. Immunoprecipitation samples were resolved by SDS-PAGE using 10% polyacrylamide gels and bound proteins detected by Western blotting as above. Samples of total cell lysate typically contained 5% of the protein used for immunoprecipitation.

5.9 CYCLOHEXIMIDE CHASE ASSAY

Cells were grown to 80% confluency and treated with 25µg/mL cycloheximide by adding it directly to the conditioned media on the cells. Cells were treated with cycloheximide for 0, 2, 4, or 8 hours and lysed. Quantification of Western blots was done in ImageJ and BCAR3 protein levels were normalized to the loading control (GAPDH or vinculin).

5.10 PHOSPHOPROTEOMICS

HeLa cells were transiently transfected with SNAP-V5-BCAR3 and the media was changed after 5 hours. 48 hours following transfection, the confluent 10cm dish of cells was treated with pervanadate for 30 minutes. At 4ºC, cells were lysed with Triton X-100 buffer with protease inhibitors, incubated with V5-antibody for 3 hours and Protein A/G agarose beads were added for 1 hour. The beads were washed three times with lysis buffer, boiled in SDS sample buffer and

resolved by SDS-PAGE (Invitrogen). The gel was stained with SimplySafe blue stain (Thermo Fisher Scientific) and the SNAP-V5-BCAR3-containing bands were cut from the gel for analysis in Shao-En Ong's lab at the University of Washington with Ho-Tak Lau. A targeted acquisition algorithm was used to sequence masses of BCAR3 pY-containing peptides.

5.11 SCRATCH WOUND ASSAY

The desired proteins were knocked down using two siRNA transfections, as previously described. Cells were plated in ImageLock 96-well dishes (Essen BioScience) for the second siRNA transfection and transfection materials were scaled down proportional to dish sizes. Cells were plated at 30% confluence at the time of the second transfection. For migration assays where dox-induction was required, the media was replaced with growth media containing dox (10 ng/mL except where noted) 6 hours after transfection and after two washes with PBS. For all migration assays, the confluent monolayers were placed in EGF-free assay media (with dox when required) 48 hours after the second transfection transfection. Monolayers were scratched using an Incucyte WoundMaker 8 hours after being placed in assay media, the wells were washed with PBS three times to remove debris and cells were placed back in assay media (with dox when required). Scratch wounds were imaged once every 2 hours on an IncuCyte S3 and images were analyzed using the scratch wound function on the IncuCyte image analysis software. Overall migration was measured using the relative wound density calculated by the analysis software. Lamellipodium length was measured using the ruler in the IncuCyte image analysis software. Membrane ruffles were visualized as dark contrast at the front of the protrusion. Ruffling was scored by counting the number of leading edge cells that did and did not have membrane ruffles to calculate a percentage of ruffling cells.

5.12 TRANSWELL MIGRATION AND INVASION ASSAYS

Cells were grown in EGF-free assay media for 24 hours before the assay. Migration assays were performed in 24-well chemotaxis chamber with an 8μm pore size polyethylene terephthalate filter that separated the upper and lower wells (Thermo Fisher Scientific). Invasion assays were performed in 24-well Matrigel invasion chambers with an 8μm pore size polyethylene

terephthalate filter coated in Matrigel matrix that separated the upper and lower wells (Thermo Fisher Scientific). In both assays, the lower wells were filled with MCF10A growth media. 80,000 cells were resuspended in EGF-free assay media and added to the top well. After 24 hours, cells on the top of the membrane were removed and the cells on the bottom of the membrane were fixed with methanol and stained with SybrSafe at 1:10,000 for 15 minutes. Membranes were rinsed in TBE, imaged and nuclei were counted.

5.13 IMMUNOFLUORESCENCE

For experiments that required protein knockdown, cells were transfected with siRNA as previously described. On the day following the second siRNA transfection, cells were plated on 12-mm #1.5 coverslips at 30% confluency in 4-well or 24-well (1.9 cm^2) plates for scratch wound assays (with dox when required). Cells were placed in assay media overnight the day before the assay and confluent monolayers were scratched with a P200 pipette tip the following morning. Cells were fixed and permeabilized 6 hours after the start of migration.

For experiments where the SNAP tag needed to be labeled, JaneliaFluor cp549JF SNAP-ligand (Lavis Lab, Janelia Farms) [97] was added to the cells at 100nM 4 hours after forming the wounds. Cells were incubated for 1 hour with the SNAP-ligand, washed three times with PBS and placed in fresh, ligand-free assay media for 1 hour.

Cells were fixed and permeabilized with 0.1% Triton X-100/4% paraformaldehyde (PFA)/PBS for 2 minutes at room temperature (RT) and further fixed with 4% PFA/PBS for 15 minutes at RT. Cells were blocked with 2% BSA + 5% normal goat serum/PBS for 30 minutes at RT. Primary antibodies were diluted in block solution (typically 1:200 dilution) and added for 3 hours are RT. Coverslips were washed three times with PBS. AlexaFluor-labeled secondary antibodies and AlexaFluor-labeled phalloidin were diluted in PBS 1:1000 or according to manufacture protocol and were added to the coverslips for 1 hour at RT. Coverslips were washed three times with PBS, mounted in Prolong Glass Antifade Mountant and left to cure at RT overnight in the dark.

5.14 IMAGING AND IMAGE ANALYSIS

Coverslips were imaged using 63x, 1.40 NA or 100x, 1.40 NA oil objectives on a Leica SP8 confocal microscope. Images were acquired and deconvolved using Leica LAS acquisition software. Images in the supplement were taken using a Zeiss LSM 780 NLO confocal microscope and 63x, 1.4 NA or 100x, 1.45 NA oil objectives. Scale and imaging settings were consistent within each experiment.

Image analysis was done in ImageJ. A line was drawn ~6μm from the front of the migrating cells, as described in [79], to isolate the leading edge. Using the threshold tool on ImageJ, paxillin-containing adhesions were identified and mean intensity of SNAP, pY-Cas, EYFP-Cas and paxillin in these leading edge adhesions and in the cytoplasm at the base of the cell were calculated. The SNAP/paxillin ratio was calculated by subtracting a ligand background mean intensity value (taken from a non-dox-induced sample) from the SNAP mean intensity, normalizing to the cytoplasmic SNAP mean intensity and then dividing by the paxillin mean intensity that was normalized to cytoplasmic paxillin mean intensity. The EYFP-Cas/paxillin ratio was calculated by normalizing the mean intensities of each in adhesions to the mean intensities in the cytoplasm and dividing normalized EYFP-Cas intensity by the normalized paxillin intensity. The pY-Cas/paxillin ratio was calculated by dividing the mean intensity of pY-Cas in adhesions by the mean intensity of paxillin.

5.15 FLUORESCENCE RECOVERY AFTER PHOTOBLEACHING AND PHOTOCONVERSION

Cells were either plated sparsely or for a scratch wound, as previously described, in glass-bottomed 35mm Fluorodishes (World Precision Instruments). For migrating cells, assays were started 7 hours after scratching the confluent monolayer of cells. A live cell imaging apparatus was used to control temperature and CO_2 levels.

FRAP experiments were conducted on a PerkinElmer Ultraview Vox spinning disk confocal microscope using a 60x objective and Perfect Focus. EYFP-Cas or EYFP-vinculin-containing adhesions were identified and photobleached using a 405nm laser at 45% laser power and 60

iterations of ablation. For short FRAP experiments, images were taken every 2 seconds for 2 minutes. For long FRAP experiments, images were taken once a minute for 1 hour. Fluorescence intensities of each adhesion at each timepoint were measured using ImageJ. Fluorescence intensities were normalized to the intensity at t=0 to generate FRAP recovery curves. Mobile fractions and half recovery times were calculated using the intensity at the last timepoint and the fraction of signal that was photobleached.

Photoconversion experiments were conducted either on a PerkinElmer Ultraview Vox spinning disk confocal microscope or a Zeiss LSM 780 NLO confocal microscope. mEos2-Cas or mEos3.2-Cas-containing adhesions were identified and photobleached using a 405nm laser at 15-60% laser power and 50-100 iterations of ablation.

APPENDIX

Supplement Figure 1. BCAR3 protein level and stability are increased in Cul5-deficient cells in low serum, EGF-free media.

MCF10A EV and Cul5-deficient cells were EGF-starved overnight and (a) lysed for Western blotting or (b) treated with CHX for 0, 2, 4 and 8 hours and lysed for Western blotting. Similar to what was observed in EGF-containing growth media, BCAR3 protein level and stability are increased in the absence of EGF.

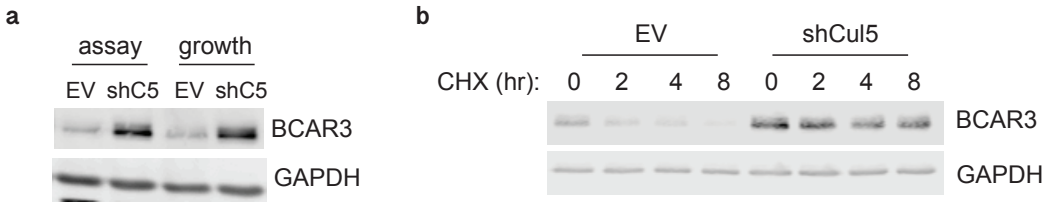

Supplement Figure 2. BCAR3 is regulated by CRL5-SOCS6 in U2OS cells, but not in HeLa cells.

(a) Control and Cul5-deficient U2OS cells were grown in DMEM supplemented with 10% FBS growth media and low serum assay media for 24 hours and lysed for Western blotting. BCAR3 protein levels are increased in Cul5-deficient cells under both growth conditions. (b) U2OS cells were transfected with control siRNA and siRNA against Cul5 and SOCS6. BCAR3 protein levels are increased when Cul5 and SOCS6 are knocked down. (c) HeLa cells were transfected with control siRNA and siRNA against Cul5 and SOCS6. BCAR3 protein levels are not increased when Cul5 and SOCS5 are knocked down. Cas levels are increased in the absence of Cul5 or SOCS6.

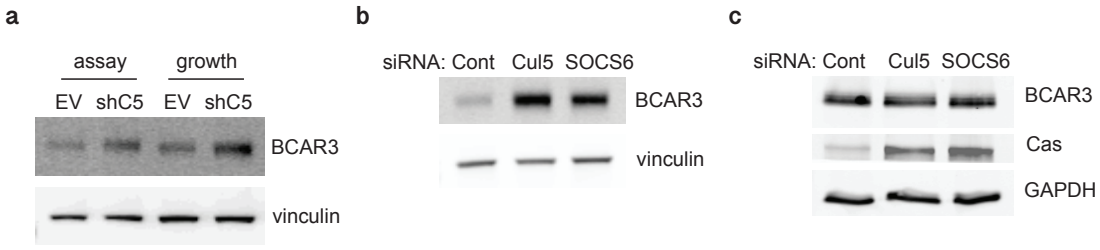

Supplement Figure 3. BCAR3 Y42, Y117, Y266 and Y341 are phosphorylated in HeLa cells and Y117 is phosphorylated at higher levels following treatment with pervanadate.

(a) HeLa cells were transfected with SNAP-V5-BCAR3 WT, treated with pervanadate for 30 minutes and lysed. Lysates were immunoprecipitated with anti-V5 antibody. The samples were run out on a gel, which was then stained with SimplySafe blue stain, and the bands corresponding to SNAP-V5-BCAR3, indicated by the arrow, were cut out of the gel for phosphoproteomic analysis. (b) A small percentage of the immunoprecipitation sample was used for Western blots, which were immunoblotted with anti-BCAR3 antibody and 4G10, to detect SNAP-V5-BCAR3 and phosphotyrosine, respectively. (c) Relative levels of phosphorylation at BCAR3 Y117 with and without treatment with pervanadate. (d) Levels of phosphorylation at BCAR3 tyrosine residues following pervanadate treatment.

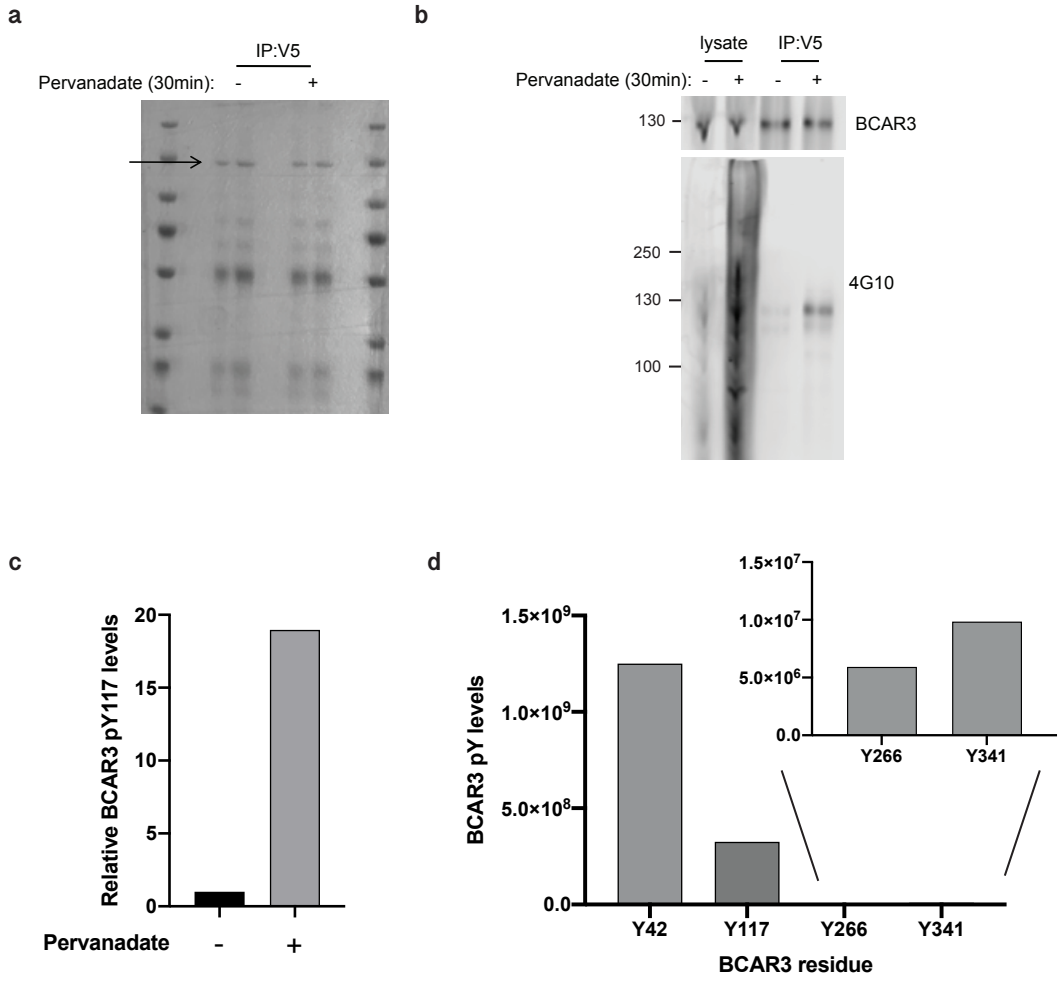

Supplement Figure 4. BCAR3 KO MCF10A cell lines were generated using CRISPR-Cas9 and BCAR3 KO reduces single cell migration and invasion.

(a) MCF10A parental subclones were grown and clone J8 was selected because cell morphology matched the morphology of MCF10A parental cell lines. The J8 clonal cell line was then infected with an all in one CRISPR plasmid, pLCV2, containing either empty vector or guide RNA against BCAR3 (guide 30 or 31). Potential knockouts were isolated through single cell expansion by dilution plating and validation of BCAR3 knockout was done by gDNA isolation and PCR, sequencing, and Western blotting. Control clonal cell lines, 8.00.3 and 8.00.4, express levels of BCAR3 and Cas similar to levels in MCF10A parental cell lines. BCAR3 KO cell lines, 8.30.3, 8.30.4, and 8.31.4, do not express detectable levels of BCAR3, but do express Cas. (b) Single cell migration of control and BCAR3 KO MCF10A toward EGF cells using a Boyden chamber assay. Mean and SEM; n=3. **p=0.003 by unpaired t-test. (c) Invasion through Matrigel toward EGF of control and BCAR3 KO MCF10A cells. Mean and SEM; n=3. **p=0.0028 by unpaired t-test.

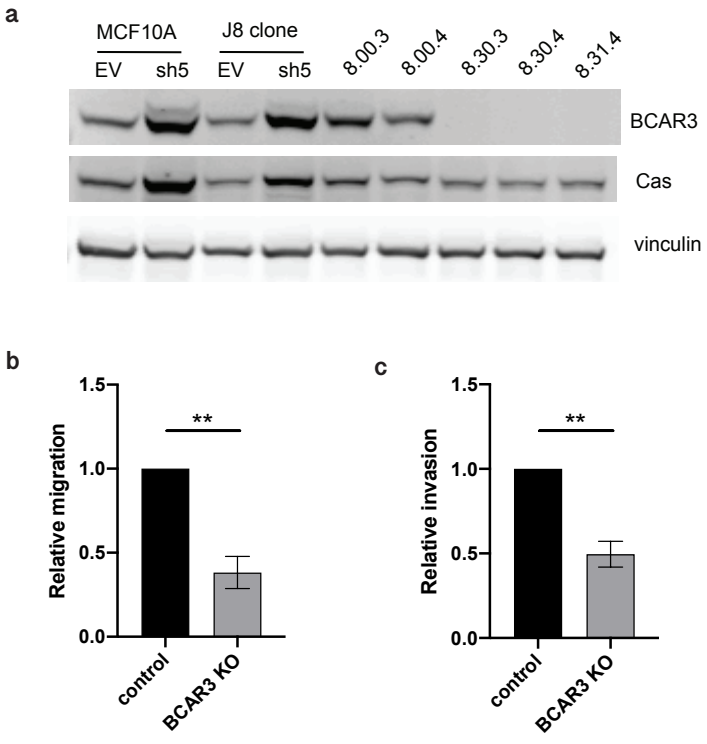

Supplement Figure 5. Dox-inducible cell lines expressing SNAP-V5-BCAR3 variants must be FACS-sorted to remove non-inducible cells.

(a) Immunofluorescence of dox-inducible MCF10A SNAP-V5-BCAR3 WT cells treated with 30ng/mL of doxycycline. A small percentage of cells express SNAP-V5-BCAR3, as only one cell shows positive staining with V5 antibody. (b) SNAP-V5-BCAR3 positive cells were isolated by treating cells with Janelia Fluor 646 SNAP-ligand and FACS-sorting for APC-positive cells. Un-induced cells treated with the SNAP-ligand have higher APC signal, indicating that the SNAP-ligand introduces background signal. (c) Cells induced with 100ng/mL of dox have two populations of cells: a SNAP-V5-BCAR3-negative population whose peak overlaps with the 0ng/mL dox control and a SNAP-V5-BCAR3-positive population, whose peak is shifted to the right, indicating these cells have higher APC signal. This SNAP-poditive peak was sorted for each cell line. (d) Immunofluorescence of dox-inducible cells treated with dox after cell sorting. Most cells express SNAP-V5-BCAR3, indicated by the positive staining with V5 antibody.

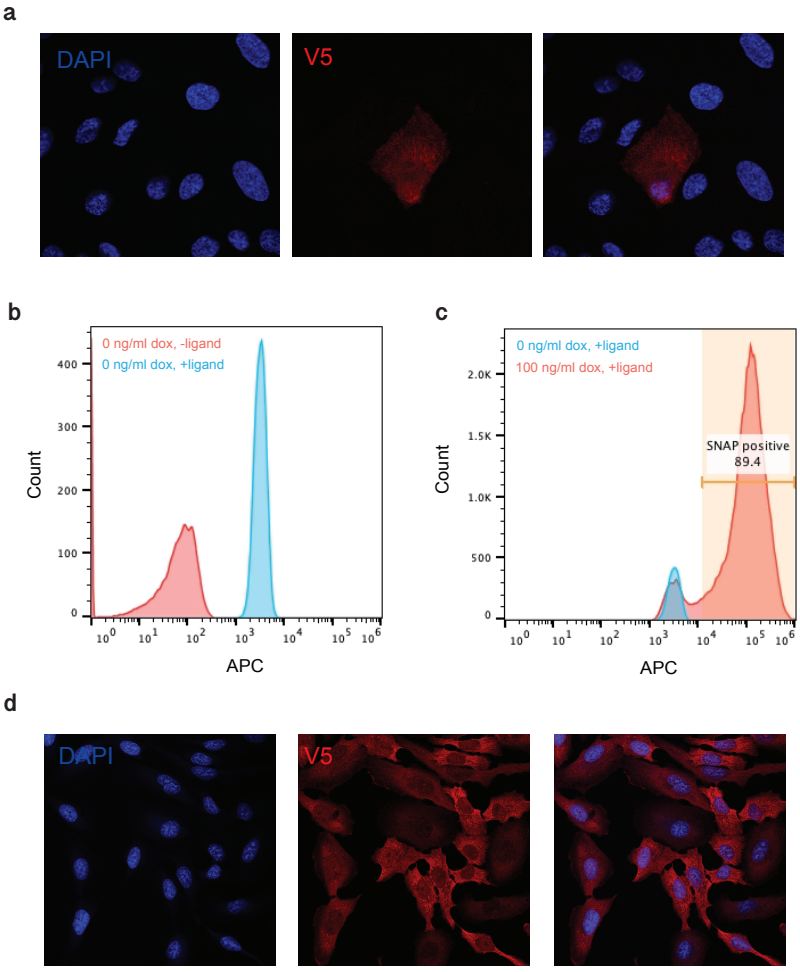

Supplement Figure 6. BCAR3 Y117 and SH2 domain are not required for binding to Cas.

Dox-inducible SNAP-V5-BCAR3 WT, Y117F, R177K, and EE MCF10A cells were induced with 10ng/mL dox for 48 hourse and lysed. Lysates were immunoprecipitated with anti-V5 antibody and probed for endogenous Cas. As expected, BCAR3 EE does not bind Cas (Figure 2.3b). BCAR3 Y117F and R177K do bind to Cas.

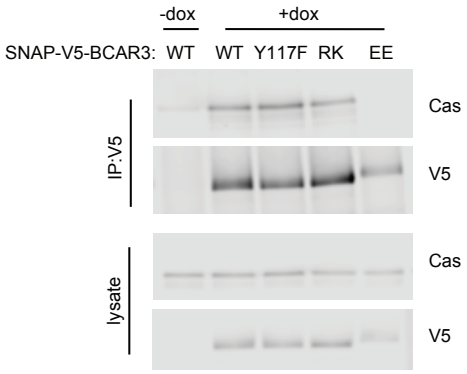

Supplement Figure 7. Endogenous BCAR3 and SNAP-V5-BCAR3 WT localize to adhesion sites.

(a) MCF10A EV cells were grown to confluence, placed in EGF-free media, scratched and allowed to migrate. Cells were fixed and stained for endogenous BCAR3 and vinculin. Scale bar = 10μm. (b) Dox-inducible SNAP-V5-BCAR3 WT cells were plated sparsely, induced with dox and allowed to spread. Cells were fixed and stained endogenous BCAR3, V5 and adhesion markers vinculin and FAK.

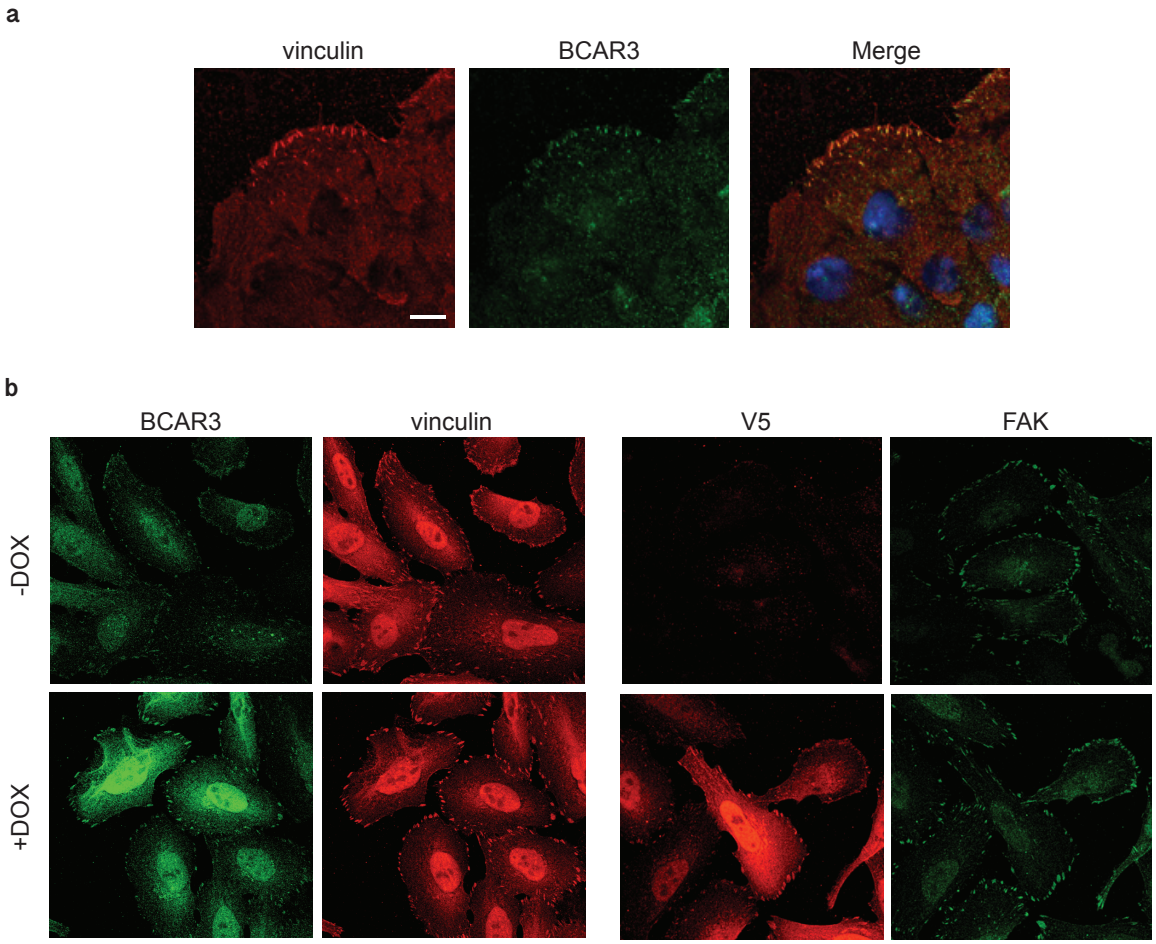

Supplement Figure 8. Photoconversion experiments need further optimization.

(a) HeLa cells were transfected with pCAG mEos2-Cas and plated sparsely. The boxed adhesions were converted using a 405nm laser on a spinning disk microscope. Images show a timecourse of green and red channels before and after photo-conversion. (b) HeLa cells were transfected with pCAG mEos3.2-Cas and plated sparsely. The boxed adhesions were converted using a 405nm laser on a confocal microscope. Images show green and red channels before and after photoconversion.

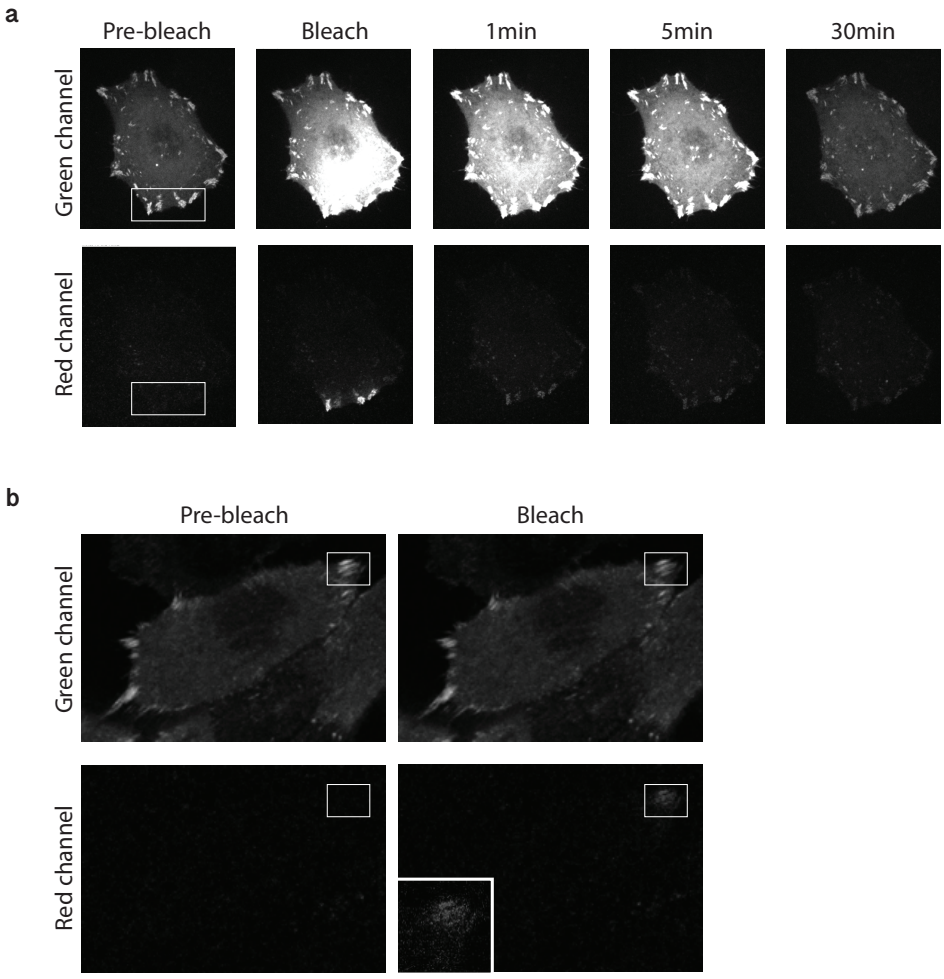

Supplement Figure 9. Fresh growth media stimulates BCAR3 degradation in Cul5-deficient MCF10A cells.

MCF10A EV and Cul5-deficient cells were treated with cycloheximide by removing the media from the cells and adding fresh CHX-containing growth media. Using these experimental methods, I observe degradation of BCAR3 in EV and shCul5 cells. As adding CHX directly to the conditioned media on the cells has shown that BCAR3 protein levels remain stable in Cul5-deficient cells, I hypothesize that a component of the growth media that was depleted in the conditioned media and present in the fresh media stimulated a Cul5-independent mechanism of BCAR3 turnover.

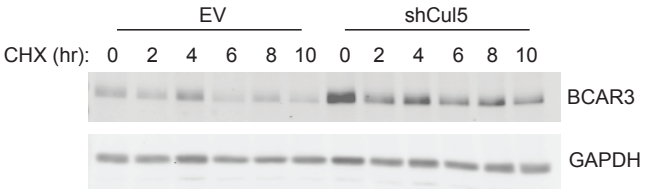

Supplement Figure 10. Cas protects BCAR3 from CRL5-independent degradation.

(a) EV and shCul5 MCF10A cells were treated with control siRNA or siRNA against Cas or BCAR3 and lysed for Western blotting. Quantification of protein levels of (b) BCAR3 when Cas is knocked down and (c) Cas when BCAR3 is knocked down was conducted for 4 independent experiments.

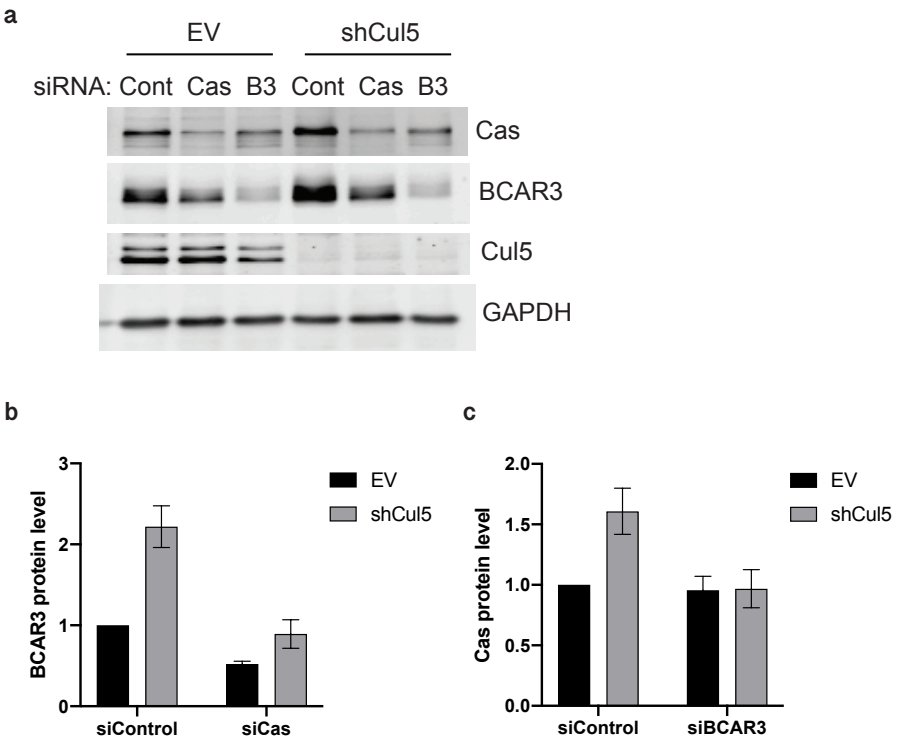

Supplement Figure 11. Growth factors stimulate phosphorylation of BCAR3 in MCF10A cells.

Dox-inducible MCF10A cells were plated and treated with doxycyline to induce expression of SNAP-V5-BCAR3. Cells were put in EGF-free media for 24 hours, followed by (a) stimulation with EGF and insulin for 30, 60, and 90 minutes or (b) stimulation with EGF alone for 5, 10, and 30 minutes, and cell lysis. Probing Western blots with anti-BCAR3 antibody show band shifts under the stimulation conditions, suggesting that EGF and/or insulin stimulate phosphorylation of BCAR3.

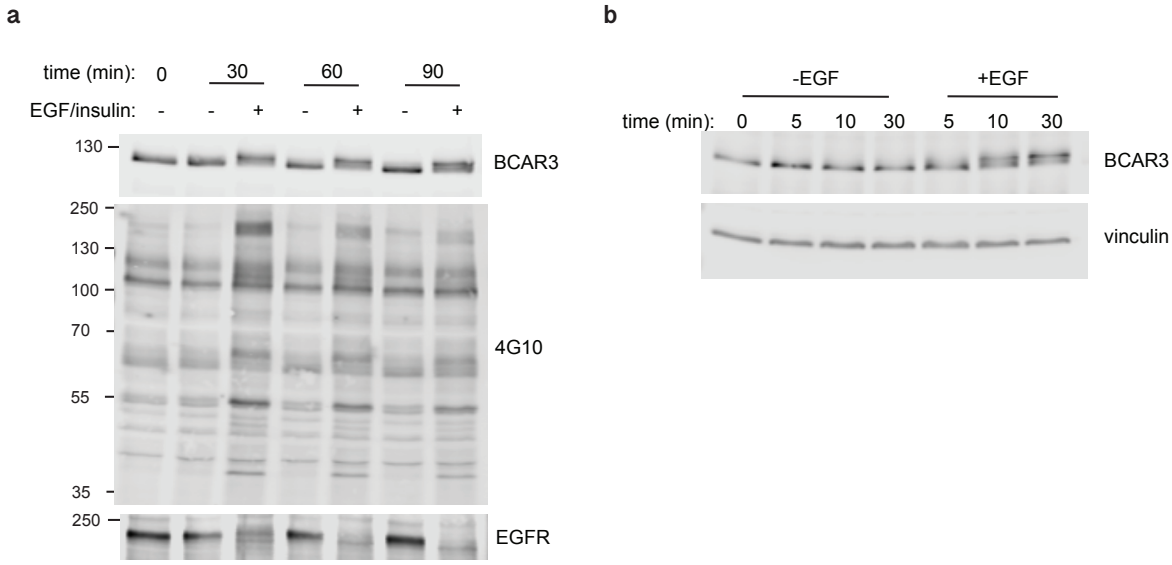

REFERENCES

1. Weijer, C.J., *Collective cell migration in development.* J Cell Sci, 2009. **122**(Pt 18): p. 3215-23.
2. Li, L., et al., *Collective cell migration: Implications for wound healing and cancer invasion.* Burns Trauma, 2013. **1**(1): p. 21-6.
3. Friedl, P. and D. Gilmour, *Collective cell migration in morphogenesis, regeneration and cancer.* Nat Rev Mol Cell Biol, 2009. **10**(7): p. 445-57.
4. Nguyen, D.X., P.D. Bos, and J. Massagué, *Metastasis: from dissemination to organ-specific colonization.* Nat Rev Cancer, 2009. **9**(4): p. 274-84.
5. Yamada, K.M. and M. Sixt, *Mechanisms of 3D cell migration.* Nat Rev Mol Cell Biol, 2019. **20**(12): p. 738-752.
6. Bear, J.E. and J.M. Haugh, *Directed migration of mesenchymal cells: where signaling and the cytoskeleton meet.* Curr Opin Cell Biol, 2014. **30**: p. 74-82.
7. Even-Ram, S. and K.M. Yamada, *Cell migration in 3D matrix.* Curr Opin Cell Biol, 2005. **17**(5): p. 524-32.
8. Paluch, E.K., I.M. Aspalter, and M. Sixt, *Focal Adhesion-Independent Cell Migration.* Annu Rev Cell Dev Biol, 2016. **32**: p. 469-490.
9. Garcin, C. and A. Straube, *Microtubules in cell migration.* Essays Biochem, 2019. **63**(5): p. 509-520.
10. Krause, M. and A. Gautreau, *Steering cell migration: lamellipodium dynamics and the regulation of directional persistence.* Nat Rev Mol Cell Biol, 2014. **15**(9): p. 577-90.
11. Price, L.S., et al., *Activation of Rac and Cdc42 by integrins mediates cell spreading.* Mol Biol Cell, 1998. **9**(7): p. 1863-71.
12. Zaidel-Bar, R., et al., *Early molecular events in the assembly of matrix adhesions at the leading edge of migrating cells.* J Cell Sci, 2003. **116**(Pt 22): p. 4605-13.
13. Case, L.B. and C.M. Waterman, *Integration of actin dynamics and cell adhesion by a three-dimensional, mechanosensitive molecular clutch.* Nat Cell Biol, 2015. **17**(8): p. 955-63.
14. Galbraith, C.G., K.M. Yamada, and M.P. Sheetz, *The relationship between force and focal complex development.* J Cell Biol, 2002. **159**(4): p. 695-705.
15. Kanchanawong, P., et al., *Nanoscale architecture of integrin-based cell adhesions.* Nature, 2010. **468**(7323): p. 580-4.
16. Burridge, K., *Focal adhesions: a personal perspective on a half century of progress.* FEBS J, 2017. **284**(20): p. 3355-3361.
17. Zamir, E. and B. Geiger, *Molecular complexity and dynamics of cell-matrix adhesions.* J Cell Sci, 2001. **114**(Pt 20): p. 3583-90.
18. Chen, W.T. and S.J. Singer, *Immunoelectron microscopic studies of the sites of cell-substratum and cell-cell contacts in cultured fibroblasts.* J Cell Biol, 1982. **95**(1): p. 205-22.
19. Brugge, J.S. and R.L. Erikson, *Identification of a transformation-specific antigen induced by an avian sarcoma virus.* Nature, 1977. **269**(5626): p. 346-8.
20. Purchio, A.F., et al., *Identification of a polypeptide encoded by the avian sarcoma virus src gene.* Proc Natl Acad Sci U S A, 1978. **75**(3): p. 1567-71.

21. Brown, M.T. and J.A. Cooper, *Regulation, substrates and functions of src.* Biochim Biophys Acta, 1996. **1287**(2-3): p. 121-49.
22. Hanks, S.K., et al., *Focal adhesion protein-tyrosine kinase phosphorylated in response to cell attachment to fibronectin.* Proc Natl Acad Sci U S A, 1992. **89**(18): p. 8487-91.
23. Mitra, S.K., D.A. Hanson, and D.D. Schlaepfer, *Focal adhesion kinase: in command and control of cell motility.* Nat Rev Mol Cell Biol, 2005. **6**(1): p. 56-68.
24. Parsons, J.T., *Focal adhesion kinase: the first ten years.* J Cell Sci, 2003. **116**(Pt 8): p. 1409-16.
25. Thomas, S.M. and J.S. Brugge, *Cellular functions regulated by Src family kinases.* Annu Rev Cell Dev Biol, 1997. **13**: p. 513-609.
26. Ilić, D., et al., *Reduced cell motility and enhanced focal adhesion contact formation in cells from FAK-deficient mice.* Nature, 1995. **377**(6549): p. 539-44.
27. Ren, X.-D., et al., *Focal adhesion kinase suppresses Rho activity to promote focal adhesion turnover.* Journal of Cell Science, 2000. **113**: p. 3673-3678.
28. Hamadi, A., et al., *Regulation of focal adhesion dynamics and disassembly by phosphorylation of FAK at tyrosine 397.* Journal of Cell Science, 2005. **118**: p. 4415-4425.
29. Webb, D., et al., *FAK-Src signaling through paxillin, ERK and MLCK regulates adhesion disassembly.* Nature Cell Biology, 2004. **6**: p. 154-161.
30. Klinghoffer, R.A., et al., *Src family kinases are required for integrin but not PDGFR signal transduction.* EMBO J, 1999. **18**(9): p. 2459-71.
31. Murphy, J.M., et al., *Targeting focal adhesion kinase in cancer cells and the tumor microenvironment.* Exp Mol Med, 2020. **52**(6): p. 877-886.
32. Sulzmaier, F.J., C. Jean, and D.D. Schlaepfer, *FAK in cancer: mechanistic findings and clinical applications.* Nat Rev Cancer, 2014. **14**(9): p. 598-610.
33. Irby, R.B. and T.J. Yeatman, *Role of Src expression and activation in human cancer.* Oncogene, 2000. **19**(49): p. 5636-42.
34. Zhang, S. and D. Yu, *Targeting Src family kinases in anti-cancer therapies: turning promise into triumph.* Trends Pharmacol Sci, 2012. **33**(3): p. 122-8.
35. Sakai, R., et al., *A novel signaling molecule, p130, forms stable complexes in vivo with v-Crk and v-Src in a tyrosine phosphorylation-dependent manner.* EMBO J, 1994. **13**(16): p. 3748-56.
36. Matsui, H., I. Harada, and Y. Sawada, *Src, p130Cas, and Mechanotransduction in Cancer Cells.* Genes Cancer, 2012. **3**(5-6): p. 394-401.
37. Wallez, Y., et al., *NSP-CAS Protein Complexes: Emerging Signaling Modules in Cancer.* Genes Cancer, 2012. **3**(5-6): p. 382-93.
38. Ridley, A.J., *Membrane ruffling and signal transduction.* Bioessays, 1994. **16**(5): p. 321-7.
39. Ridley, A.J., et al., *The small GTP-binding protein rac regulates growth factor-induced membrane ruffling.* Cell, 1992. **70**(3): p. 401-10.
40. Kiyokawa, E., et al., *Activation of Rac1 by a Crk SH3-binding protein, DOCK180.* Genes Dev, 1998. **12**(21): p. 3331-6.
41. Klemke, R.L., et al., *CAS/Crk coupling serves as a "molecular switch" for induction of cell migration.* J Cell Biol, 1998. **140**(4): p. 961-72.
42. Cheresh, D.A., J. Leng, and R.L. Klemke, *Regulation of cell contraction and membrane ruffling by distinct signals in migratory cells.* J Cell Biol, 1999. **146**(5): p. 1107-16.

43. Sharma, A. and B.J. Mayer, *Phosphorylation of p130Cas initiates Rac activation and membrane ruffling.* BMC Cell Biol, 2008. **9**: p. 50.
44. van Agthoven, T., et al., *Identification of BCAR3 by a random search for genes involved in antiestrogen resistance of human breast cancer cells.* EMBO J, 1998. **17**(10): p. 2799-808.
45. Schrecengost, R.S., et al., *Breast cancer antiestrogen resistance-3 expression regulates breast cancer cell migration through promotion of p130Cas membrane localization and membrane ruffling.* Cancer Res, 2007. **67**(13): p. 6174-82.
46. Cross, A.M., et al., *Breast cancer antiestrogen resistance 3-p130(Cas) interactions promote adhesion disassembly and invasion in breast cancer cells.* Oncogene, 2016. **35**(45): p. 5850-5859.
47. Zhang, W., et al., *Prediction and prognostic significance of BCAR3 expression in patients with multiple myeloma.* Journal of Translational Medicine, 2018. **16**: p. 363.
48. Guo, J., et al., *Breast cancer anti-estrogen resistance 3 inhibits transforming growth factor β/Smad signaling and associates with favorable breast cancer disease outcomes.* Breast Cancer Res, 2014. **16**(6): p. 476.
49. Hochgräfe, F., et al., *Tyrosine phosphorylation profiling reveals the signaling network characteristics of Basal breast cancer cells.* Cancer Res, 2010. **70**(22): p. 9391-401.
50. Oh, M.J., et al., *BCAR3 regulates EGF-induced DNA synthesis in normal human breast MCF-12A cells.* Biochem Biophys Res Commun, 2008. **375**(3): p. 430-4.
51. Jones, R.B., et al., *A quantitative protein interaction network for the ErbB receptors using protein microarrays.* Nature, 2006. **439**(7073): p. 168-74.
52. Sun, G., et al., *Protein tyrosine phosphatase α phosphotyrosyl-789 binds BCAR3 to position Cas for activation at integrin-mediated focal adhesions.* Mol Cell Biol, 2012. **32**(18): p. 3776-89.
53. Mace, P.D., et al., *NSP-Cas protein structures reveal a promiscuous interaction module in cell signaling.* Nat Struct Mol Biol, 2011. **18**(12): p. 1381-7.
54. Wilson, A.L., et al., *Breast cancer antiestrogen resistance 3 (BCAR3) promotes cell motility by regulating actin cytoskeletal and adhesion remodeling in invasive breast cancer cells.* PLoS One, 2013. **8**(6): p. e65678.
55. Cai, D., et al., *AND-34/BCAR3, a GDP exchange factor whose overexpression confers antiestrogen resistance, activates Rac, PAK1, and the cyclin D1 promoter.* Cancer Res, 2003. **63**(20): p. 6802-8.
56. Schuh, N.R., et al., *BCAR3 regulates Src/p130 Cas association, Src kinase activity, and breast cancer adhesion signaling.* J Biol Chem, 2010. **285**(4): p. 2309-17.
57. Felekkis, K.N., et al., *AND-34 activates phosphatidylinositol 3-kinase and induces anti-estrogen resistance in a SH2 and GDP exchange factor-like domain-dependent manner.* Mol Cancer Res, 2005. **3**(1): p. 32-41.
58. Riggins, R.B., L.A. Quilliam, and A.H. Bouton, *Synergistic promotion of c-Src activation and cell migration by Cas and AND-34/BCAR3.* J Biol Chem, 2003. **278**(30): p. 28264-73.
59. Wallez, Y., S.J. Riedl, and E.B. Pasquale, *Association of the breast cancer antiestrogen resistance protein 1 (BCAR1) and BCAR3 scaffolding proteins in cell signaling and antiestrogen resistance.* J Biol Chem, 2014. **289**(15): p. 10431-44.
60. Cai, D., et al., *AND-34, a novel p130Cas-binding thymic stromal cell protein regulated by adhesion and inflammatory cytokines.* J Immunol, 1999. **163**(4): p. 2104-12.

61. Hornbeck, P.V., et al., *PhosphoSitePlus, 2014: mutations, PTMs and recalibrations.* Nucleic Acids Res, 2015. **43**(Database issue): p. D512-20.
62. Oh, M.J., et al., *Functional roles of BCAR3 in the signaling pathways of insulin leading to DNA synthesis, membrane ruffling and GLUT4 translocation.* Biochem Biophys Res Commun, 2013. **441**(4): p. 911-6.
63. Alonso, A., et al., *Protein tyrosine phosphatases in the human genome.* Cell, 2004. **117**(6): p. 699-711.
64. Nijman, S.M., et al., *A genomic and functional inventory of deubiquitinating enzymes.* Cell, 2005. **123**(5): p. 773-86.
65. Pickart, C.M., *Back to the future with ubiquitin.* Cell, 2004. **116**(2): p. 181-90.
66. Hochstrasser, M., *Lingering mysteries of ubiquitin-chain assembly.* Cell, 2006. **124**(1): p. 27-34.
67. Hershko, A., et al., *Components of ubiquitin-protein ligase system. Resolution, affinity purification, and role in protein breakdown.* J Biol Chem, 1983. **258**(13): p. 8206-14.
68. Metzger, M.B., V.A. Hristova, and A.M. Weissman, *HECT and RING finger families of E3 ubiquitin ligases at a glance.* J Cell Sci, 2012. **125**(Pt 3): p. 531-7.
69. Vijay-Kumar, S., C.E. Bugg, and W.J. Cook, *Structure of ubiquitin refined at 1.8 A resolution.* J Mol Biol, 1987. **194**(3): p. 531-44.
70. Swatek, K.N. and D. Komander, *Ubiquitin modifications.* Cell Res, 2016. **26**(4): p. 399-422.
71. Clague, M.J. and S. Urbé, *Ubiquitin: same molecule, different degradation pathways.* Cell, 2010. **143**(5): p. 682-5.
72. Cooper, J.A., T. Kaneko, and S.S. Li, *Cell regulation by phosphotyrosine-targeted ubiquitin ligases.* Mol Cell Biol, 2015. **35**(11): p. 1886-97.
73. Lydeard, J.R., B.A. Schulman, and J.W. Harper, *Building and remodelling Cullin-RING E3 ubiquitin ligases.* EMBO Rep, 2013. **14**(12): p. 1050-61.
74. Petroski, M.D. and R.J. Deshaies, *Function and regulation of cullin-RING ubiquitin ligases.* Nat Rev Mol Cell Biol, 2005. **6**(1): p. 9-20.
75. Kile, B.T., et al., *The SOCS box: a tale of destruction and degradation.* Trends Biochem Sci, 2002. **27**(5): p. 235-41.
76. Teckchandani, A., et al., *Cullin 5 destabilizes Cas to inhibit Src-dependent cell transformation.* J Cell Sci, 2014. **127**(Pt 3): p. 509-20.
77. Simó, S. and J.A. Cooper, *Rbx2 regulates neuronal migration through different cullin 5-RING ligase adaptors.* Dev Cell, 2013. **27**(4): p. 399-411.
78. Laszlo, G.S. and J.A. Cooper, *Restriction of Src activity by Cullin-5.* Curr Biol, 2009. **19**(2): p. 157-62.
79. Teckchandani, A. and J.A. Cooper, *The ubiquitin-proteasome system regulates focal adhesions at the leading edge of migrating cells.* Elife, 2016. **5**.
80. von Wichert, G., et al., *RPTP-alpha acts as a transducer of mechanical force on alphav/beta3-integrin-cytoskeleton linkages.* J Cell Biol, 2003. **161**(1): p. 143-53.
81. Zhang, X., et al., *Talin depletion reveals independence of initial cell spreading from integrin activation and traction.* Nat Cell Biol, 2008. **10**(9): p. 1062-8.
82. Roca-Cusachs, P., et al., *Integrin-dependent force transmission to the extracellular matrix by α-actinin triggers adhesion maturation.* Proc Natl Acad Sci U S A, 2013. **110**(15): p. E1361-70.

83. Rottner, K., A. Hall, and J.V. Small, *Interplay between Rac and Rho in the control of substrate contact dynamics.* Curr Biol, 1999. **9**(12): p. 640-8.
84. Nobes, C.D. and A. Hall, *Rho, rac, and cdc42 GTPases regulate the assembly of multimolecular focal complexes associated with actin stress fibers, lamellipodia, and filopodia.* Cell, 1995. **81**(1): p. 53-62.
85. Ponniah, S., et al., *Targeted disruption of the tyrosine phosphatase PTPalpha leads to constitutive downregulation of the kinases Src and Fyn.* Curr Biol, 1999. **9**(10): p. 535-8.
86. Su, J., M. Muranjan, and J. Sap, *Receptor protein tyrosine phosphatase alpha activates Src-family kinases and controls integrin-mediated responses in fibroblasts.* Curr Biol, 1999. **9**(10): p. 505-11.
87. Schaller, M.D. and J.T. Parsons, *pp125FAK-dependent tyrosine phosphorylation of paxillin creates a high-affinity binding site for Crk.* Mol Cell Biol, 1995. **15**(5): p. 2635-45.
88. Yano, H., et al., *Paxillin alpha and Crk-associated substrate exert opposing effects on cell migration and contact inhibition of growth through tyrosine phosphorylation.* Proc Natl Acad Sci U S A, 2000. **97**(16): p. 9076-81.
89. Sanders, M.A. and M.D. Basson, *p130cas but not paxillin is essential for Caco-2 intestinal epithelial cell spreading and migration on collagen IV.* J Biol Chem, 2005. **280**(25): p. 23516-22.
90. Pilling, C., *Cullin5 and SOCS Protein Regulation of Receptor Tyrosine Kinases*, in *Molecular and Cellular Biology*. 2017, University of Washington. p. 128.
91. Defilippi, P., P. Di Stefano, and S. Cabodi, *p130Cas: a versatile scaffold in signaling networks.* Trends Cell Biol, 2006. **16**(5): p. 257-63.
92. Nikonova, A.S., et al., *CAS proteins in health and disease: an update.* IUBMB Life, 2014. **66**(6): p. 387-95.
93. Harte, M.T., et al., *p130Cas, a substrate associated with v-Src and v-Crk, localizes to focal adhesions and binds to focal adhesion kinase.* J Biol Chem, 1996. **271**(23): p. 13649-55.
94. Vuori, K., et al., *Introduction of p130cas signaling complex formation upon integrin-mediated cell adhesion: a role for Src family kinases.* Mol Cell Biol, 1996. **16**(6): p. 2606-13.
95. Garron, M.L., et al., *Structural insights into the association between BCAR3 and Cas family members, an atypical complex implicated in anti-oestrogen resistance.* J Mol Biol, 2009. **386**(1): p. 190-203.
96. Keppler, A., et al., *A general method for the covalent labeling of fusion proteins with small molecules in vivo.* Nat Biotechnol, 2003. **21**(1): p. 86-9.
97. Grimm, J.B., et al., *A general method to improve fluorophores for live-cell and single-molecule microscopy.* Nat Methods, 2015. **12**(3): p. 244-50, 3 p following 250.
98. Makkinje, A., et al., *AND-34/BCAR3 regulates adhesion-dependent p130Cas serine phosphorylation and breast cancer cell growth pattern.* Cell Signal, 2009. **21**(9): p. 1423-35.
99. Ruest, P.J., et al., *Mechanisms of CAS substrate domain tyrosine phosphorylation by FAK and Src.* Mol Cell Biol, 2001. **21**(22): p. 7641-52.
100. Nakamoto, T., et al., *Requirements for localization of p130cas to focal adhesions.* Mol Cell Biol, 1997. **17**(7): p. 3884-97.

101. Donato, D.M., et al., *Dynamics and mechanism of p130Cas localization to focal adhesions.* J Biol Chem, 2010. **285**(27): p. 20769-79.
102. Braniš, J., et al., *The role of focal adhesion anchoring domains of CAS in mechanotransduction.* Sci Rep, 2017. **7**: p. 46233.
103. Janoštiak, R., et al., *CAS directly interacts with vinculin to control mechanosensing and focal adhesion dynamics.* Cell Mol Life Sci, 2014. **71**(4): p. 727-44.
104. Stutchbury, B., et al., *Distinct focal adhesion protein modules control different aspects of mechanotransduction.* J Cell Sci, 2017. **130**(9): p. 1612-1624.
105. Wolfenson, H., et al., *A role for the juxtamembrane cytoplasm in the molecular dynamics of focal adhesions.* PLoS One, 2009. **4**(1): p. e4304.
106. Rothenberg, K.E., et al., *Vinculin Force-Sensitive Dynamics at Focal Adhesions Enable Effective Directed Cell Migration.* Biophys J, 2018. **114**(7): p. 1680-1694.
107. Humphries, J.D., et al., *Vinculin controls focal adhesion formation by direct interactions with talin and actin.* J Cell Biol, 2007. **179**(5): p. 1043-57.
108. Legerstee, K., et al., *Dynamics and distribution of paxillin, vinculin, zyxin and VASP depend on focal adhesion location and orientation.* Sci Rep, 2019. **9**(1): p. 10460.
109. Ishikawa-Ankerhold, H.C., R. Ankerhold, and G.P. Drummen, *Advanced fluorescence microscopy techniques--FRAP, FLIP, FLAP, FRET and FLIM.* Molecules, 2012. **17**(4): p. 4047-132.
110. Carisey, A., et al., *Fluorescence recovery after photobleaching.* Methods Mol Biol, 2011. **769**: p. 387-402.
111. McKinney, S.A., et al., *A bright and photostable photoconvertible fluorescent protein.* Nat Methods, 2009. **6**(2): p. 131-3.
112. Zhang, M., et al., *Rational design of true monomeric and bright photoactivatable fluorescent proteins.* Nat Methods, 2012. **9**(7): p. 727-9.
113. Sprague, B.L. and J.G. McNally, *FRAP analysis of binding: proper and fitting.* Trends Cell Biol, 2005. **15**(2): p. 84-91.
114. Kondo, T., et al., *A novel spontaneous mutation of BCAR3 results in extrusion cataracts in CF#1 mouse strain.* Mamm Genome, 2016. **27**(9-10): p. 451-9.
115. Makkinje, A., et al., *Breast cancer anti-estrogen resistance 3 (BCAR3) protein augments binding of the c-Src SH3 domain to Crk-associated substrate (p130cas).* J Biol Chem, 2012. **287**(33): p. 27703-14.
116. Near, R.I., et al., *AND-34/BCAR3 differs from other NSP homologs in induction of anti-estrogen resistance, cyclin D1 promoter activation and altered breast cancer cell morphology.* J Cell Physiol, 2007. **212**(3): p. 655-65.
117. Near, R.I., et al., *Loss of AND-34/BCAR3 expression in mice results in rupture of the adult lens.* Mol Vis, 2009. **15**: p. 685-99.
118. Meng, X., et al., *MicroRNA-126-5p downregulates BCAR3 expression to promote cell migration and invasion in endometriosis.* Mol Cell Endocrinol, 2019. **494**: p. 110486.
119. Yang, X., et al., *A public genome-scale lentiviral expression library of human ORFs.* Nat Methods, 2011. **8**(8): p. 659-61.

VITA

Elizabeth Steenkiste attended Denison University where she received a Bachelor of Science in Biology and graduated Summa Cum Laude in 2014. While studying at Denison, Elizabeth conducted research in the labs of Dr. Eric Liebl and Dr. Jeffrey Thompson. In Dr. Liebl's lab, she studied dominant enhancers of Trio and Abl mutant phenotypes in *Drosophila*. Elizabeth completed her senior research project in Dr. Thompson's lab, where she studied the role of histone H3 methylation patterns in UV-induced DNA repair in *Saccharomyces cerevisiae*. Elizabeth joined the Molecular and Cellular Biology graduate program at the University of Washington in 2014, where she received the Cell and Molecular Biology training grant funded through the National Institutes of Health. Elizabeth worked closely with the Science Education Partnership at the Fred Hutchinson Cancer Research Center. She also designed and co-taught an undergraduate elective Biology class at the University of Washington through the Science Teaching Experience Program for Upcoming PhDs. These teaching experiences provided her with valuable skills and training that have prepared her for a teaching career in higher education. Elizabeth defended her dissertation investigating phosphorylation and protein turnover in epithelial cell migration on December 8th, 2020. Elizabeth will be pursuing a job in teaching following graduate school.